Quantum phase transitions: from antiferromagnets and superconductors to black holes

Reviews:
arXiv:0907.0008
arXiv:0810.3005 (with Markus Mueller)

Talk online: sachdev.physics.harvard.edu

Lars Fritz, Harvard
Victor Galitski, Maryland
Max Metlitski, Harvard
Eun Gook Moon, Harvard
Markus Mueller, Trieste
Joerg Schmalian, Iowa

Frederik Denef, Harvard+Leuven
Sean Hartnoll, Harvard
Christopher Herzog, Princeton
Pavel Kovtun, Victoria
Dam Son, Washington

PHYSICS
HARVARD

Outline

1. Coupled dimer antiferromagnets

   Order parameters and Landau-Ginzburg criticality

2. Graphene

   `Topological' Fermi surface transitions

3. Quantum criticality and black holes

   AdS_4 theory of compressible quantum liquids

4. Quantum criticality in the cuprates

   Global phase diagram and the spin density wave transition in metals

Outline

1. Coupled dimer antiferromagnets

   Order parameters and Landau-Ginzburg criticality

2. Graphene

   `Topological' Fermi surface transitions

3. Quantum criticality and black holes

   AdS_4 theory of compressible quantum liquids

4. Quantum criticality in the cuprates

   Global phase diagram and the spin density wave transition in metals

$TlCuCl_3$

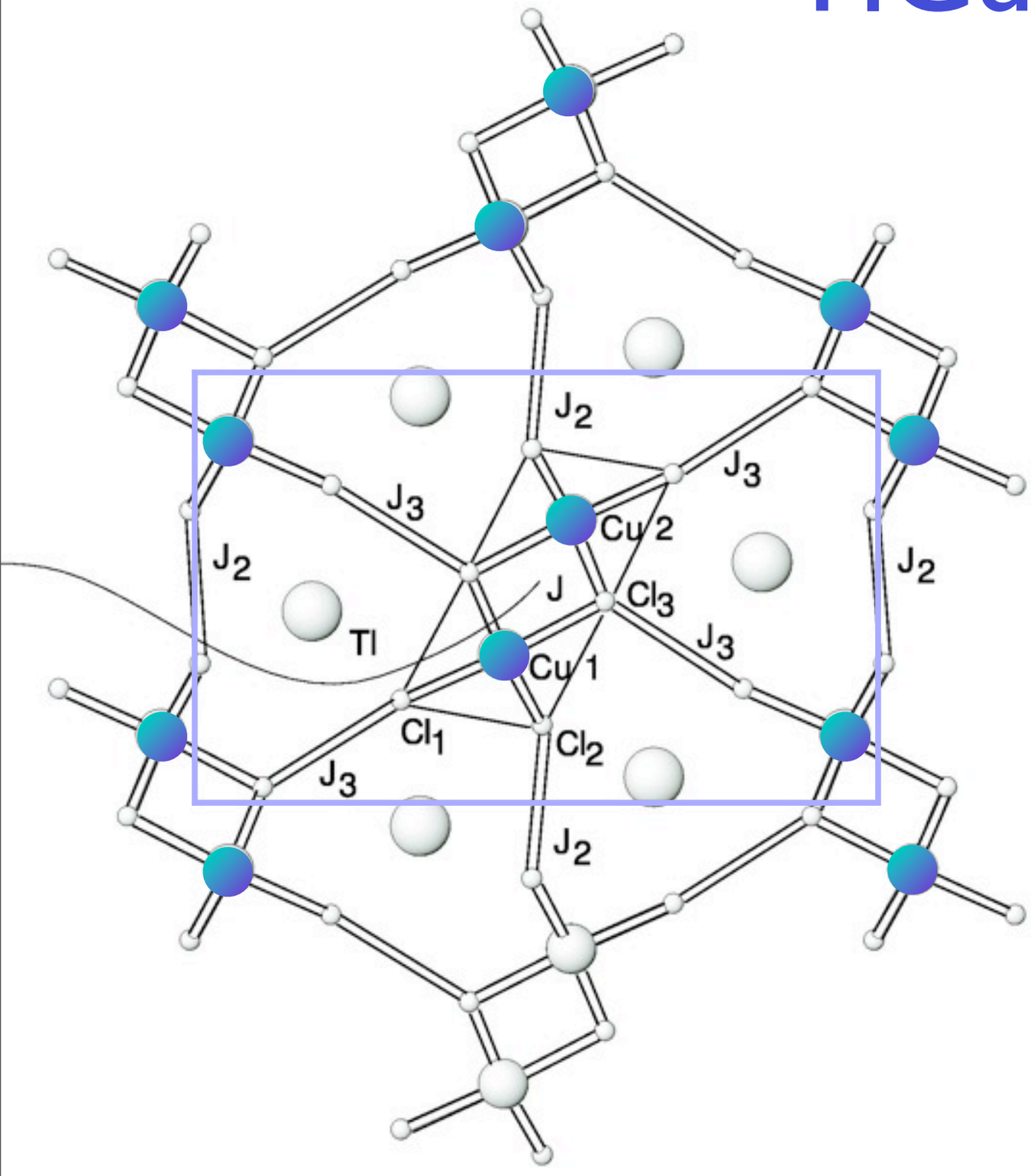
J2
J3
J3
J2
Cu2
J
Cl3
J2
Tl
J3
Cu1
Cl1
Cl2
J3
J2

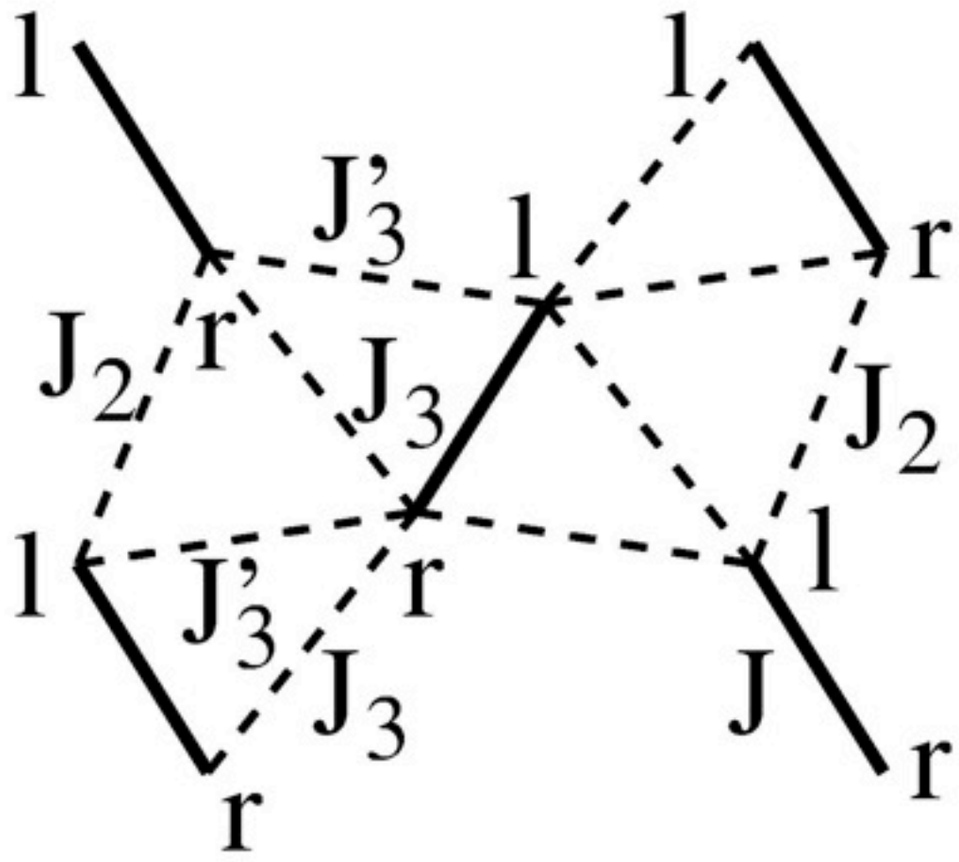
l
J'3
l
r
J2
r
J3
J2
l
J'3
r
l
J3
J
r
r

$TlCuCl_3$

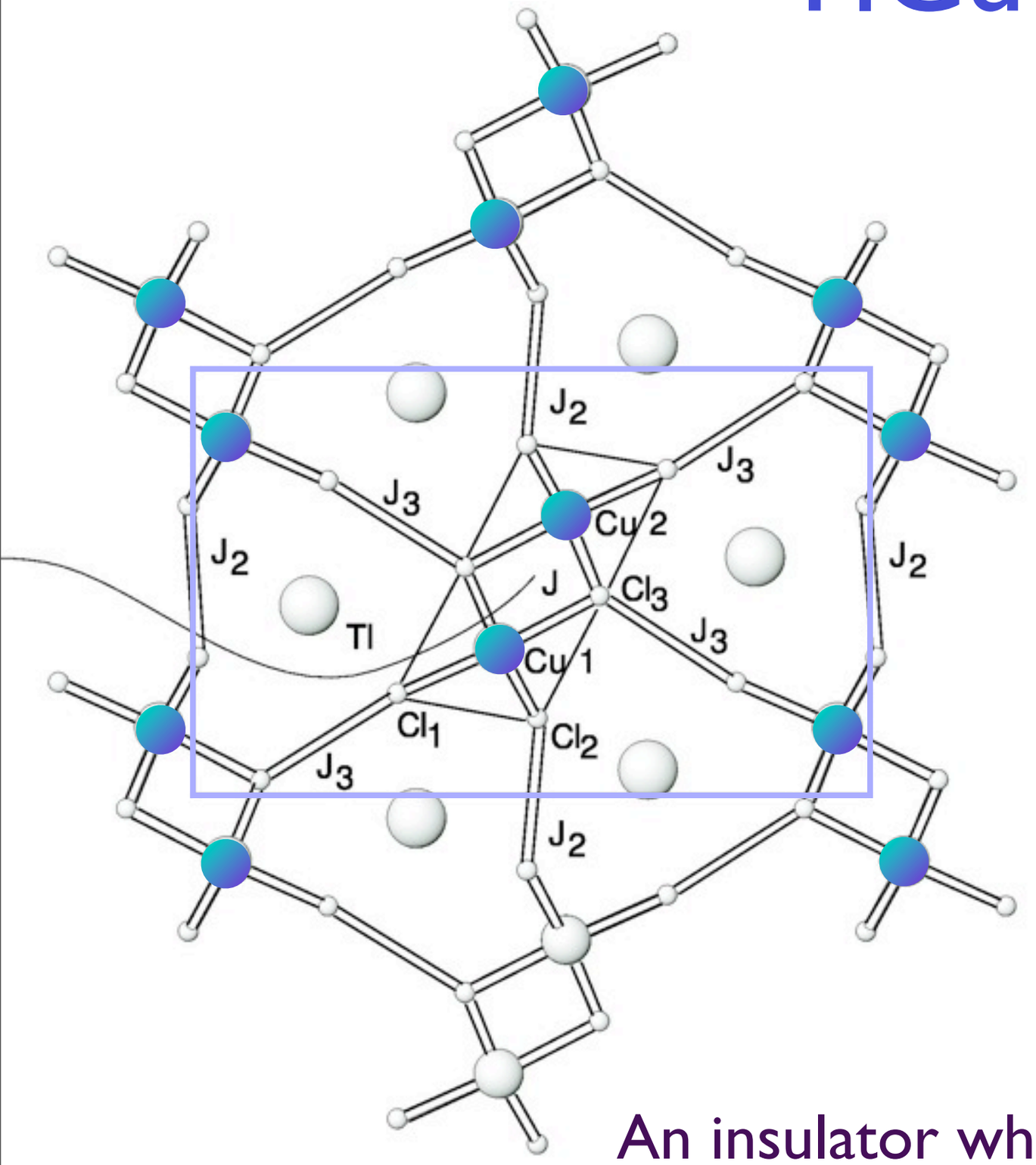

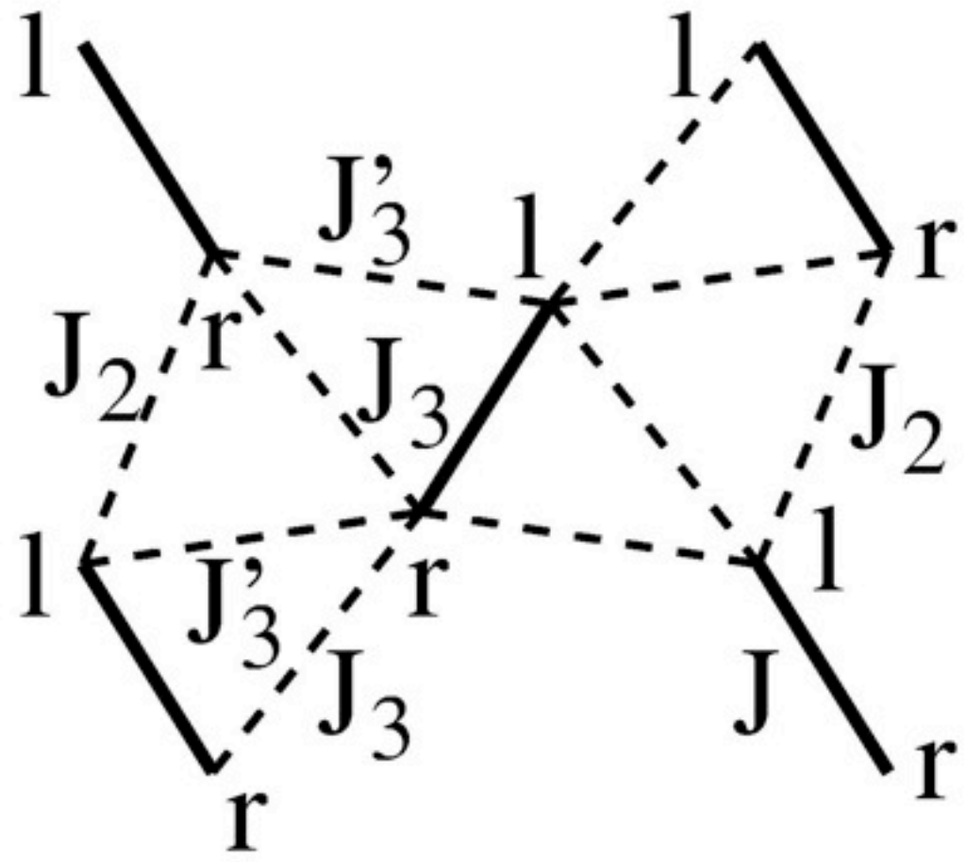

An insulator whose spin susceptibility vanishes exponentially as the temperature T tends to zero.

Square lattice antiferromagnet

$$H = \sum_{\langle ij \rangle} J_{ij} \vec{S}_i \cdot \vec{S}_j$$

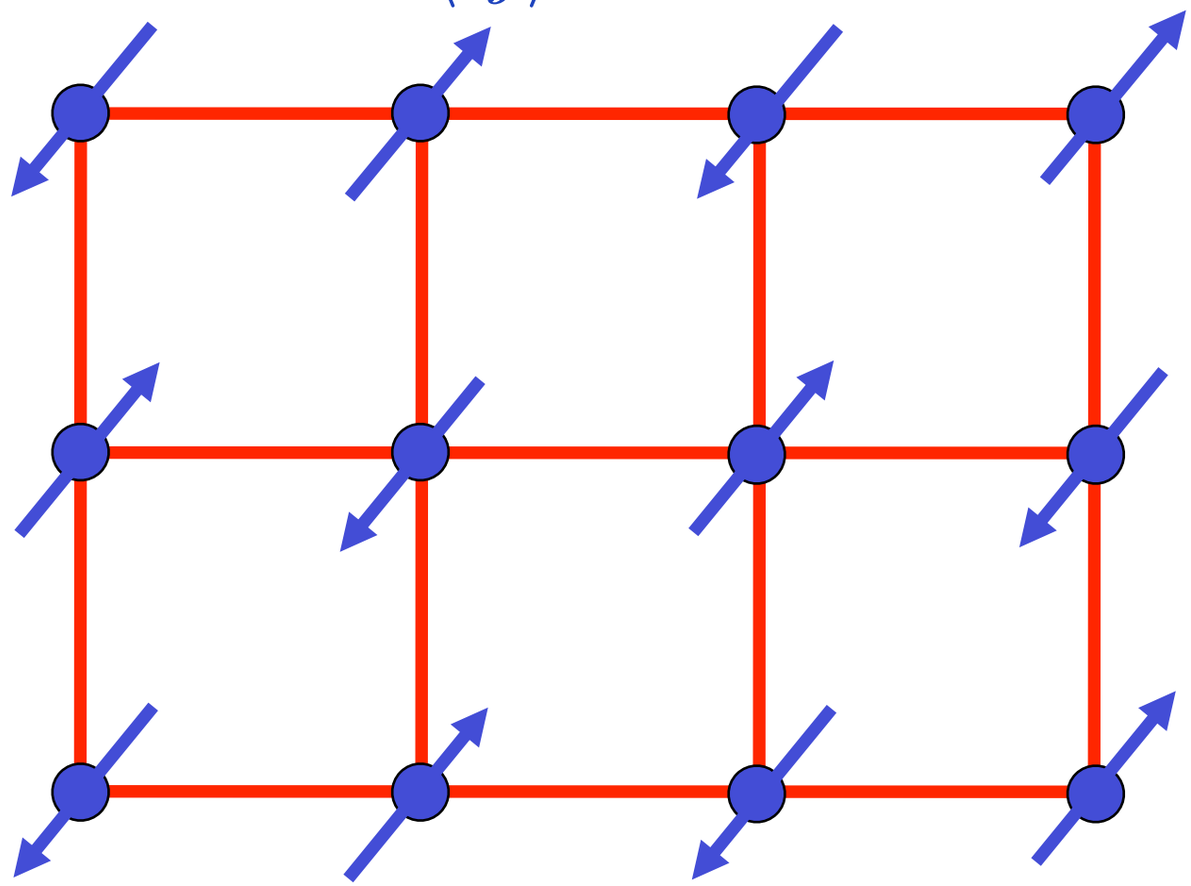

Ground state has long-range Néel order

Order parameter is a single vector field $\vec{\varphi} = \eta_i \vec{S}_i$

$\eta_i = \pm 1$ on two sublattices

$\langle \vec{\varphi} \rangle \neq 0$ in Néel state.

Square lattice antiferromagnet

$$H = \sum_{\langle ij \rangle} J_{ij} \vec{S}_i \cdot \vec{S}_j$$

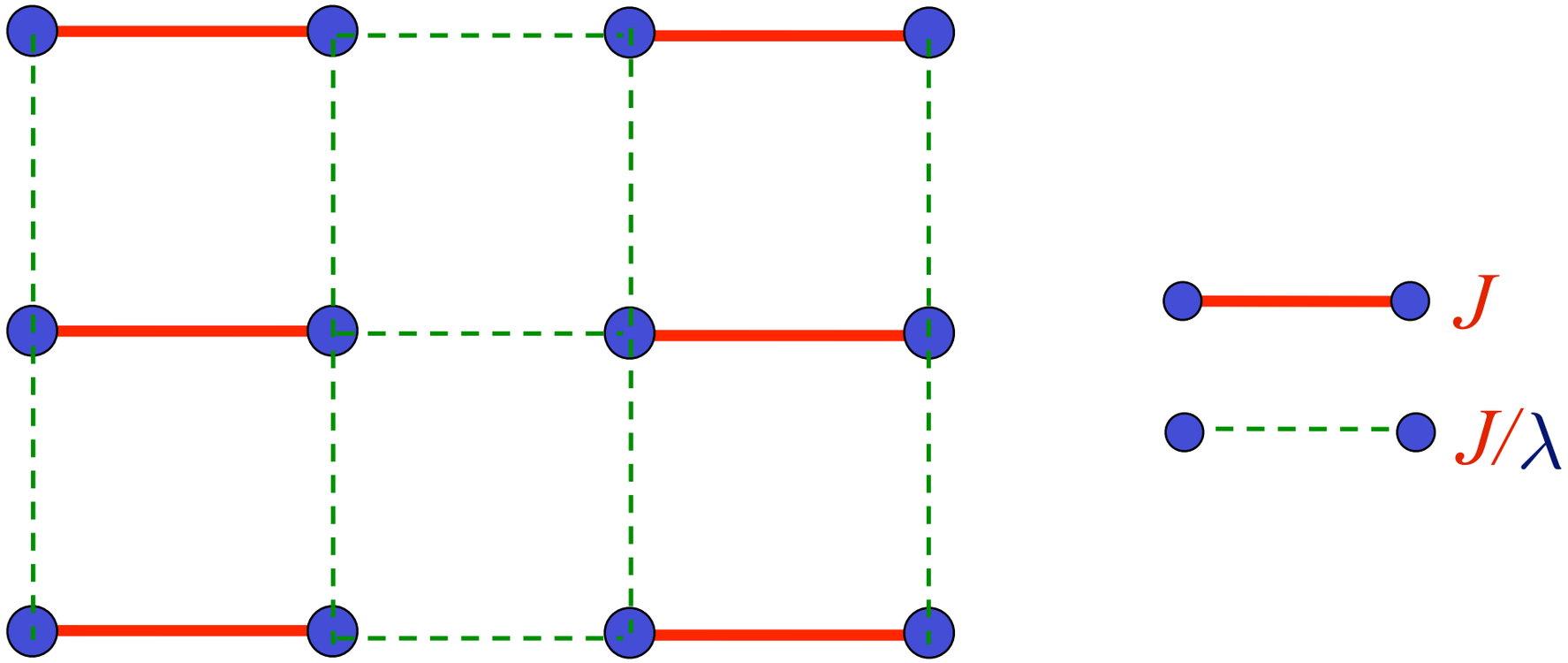

Weaken some bonds to induce spin entanglement in a new quantum phase

Square lattice antiferromagnet

$$H = \sum_{\langle ij \rangle} J_{ij} \vec{S}_i \cdot \vec{S}_j$$

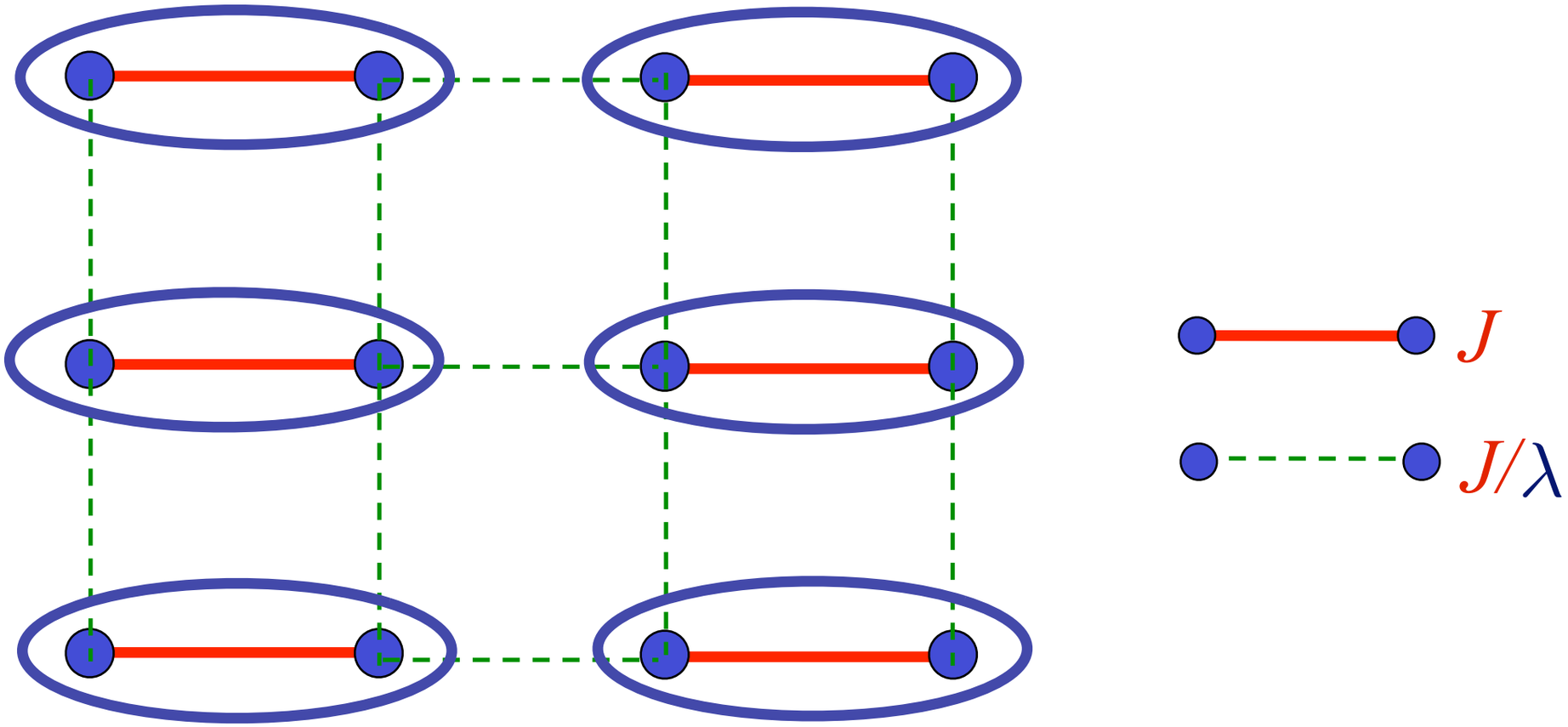

Ground state is a "quantum paramagnet"
with spins locked in valence bond singlets

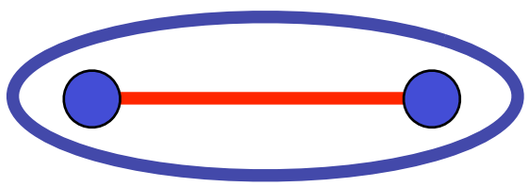

$$= \frac{1}{\sqrt{2}} \left(\left| \uparrow\downarrow \right\rangle - \left| \downarrow\uparrow \right\rangle \right)$$

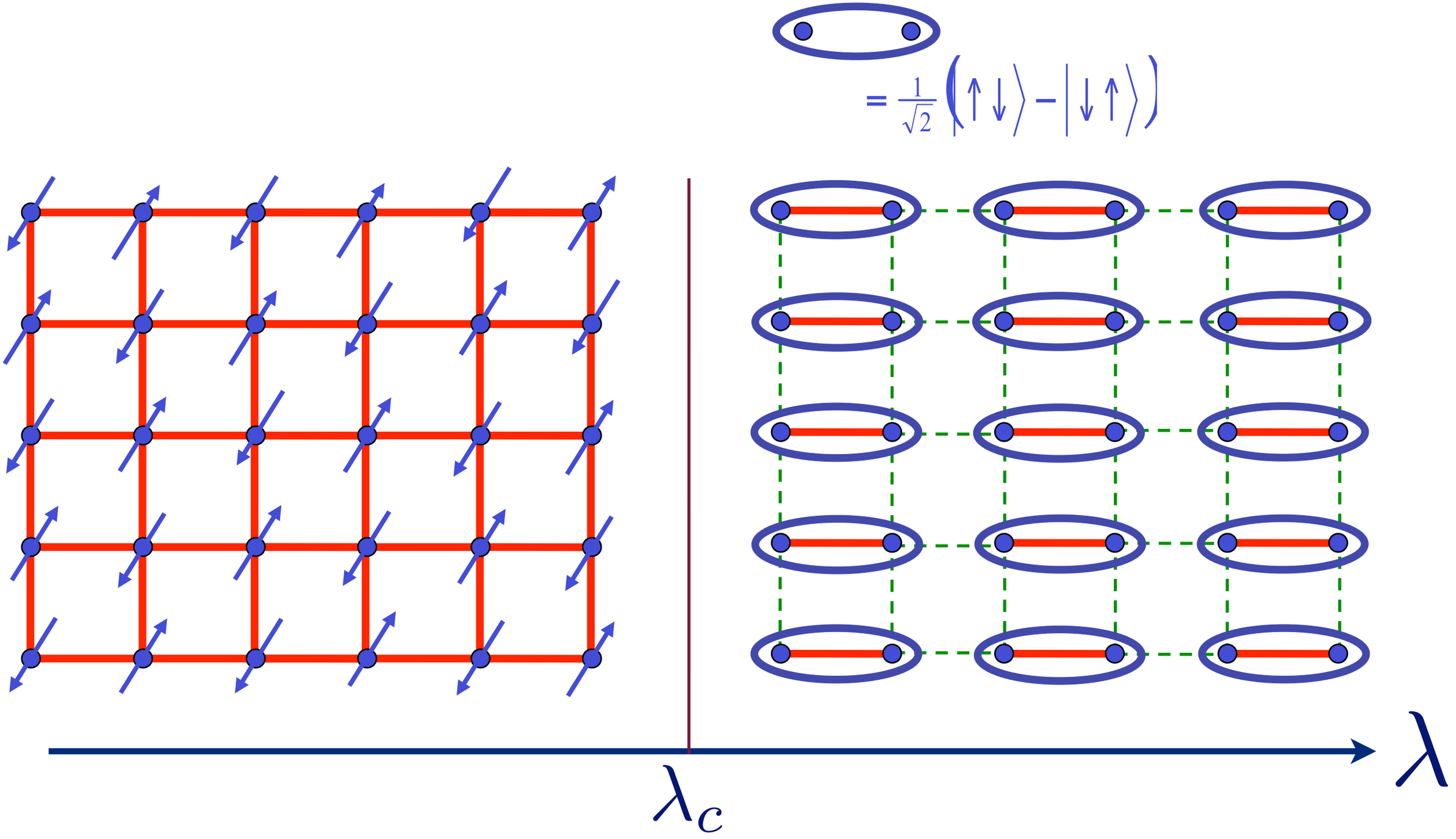

Pressure in $TlCuCl_3$

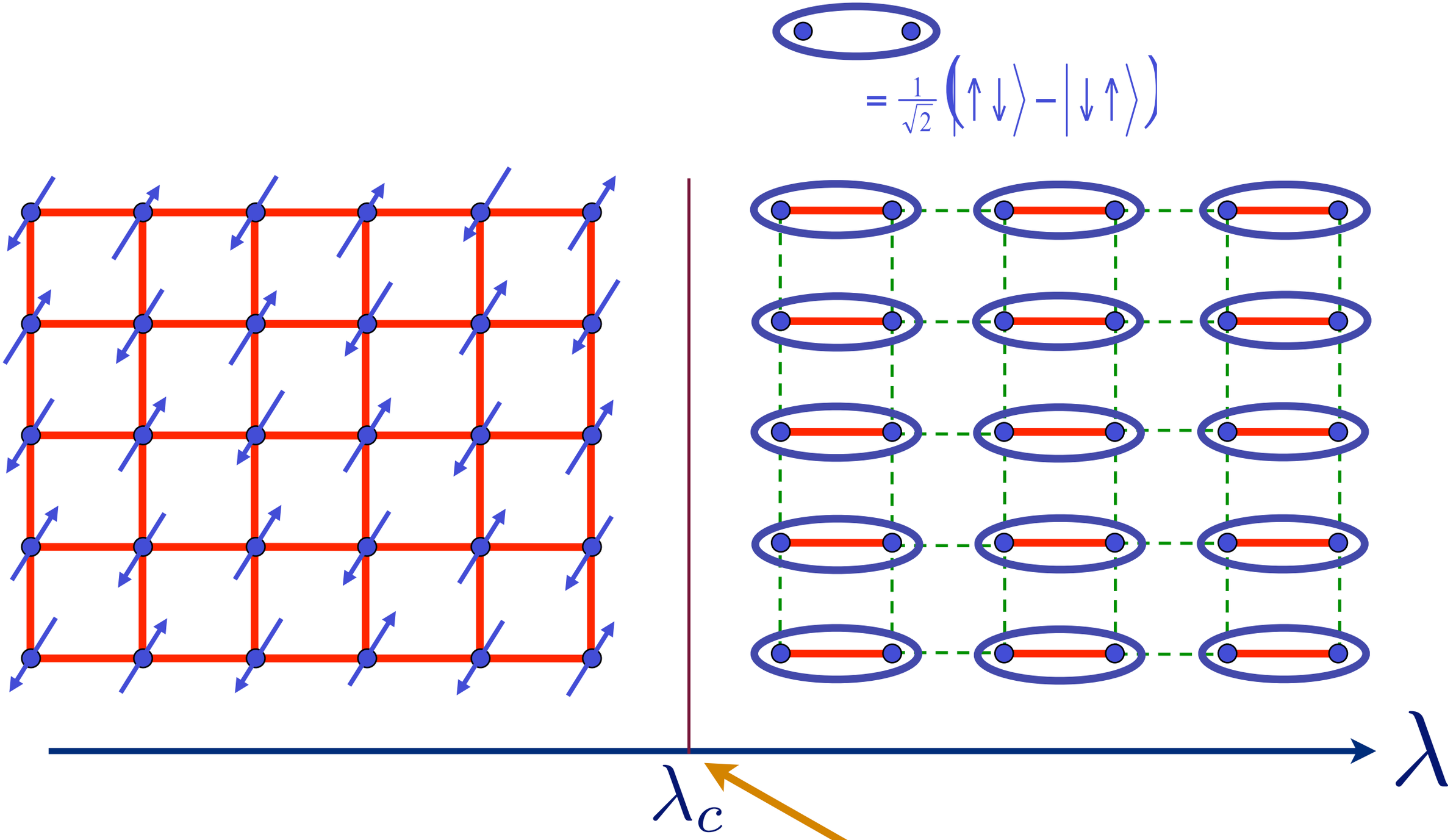

Quantum critical point with non-local entanglement in spin wavefunction

Excitation spectrum in the paramagnetic phase

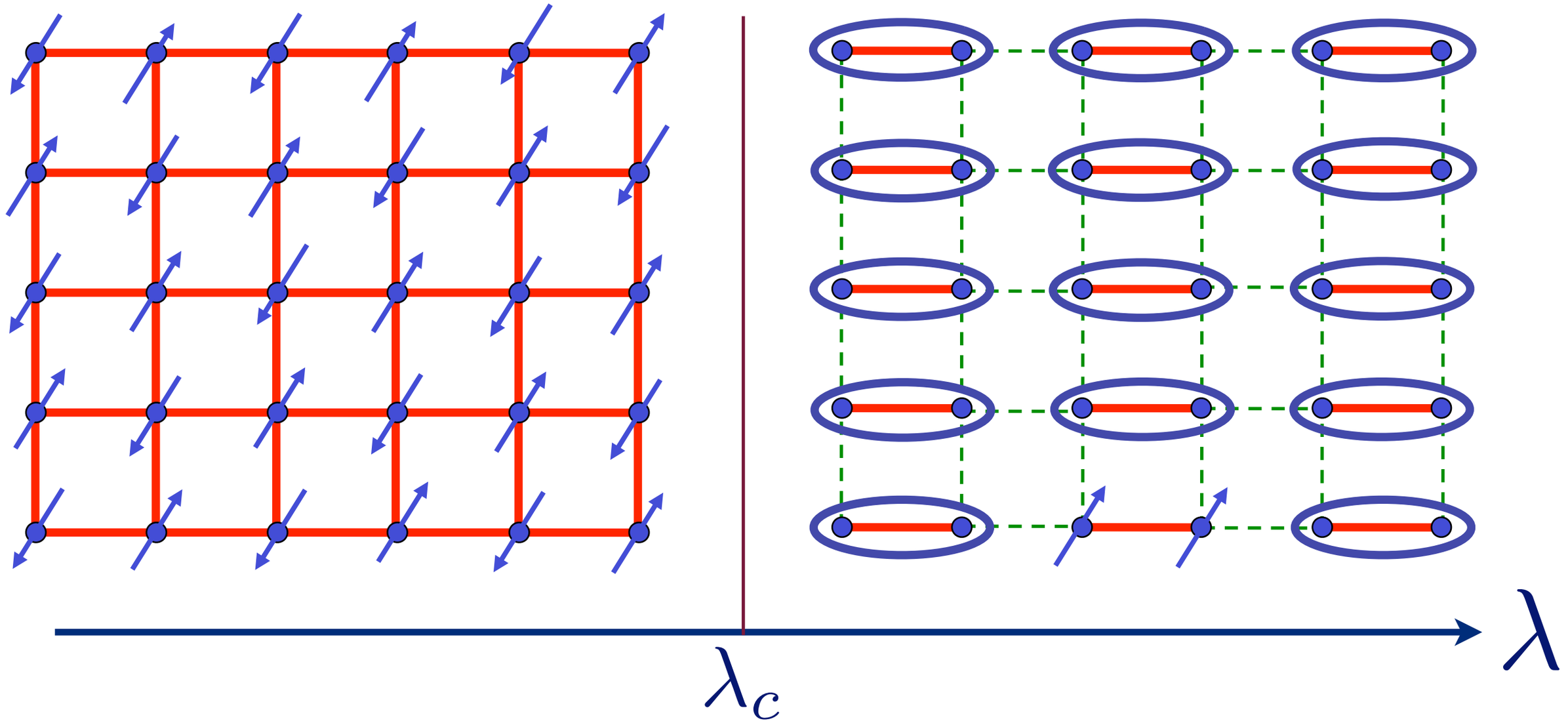

Excitation spectrum in the paramagnetic phase

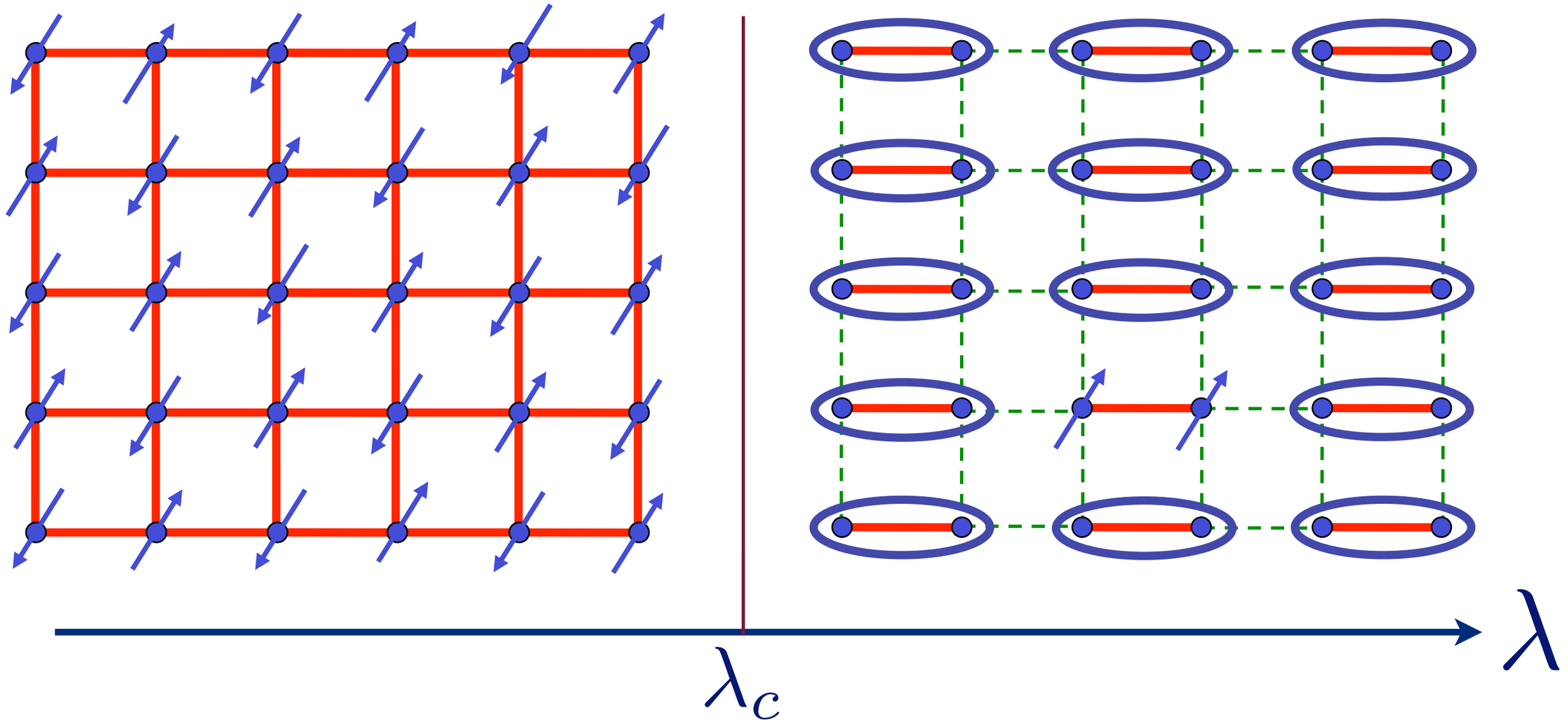

Excitation spectrum in the paramagnetic phase

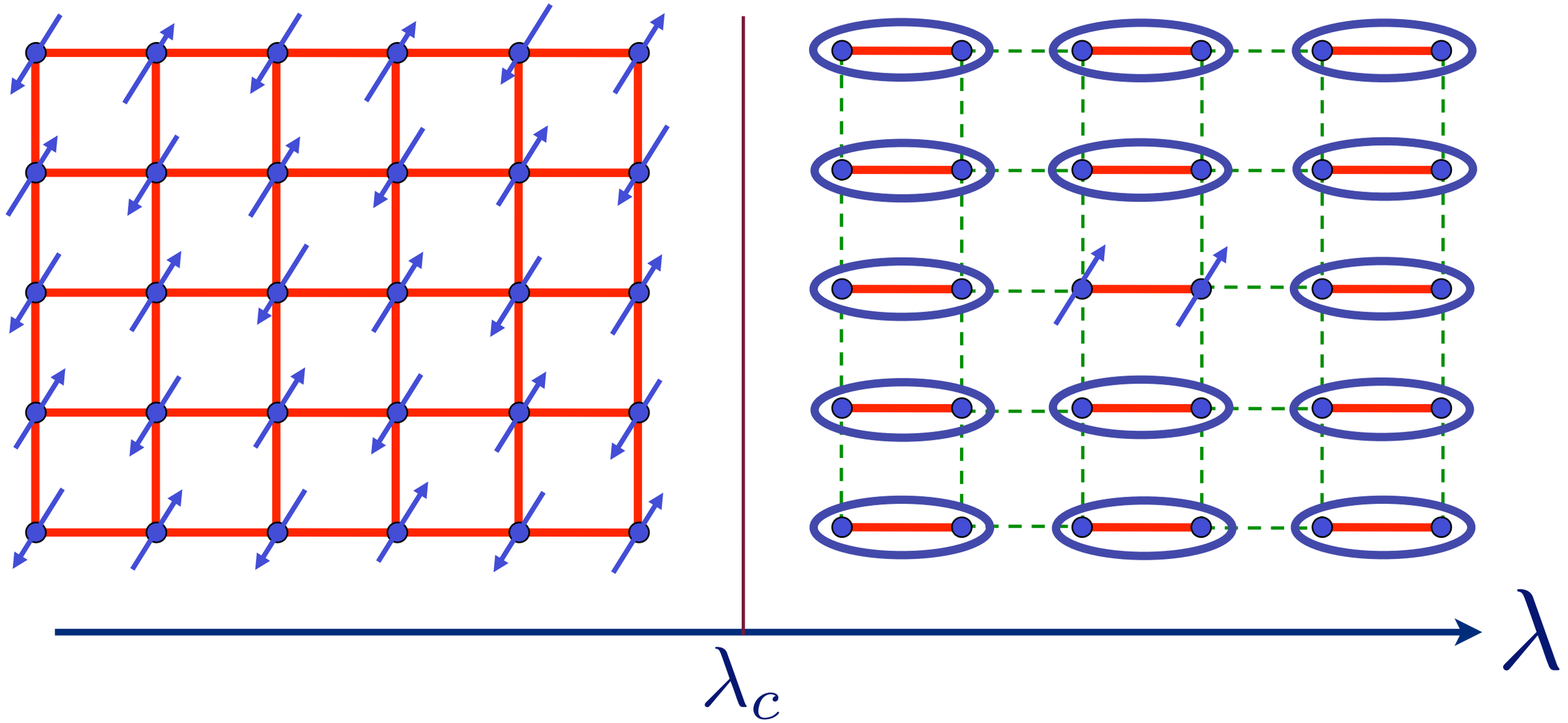

Excitation spectrum in the paramagnetic phase

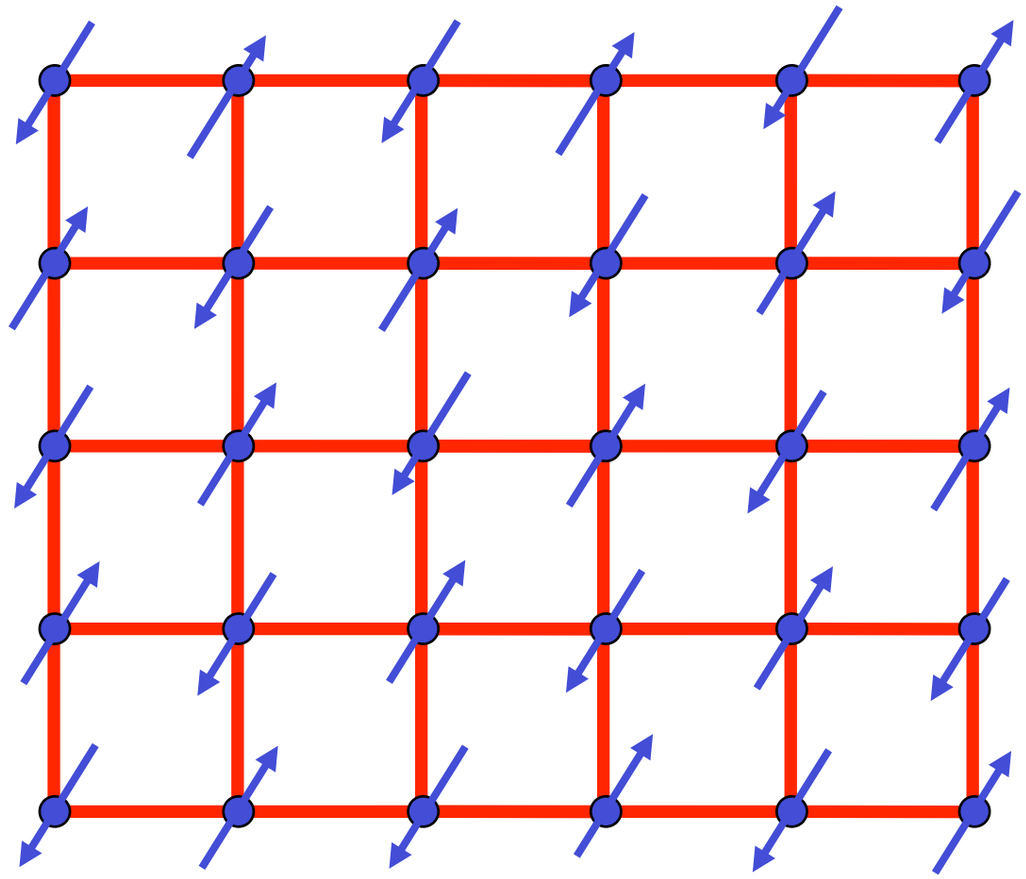

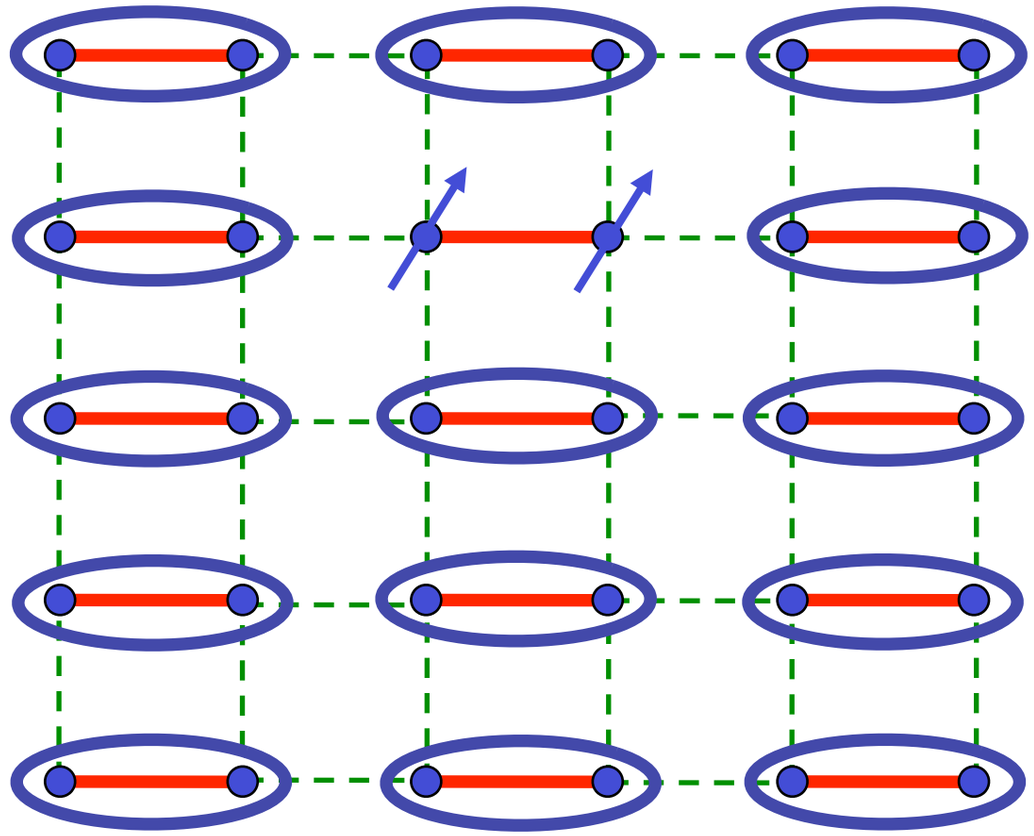

λ_c

λ

Excitation spectrum in the paramagnetic phase

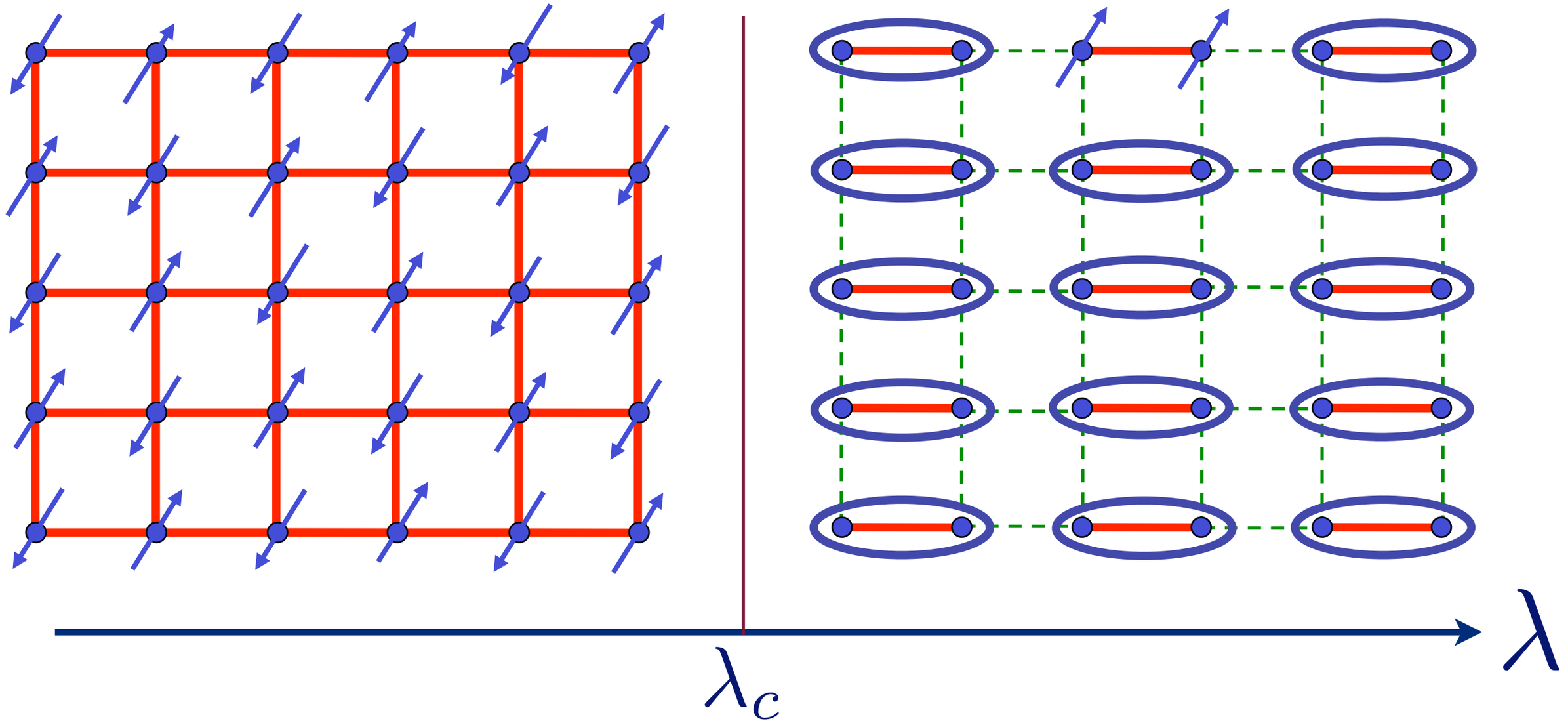

$TlCuCl_3$ at ambient pressure

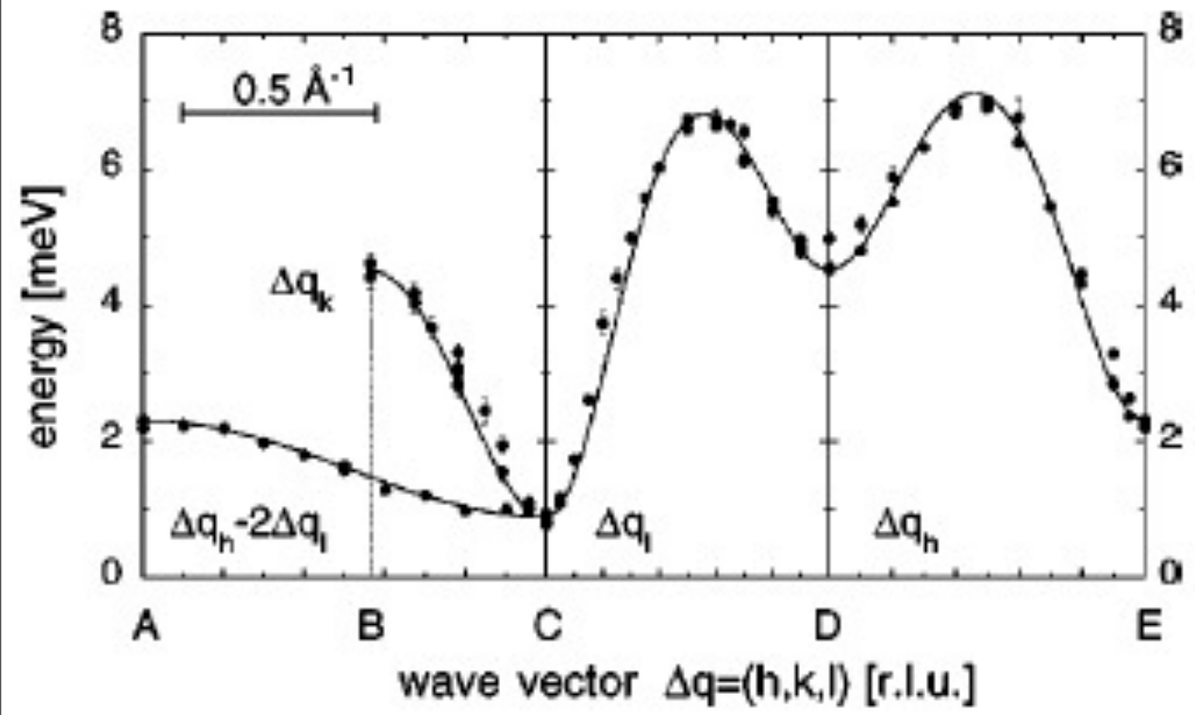

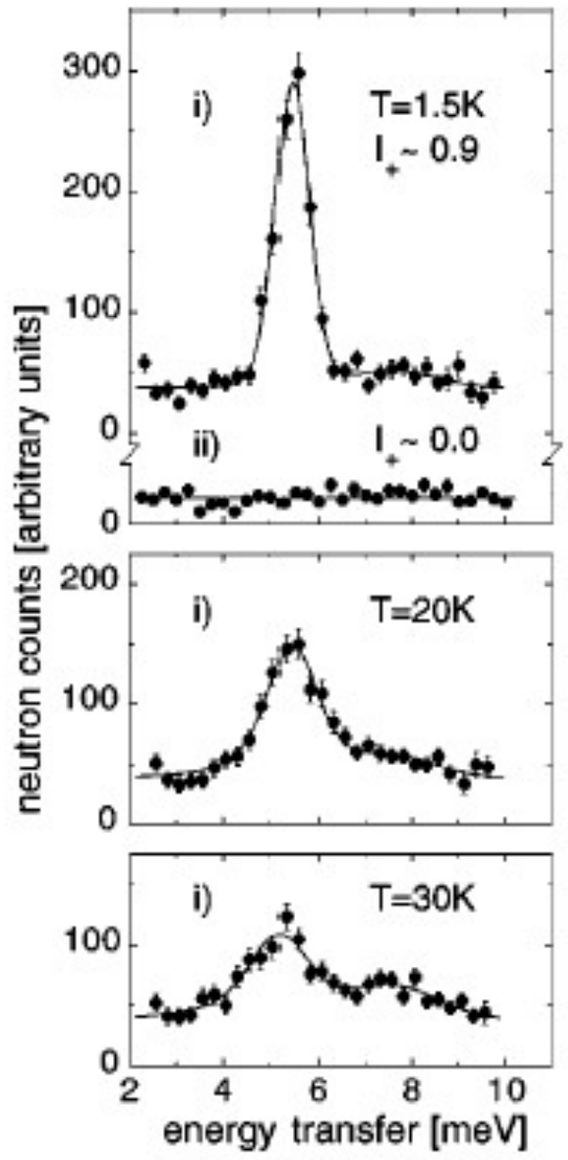

FIG. 1. Measured neutron profiles in the a^*c^* plane of $TlCuCl_3$ for $i=(1.35,0,0)$, $ii=(0,0,3.15)$ [r.l.u]. The spectrum at $T=1.5$ K

N. Cavadini, G. Heigold, W. Henggeler, A. Furrer, H.-U. Güdel, K. Krämer and H. Mutka, *Phys. Rev.* B 63 172414 (2001).

$TlCuCl_3$ at ambient pressure

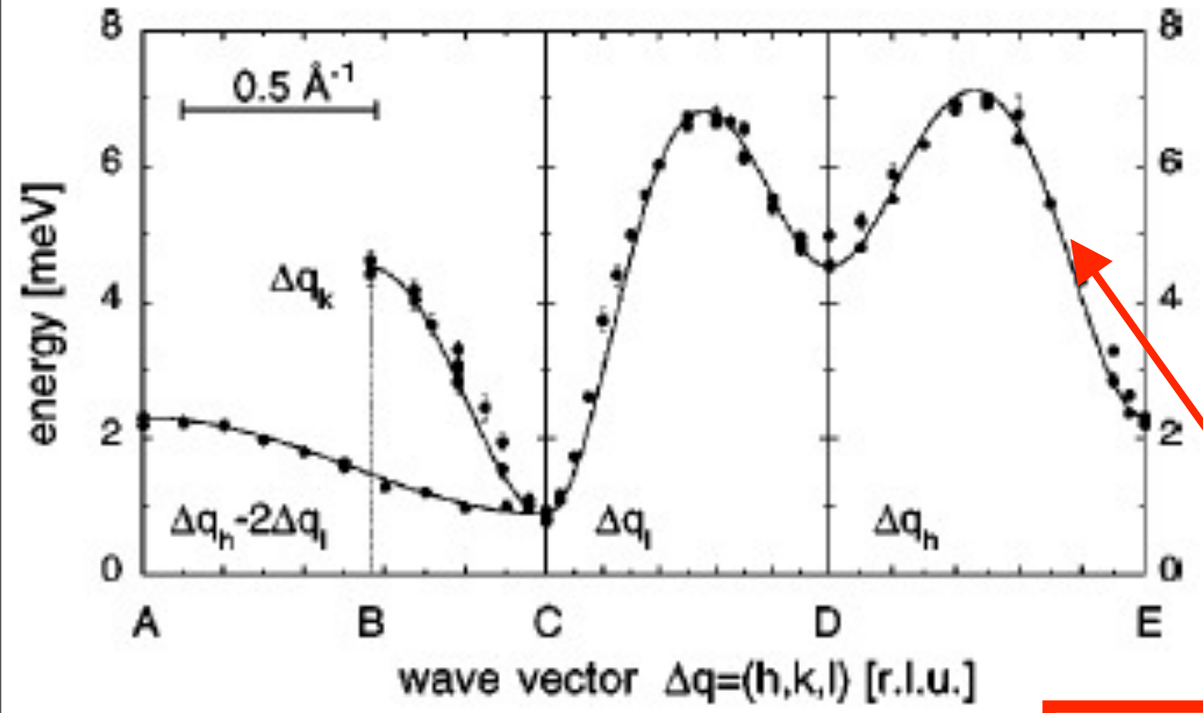

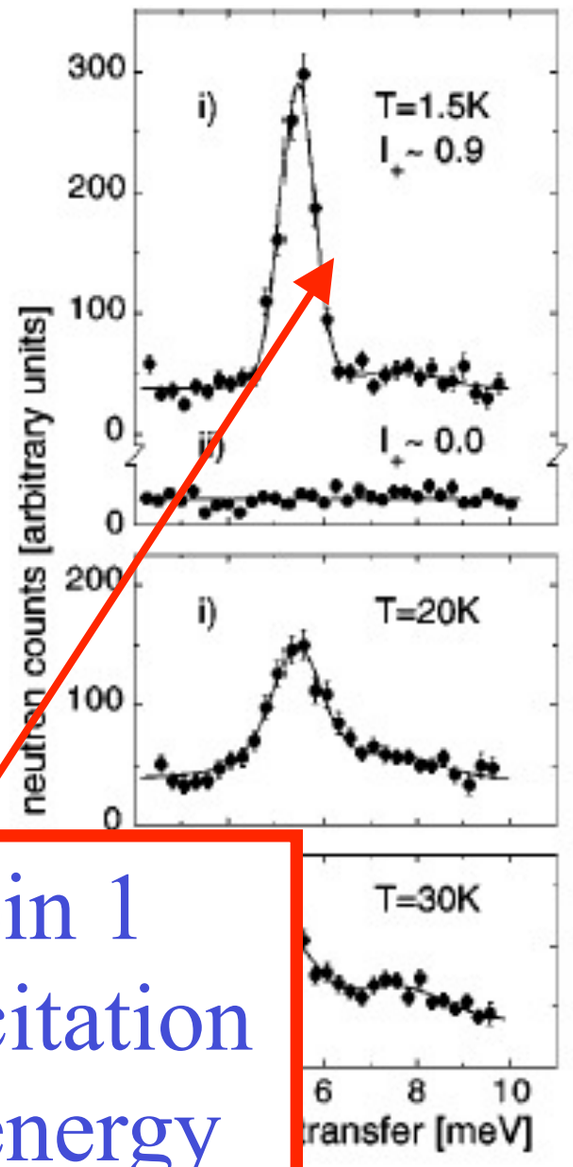

Sharp spin 1 particle excitation above an energy gap (spin gap)

...les in the a^*c^* plane of $TlCuCl_3$ ...r.l.u]. The spectrum at $T = 1.5$ K

N. Cavadini, G. Heigold, W. Henggeler, A. Furrer, H.-U. Güdel, K. Krämer and H. Mutka, *Phys. Rev.* B 63 172414 (2001).

Excitation spectrum in the Néel phase

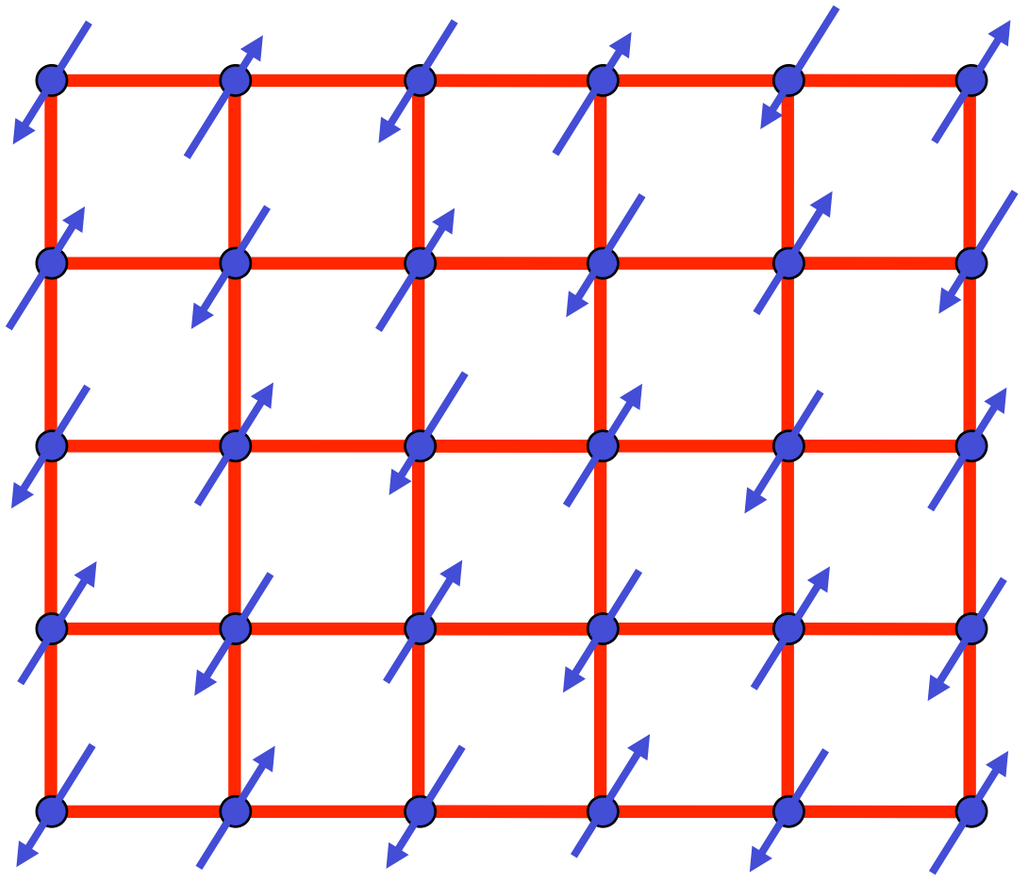

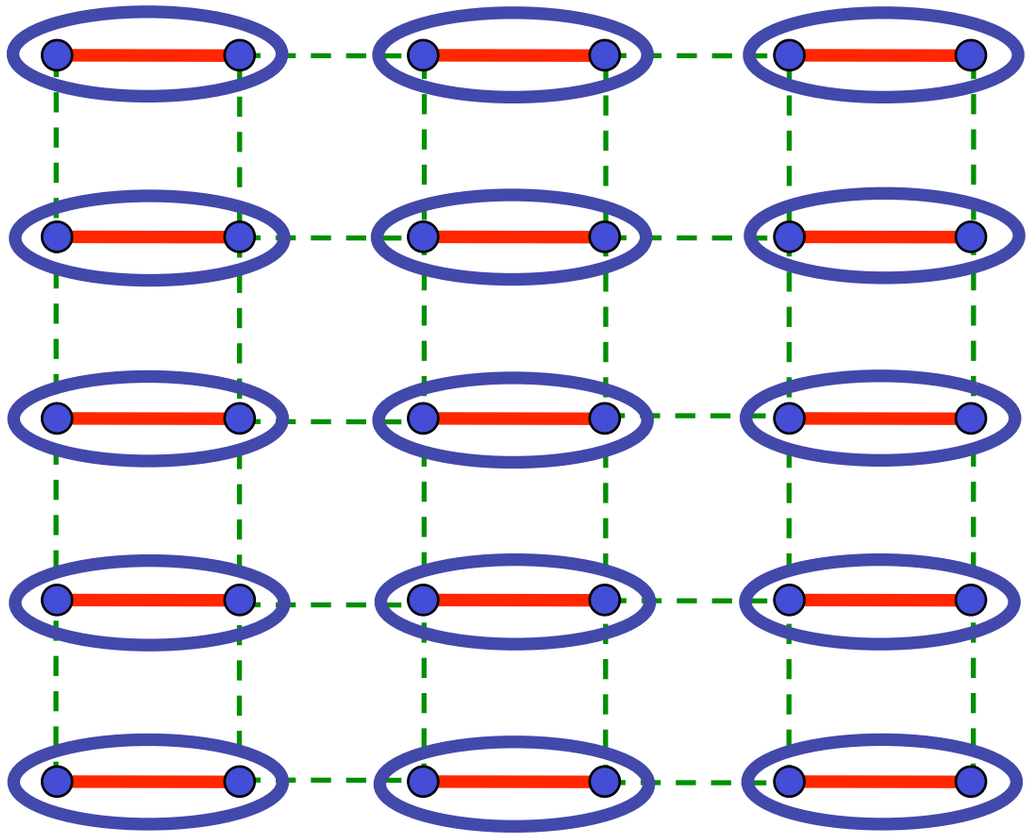

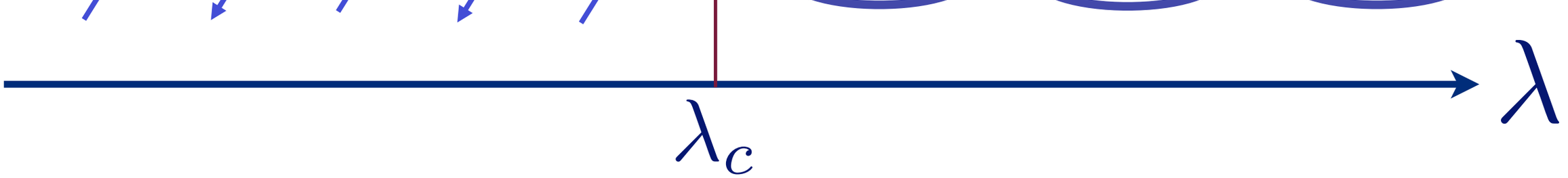

Excitation spectrum in the Néel phase

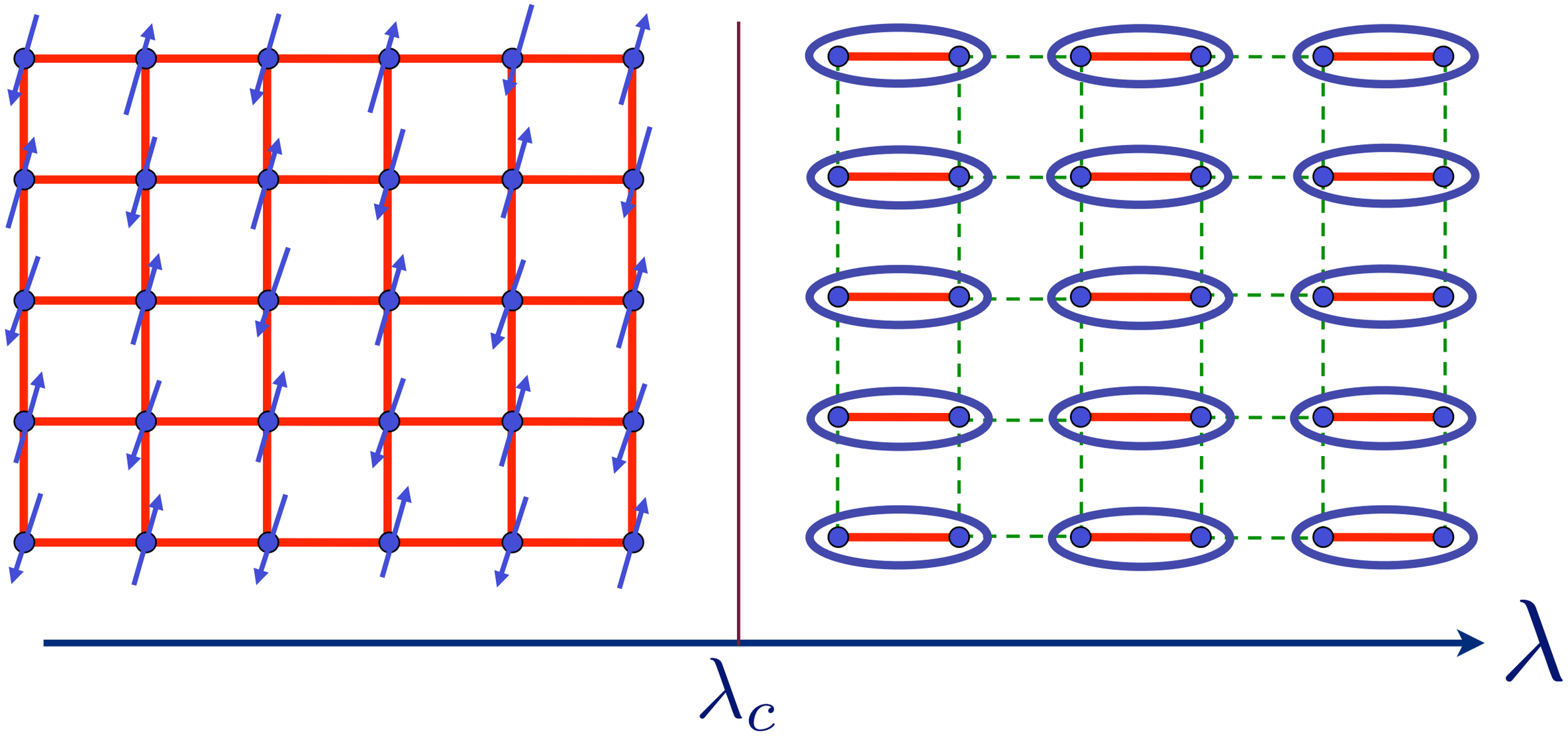

Spin waves

Excitation spectrum in the Néel phase

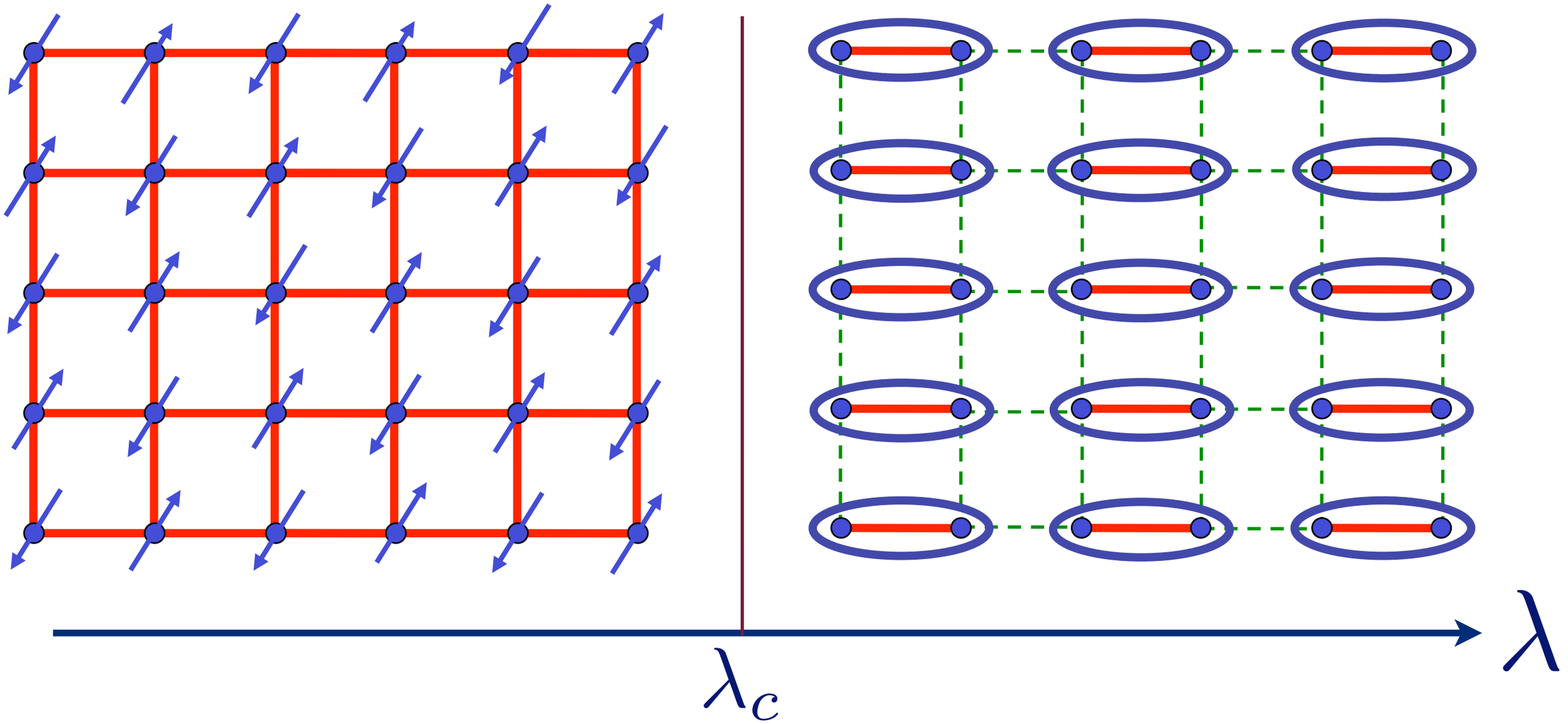

Spin waves

Description using Landau-Ginzburg field theory

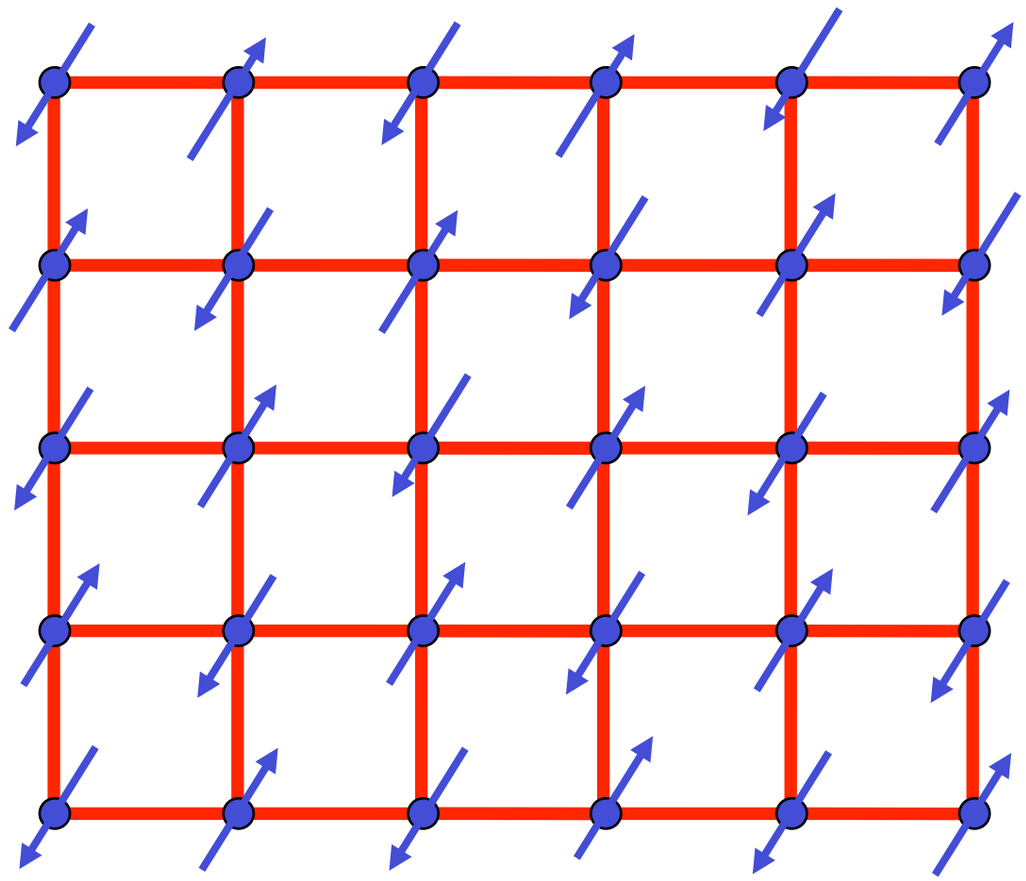

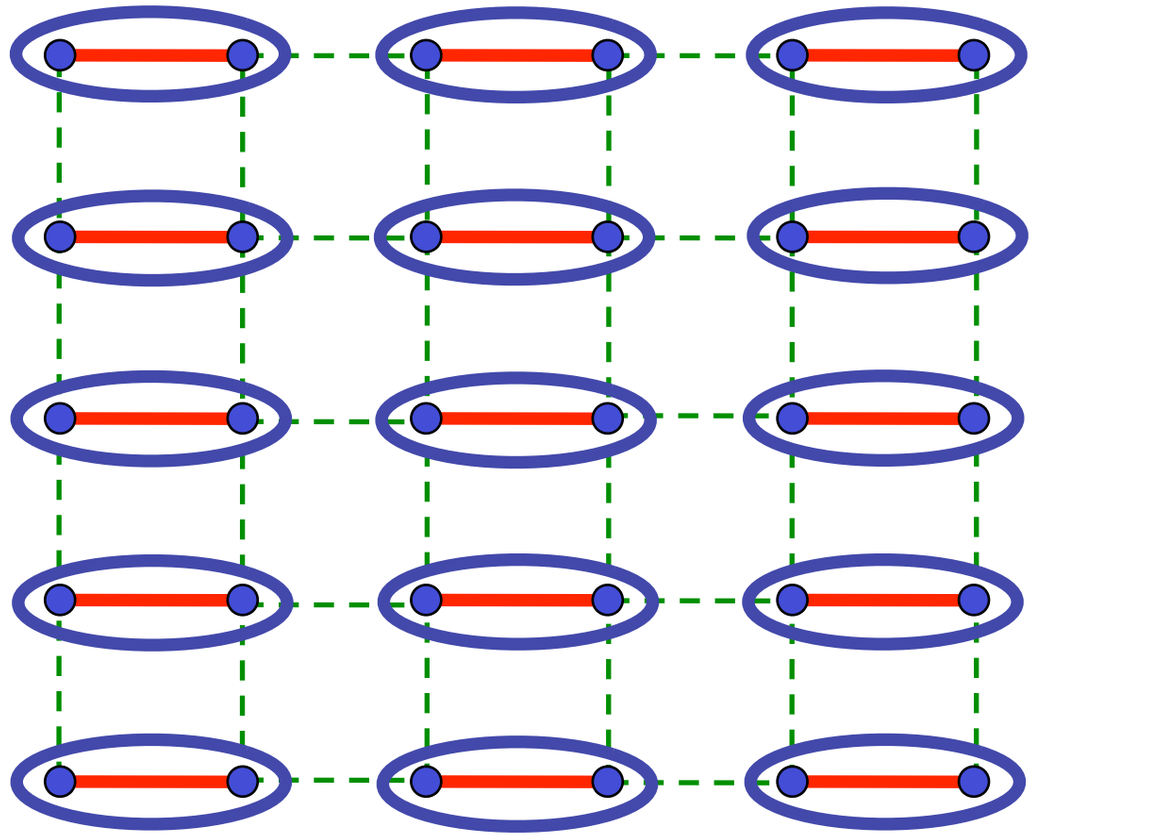

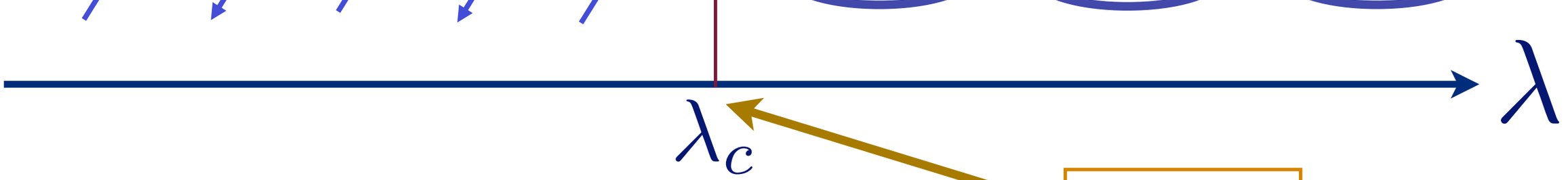

O(3) order parameter $\vec{\varphi}$

$$\mathcal{S} = \int d^2 r d\tau \left[(\partial_\tau \varphi)^2 + c^2 (\nabla_r \vec{\varphi})^2 + (\lambda - \lambda_c)\vec{\varphi}^2 + u\left(\vec{\varphi}^2\right)^2 \right]$$

Excitation spectrum in the paramagnetic phase

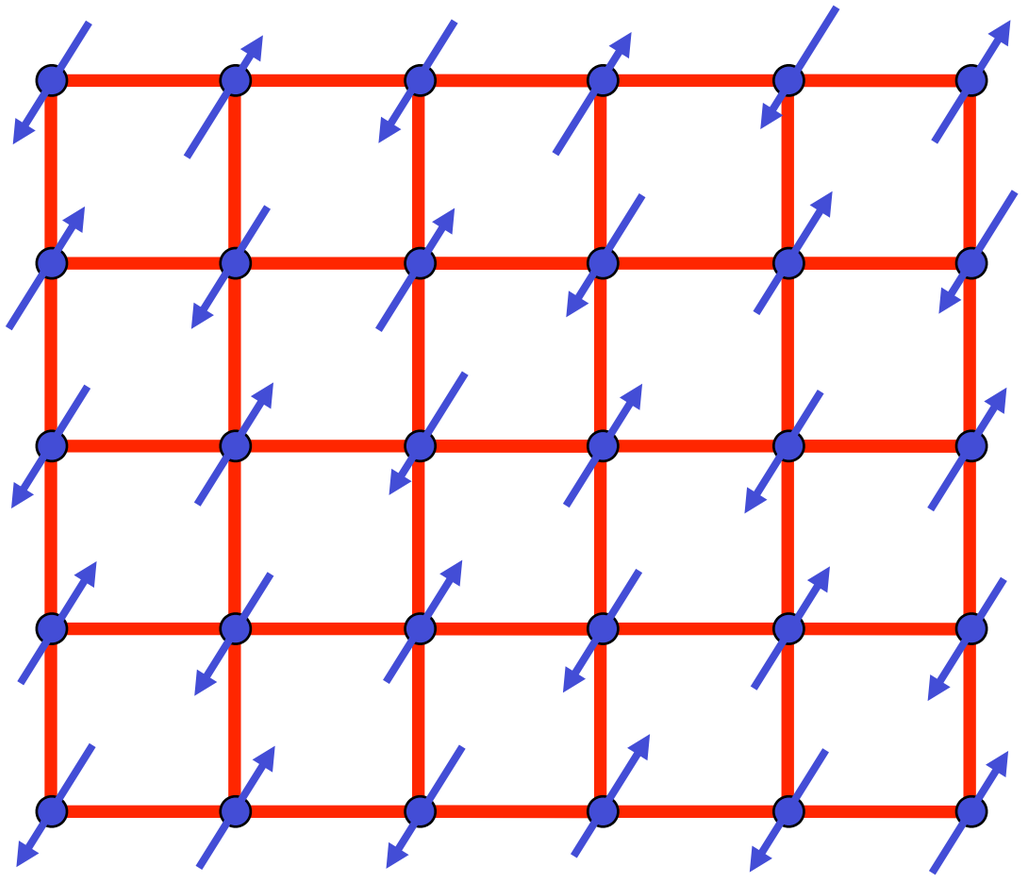

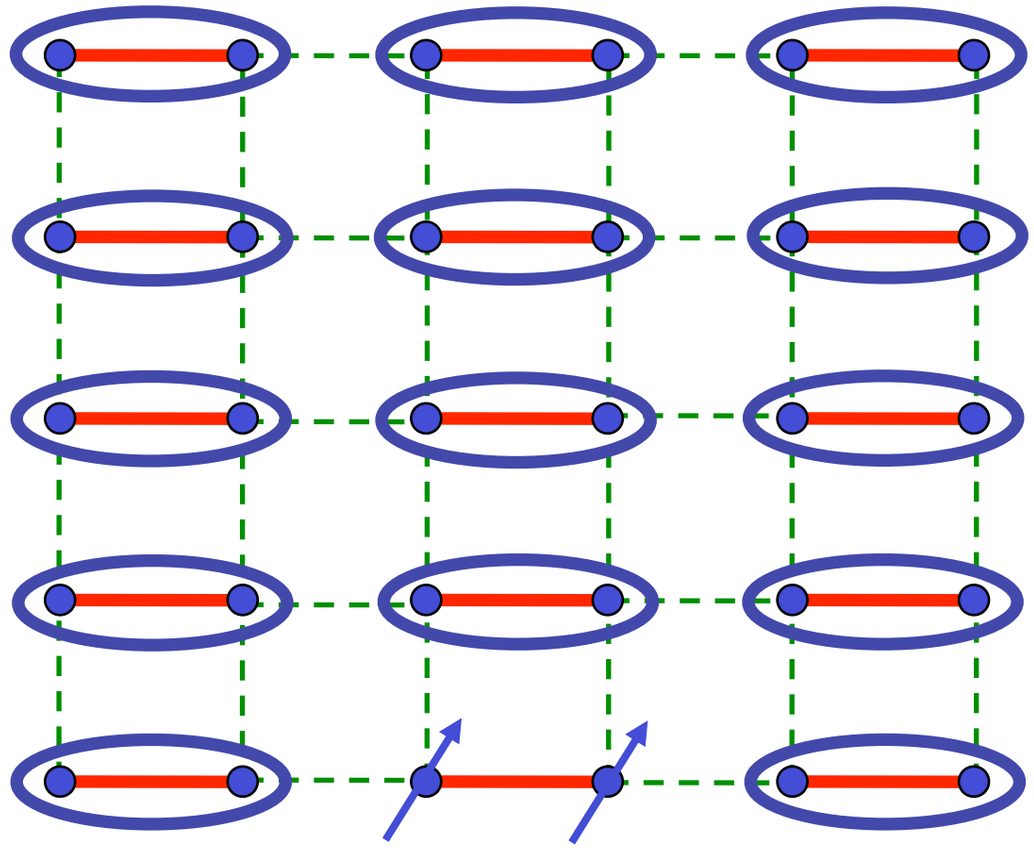

λ

λ_c

$$V(\vec{\varphi}) = (\lambda - \lambda_c)\vec{\varphi}^2 + u\left(\vec{\varphi}^2\right)^2$$

$$\lambda > \lambda_c$$

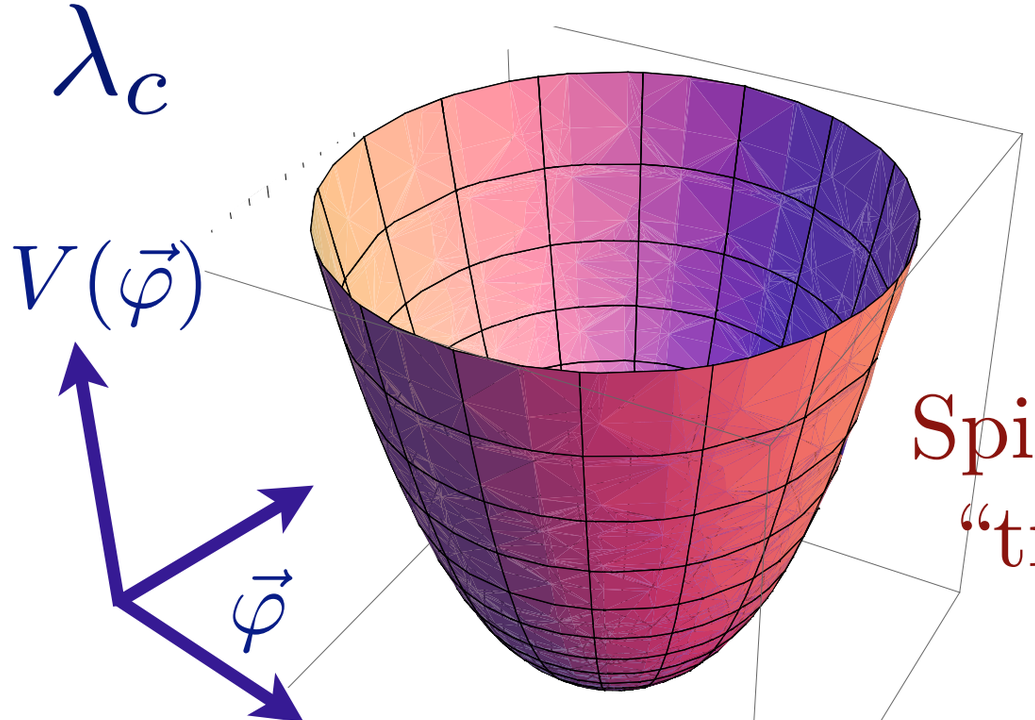

Spin $S = 1$
"triplon"

Excitation spectrum in the paramagnetic phase

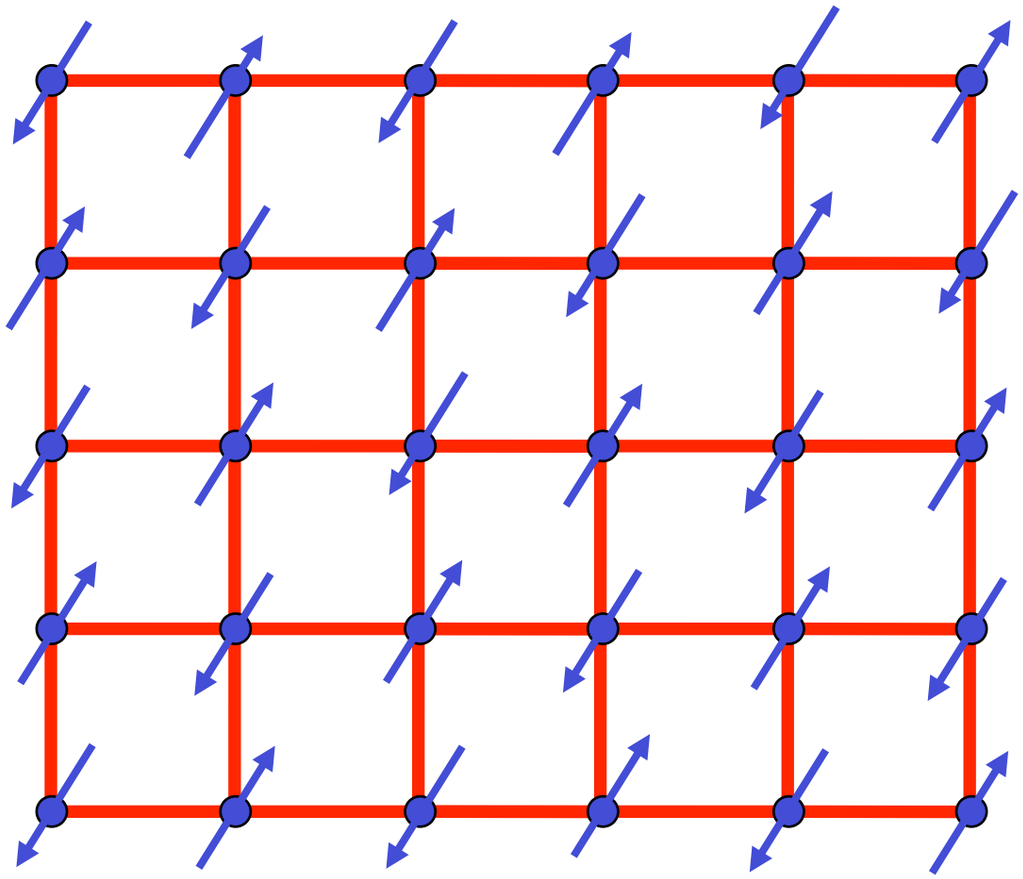

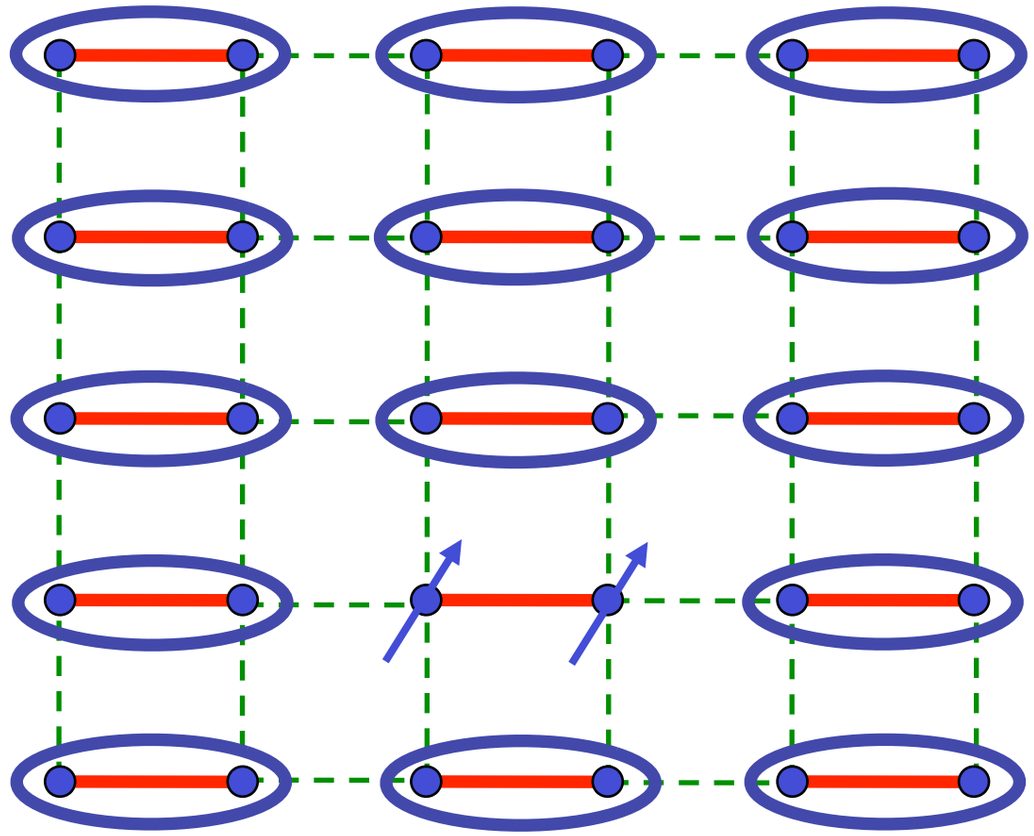

$$V(\vec{\varphi}) = (\lambda - \lambda_c)\vec{\varphi}^2 + u\left(\vec{\varphi}^2\right)^2$$

$$\lambda > \lambda_c$$

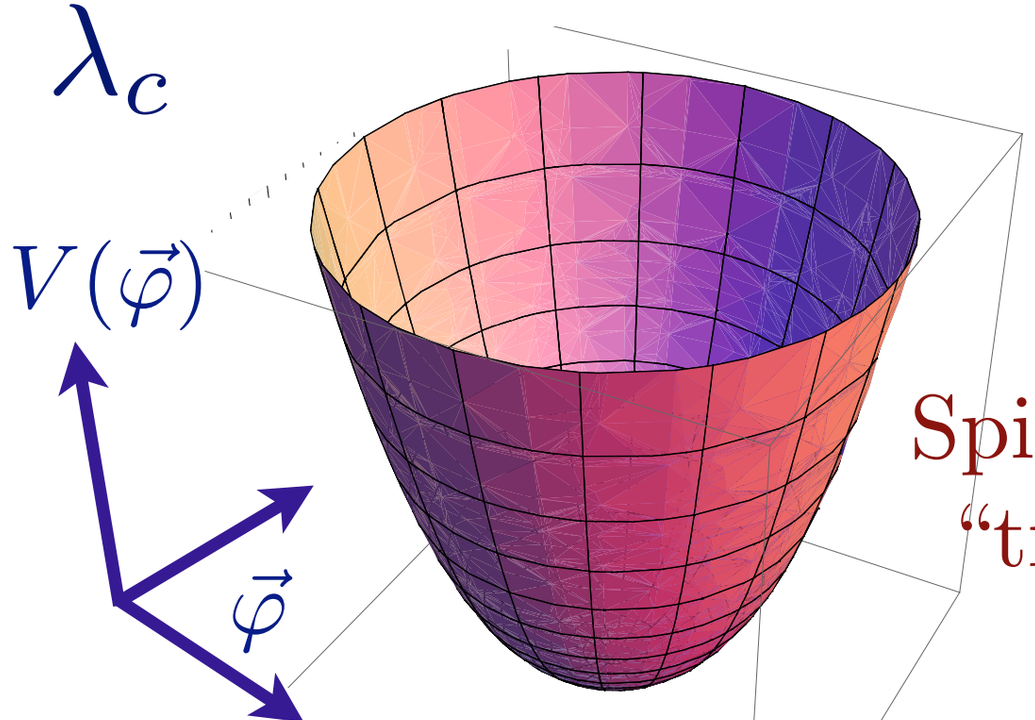

Spin $S = 1$
"triplon"

Excitation spectrum in the paramagnetic phase

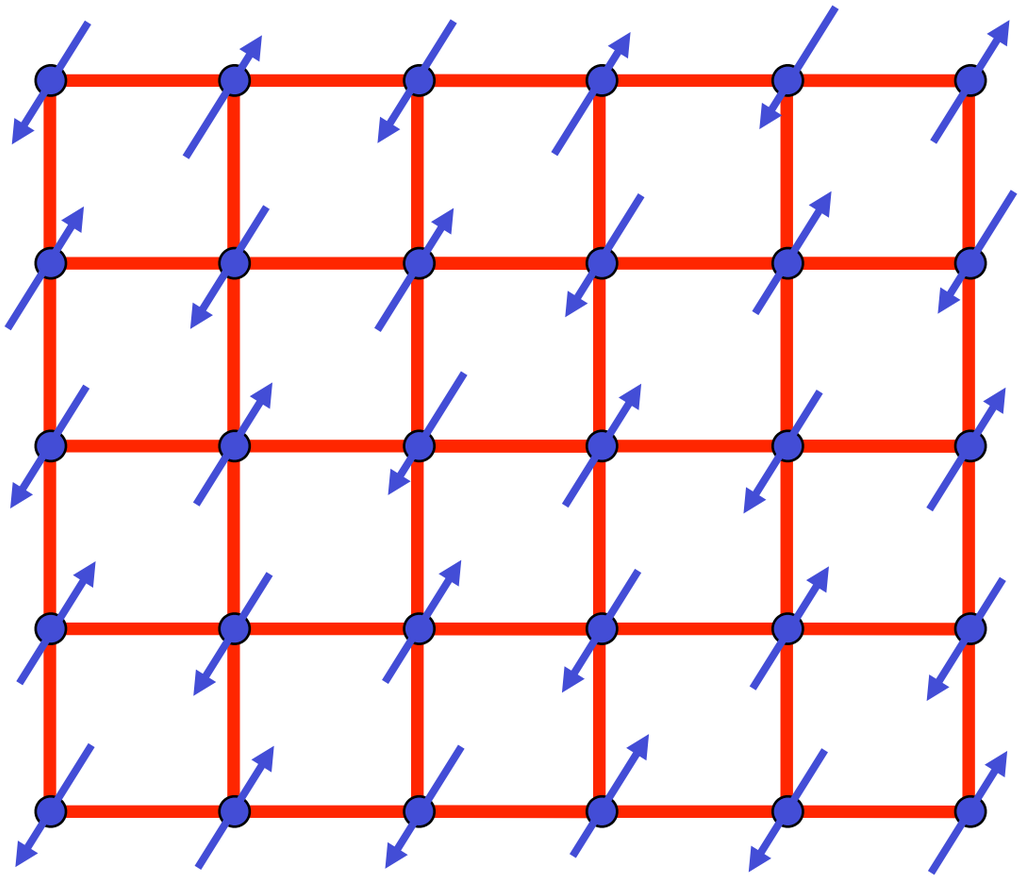

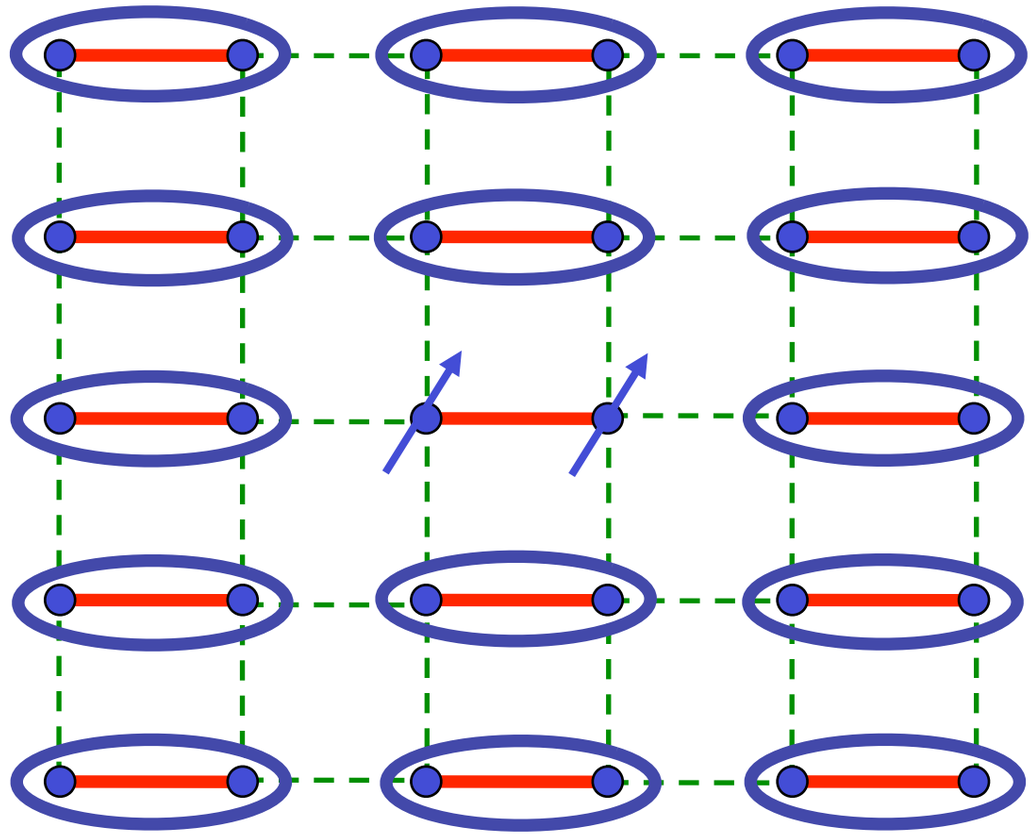

$$V(\vec{\varphi}) = (\lambda - \lambda_c)\vec{\varphi}^2 + u\left(\vec{\varphi}^2\right)^2$$

$$\lambda > \lambda_c$$

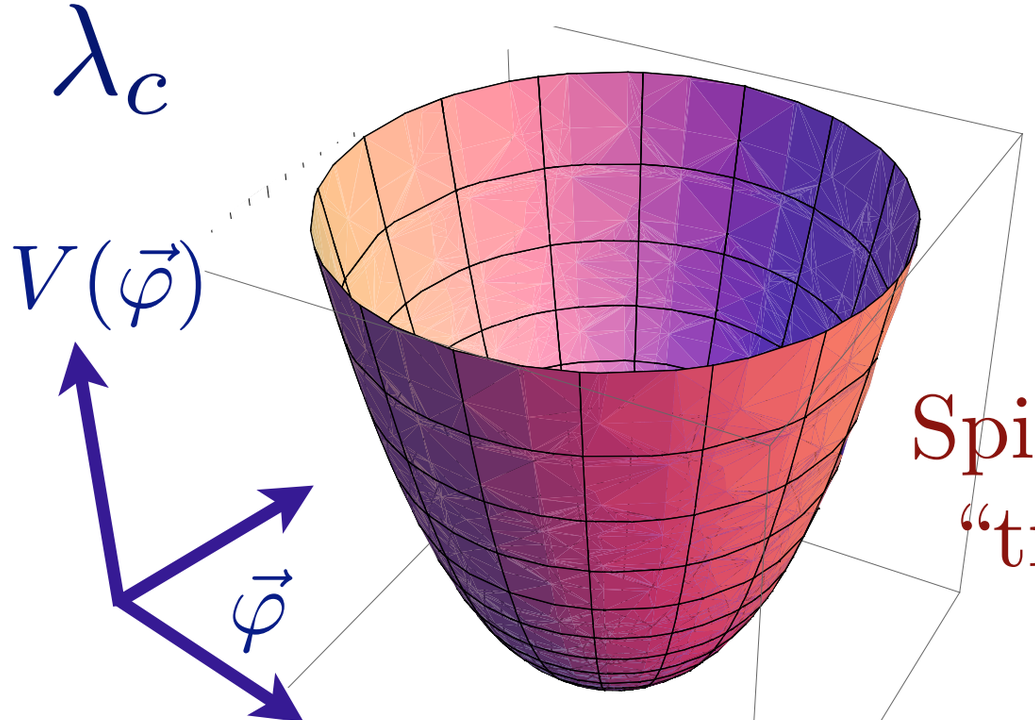

Spin $S = 1$
"triplon"

Excitation spectrum in the paramagnetic phase

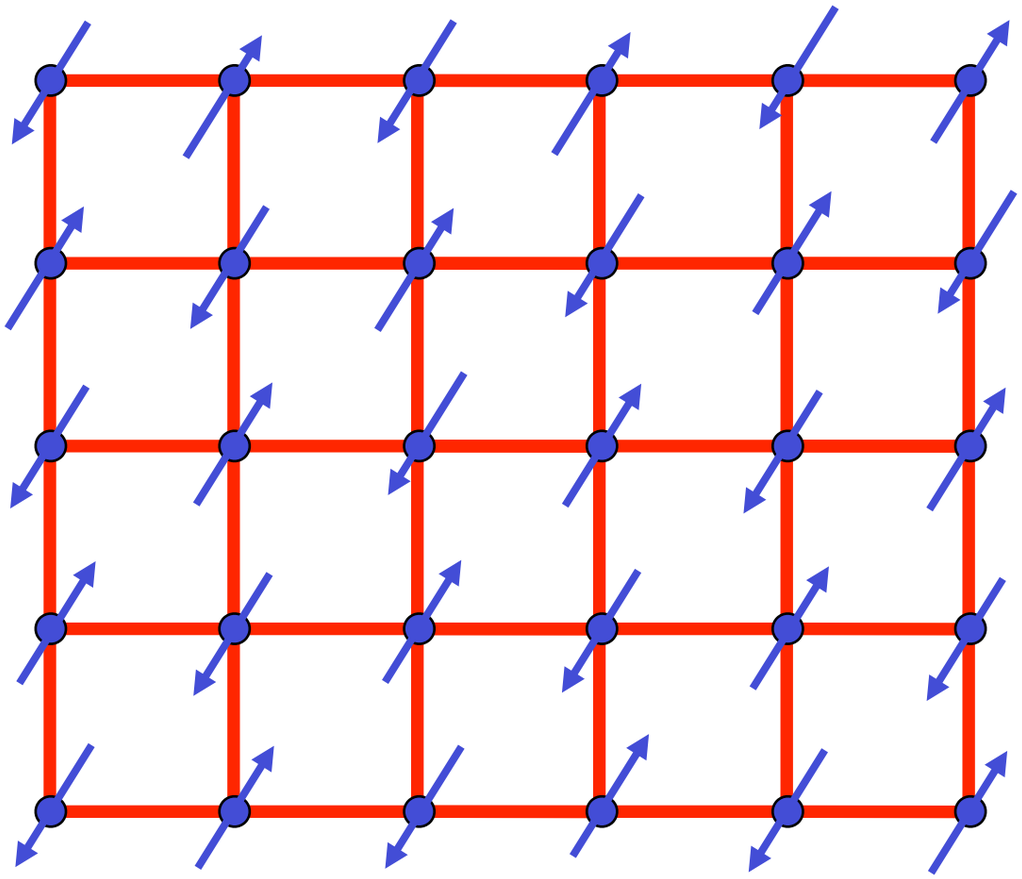

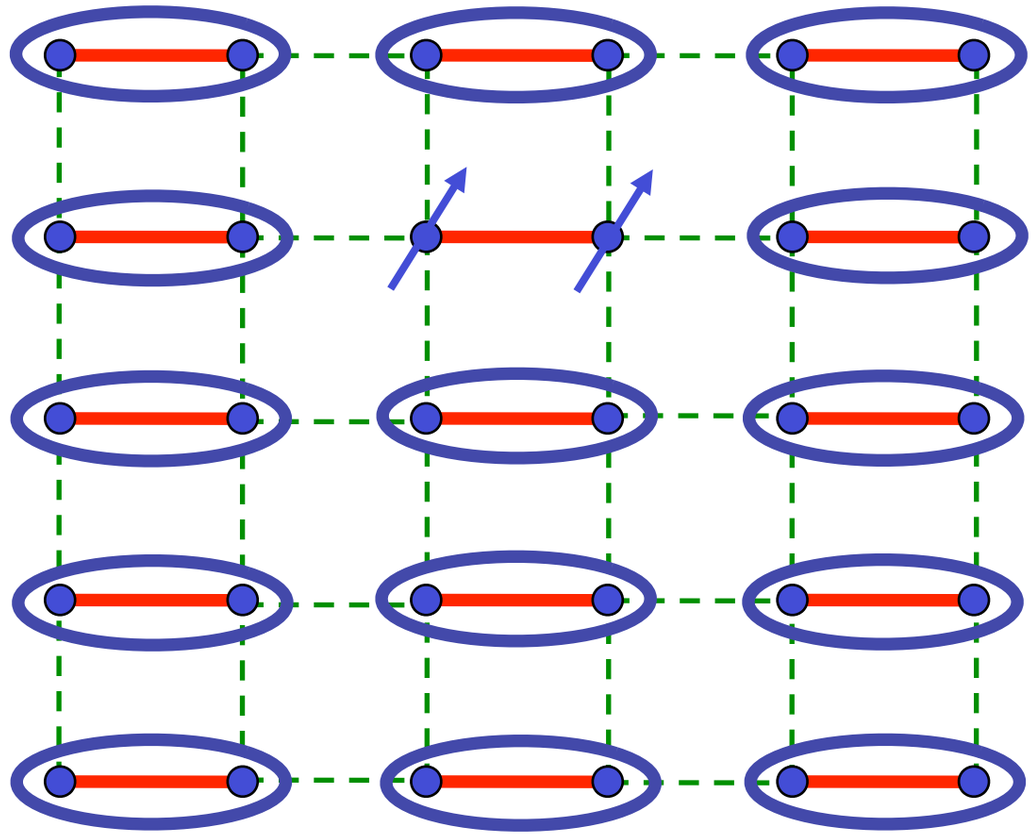

$$V(\vec{\varphi}) = (\lambda - \lambda_c)\vec{\varphi}^2 + u\left(\vec{\varphi}^2\right)^2$$

$$\lambda > \lambda_c$$

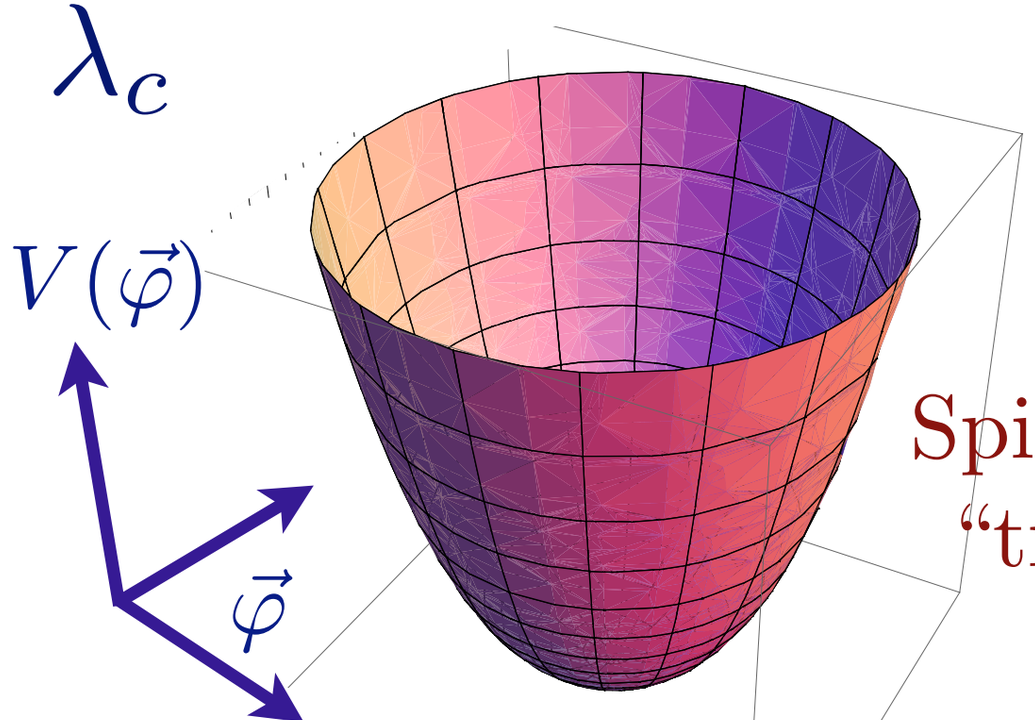

Spin $S = 1$
"triplon"

Excitation spectrum in the paramagnetic phase

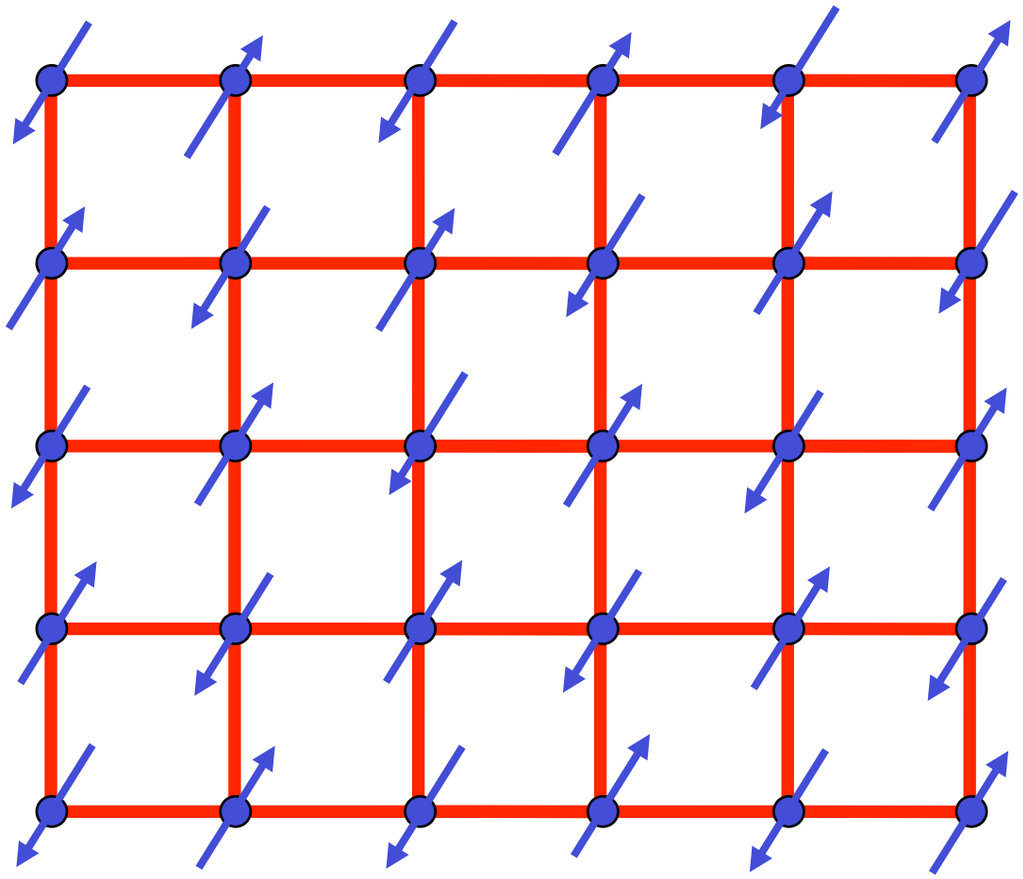

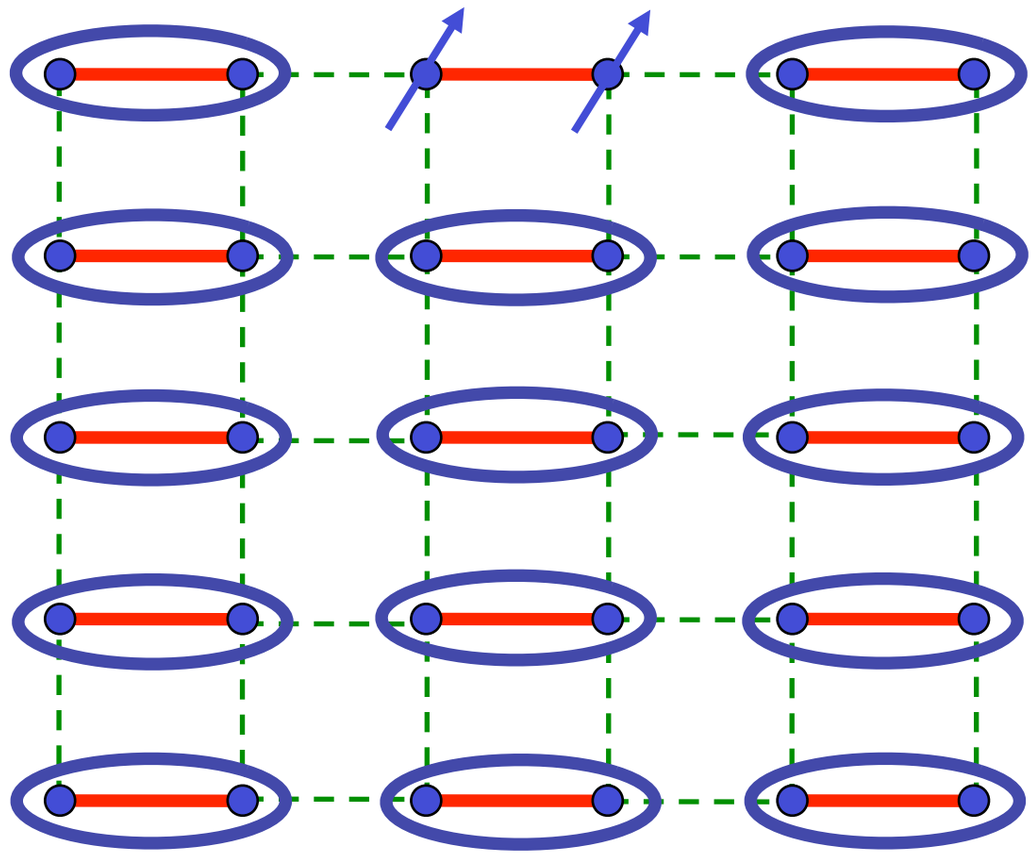

λ

λ_c

$$V(\vec{\varphi}) = (\lambda - \lambda_c)\vec{\varphi}^2 + u\left(\vec{\varphi}^2\right)^2$$

$$\lambda > \lambda_c$$

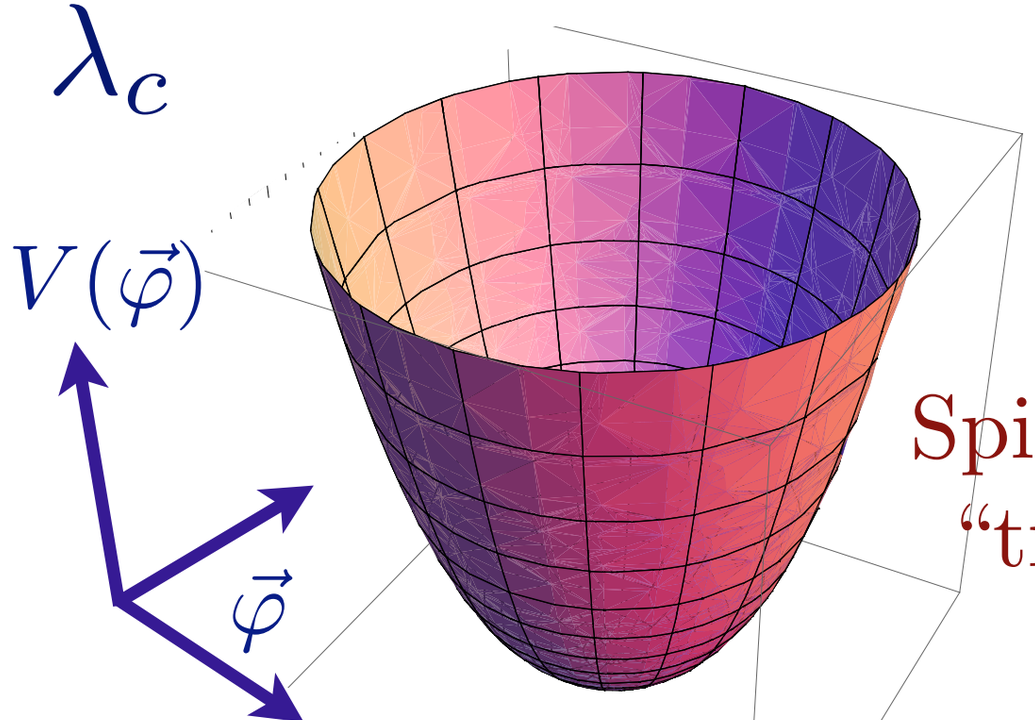

Spin $S = 1$
"triplon"

Excitation spectrum in the Néel phase

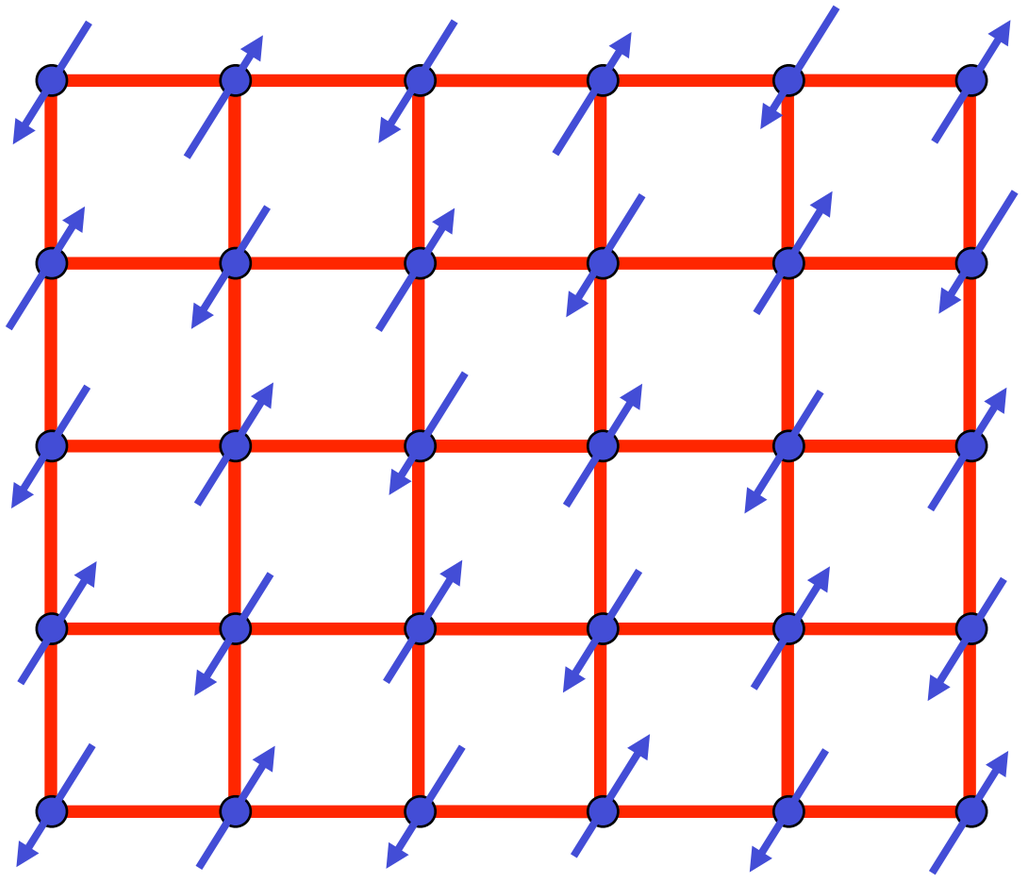

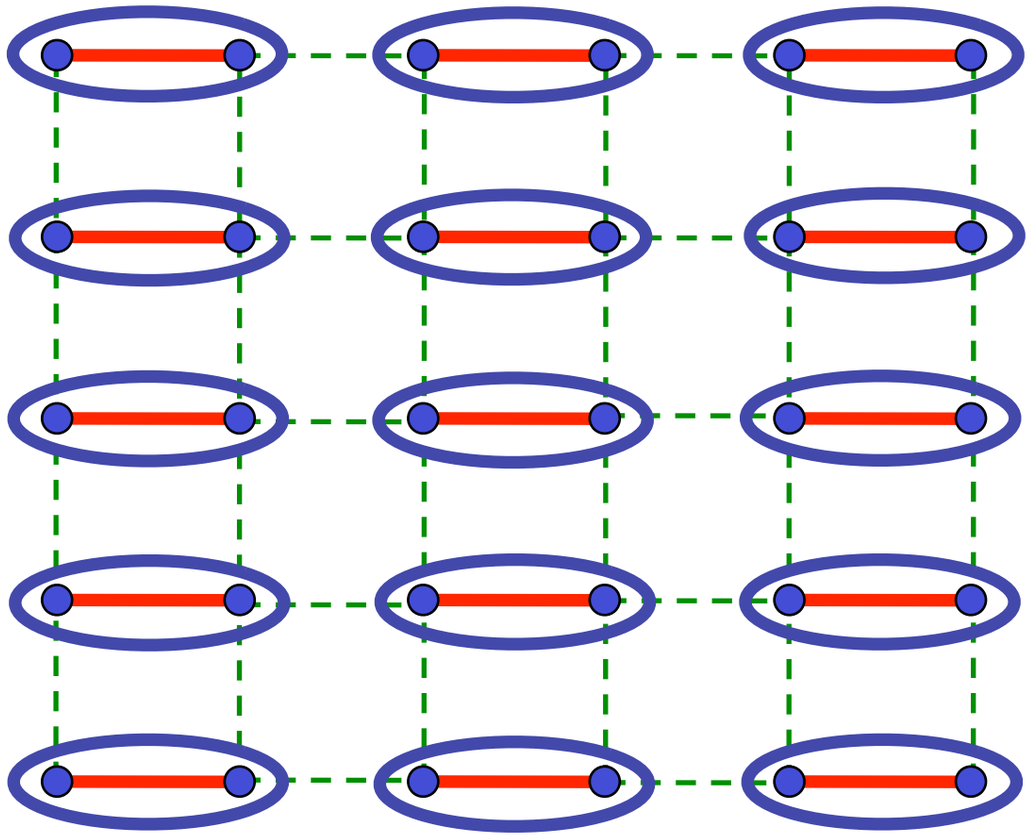

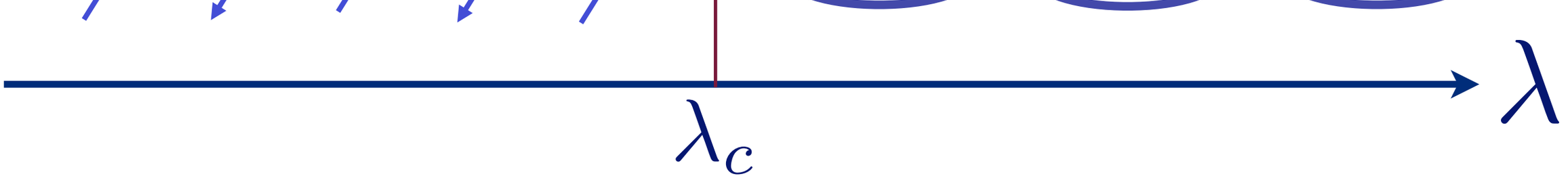

Excitation spectrum in the Néel phase

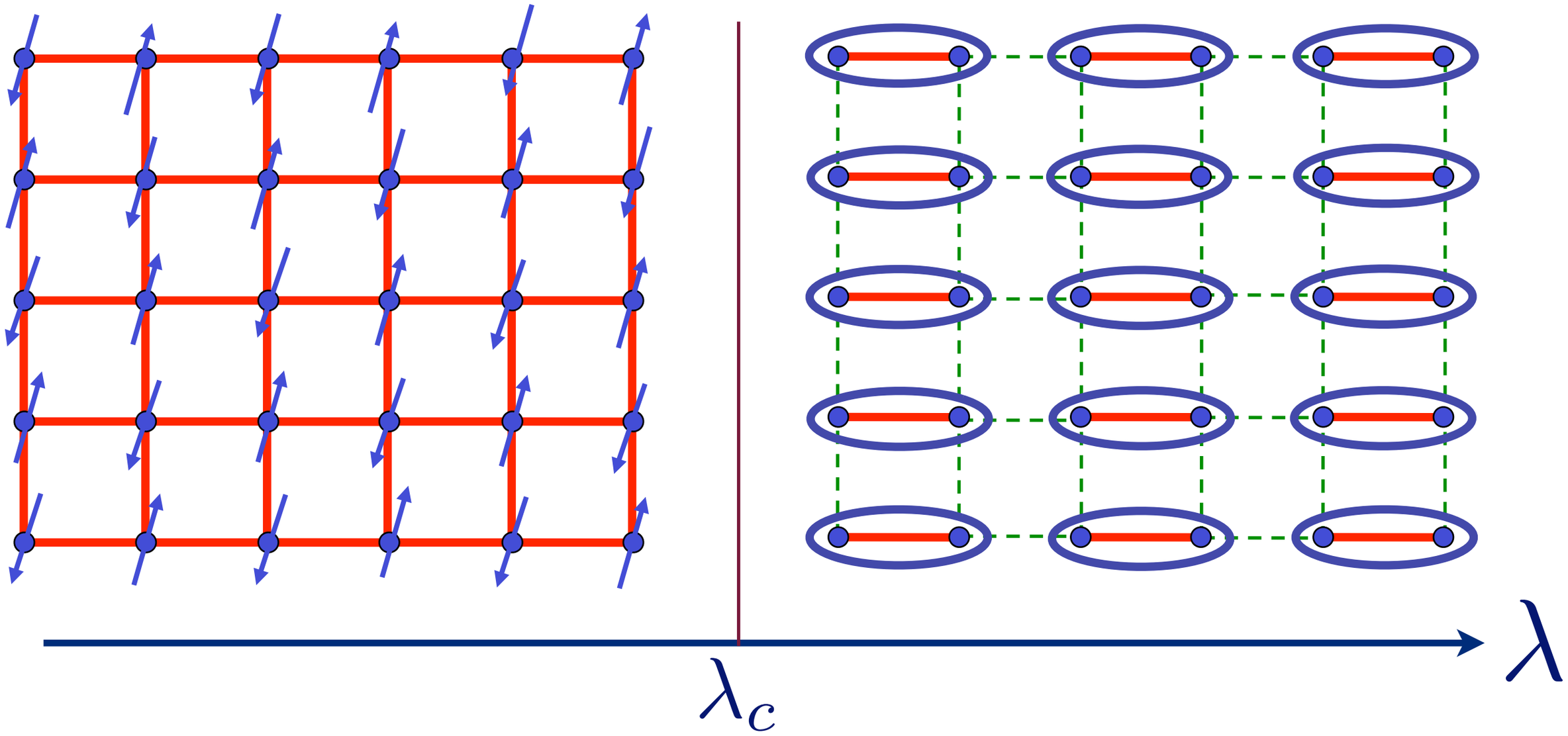

Spin waves

Excitation spectrum in the Néel phase

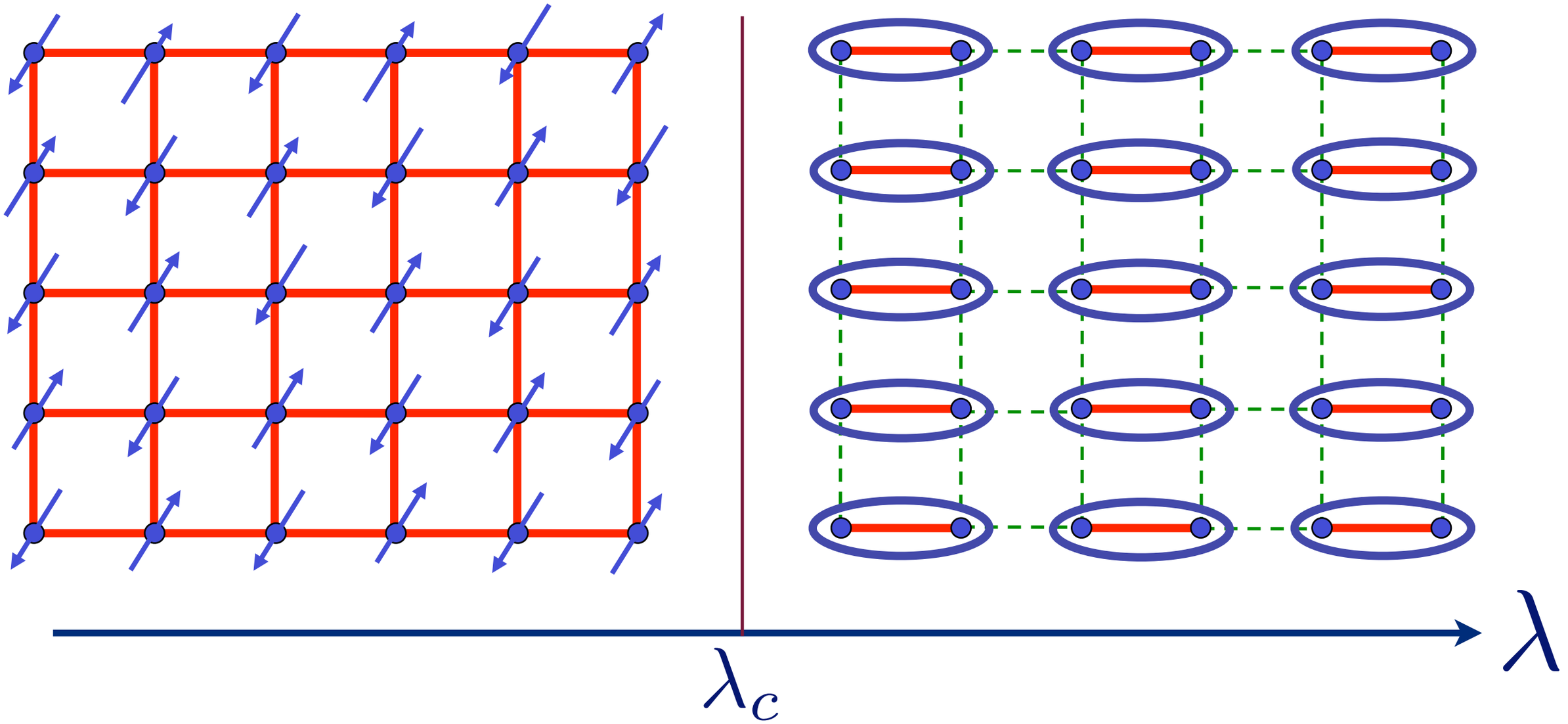

Spin waves

Excitation spectrum in the Néel phase

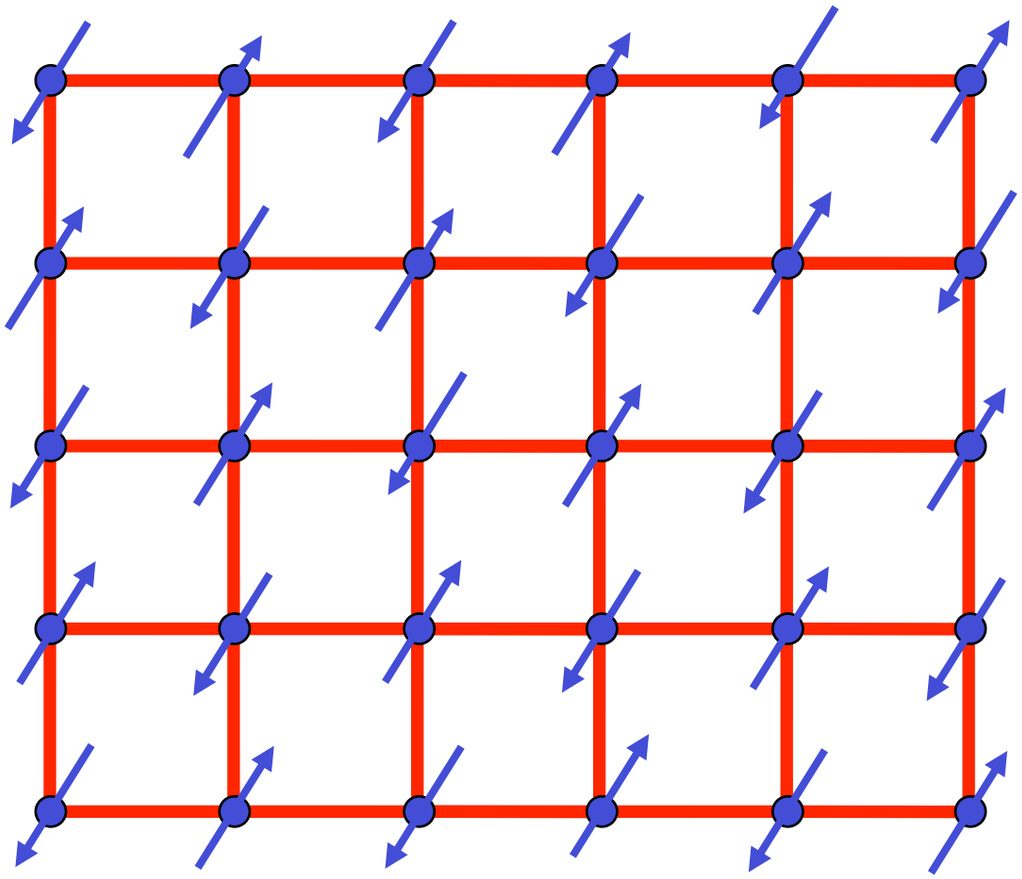

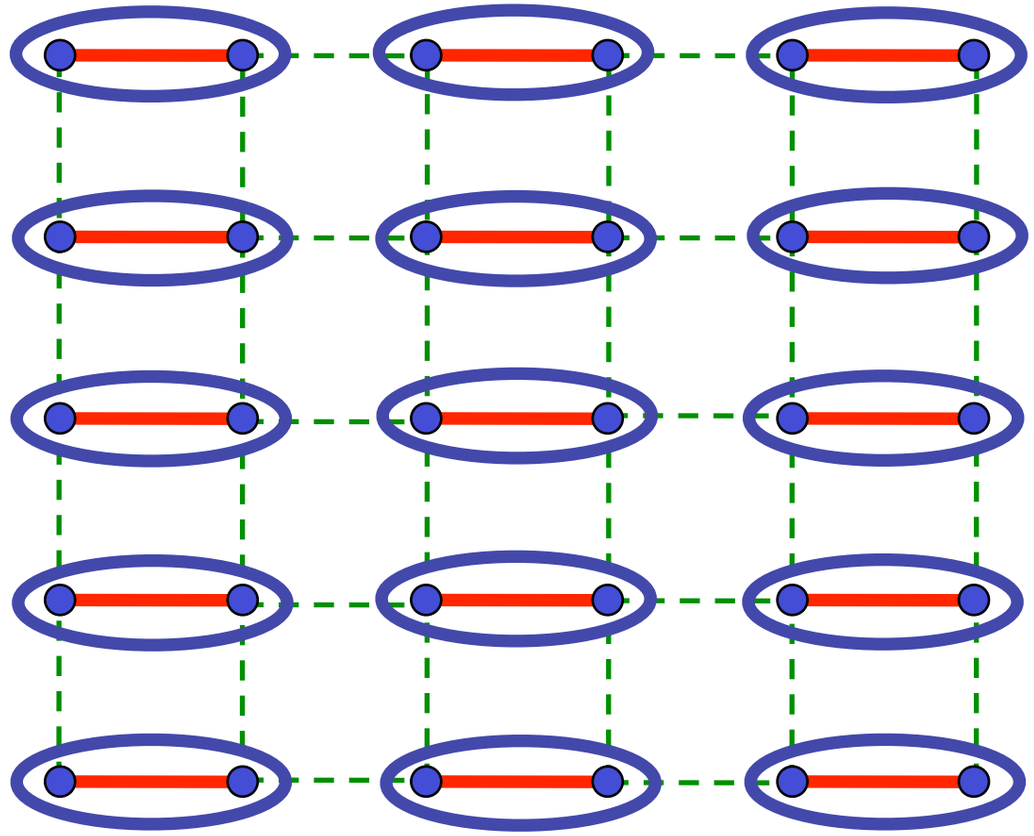

λ

λ_c

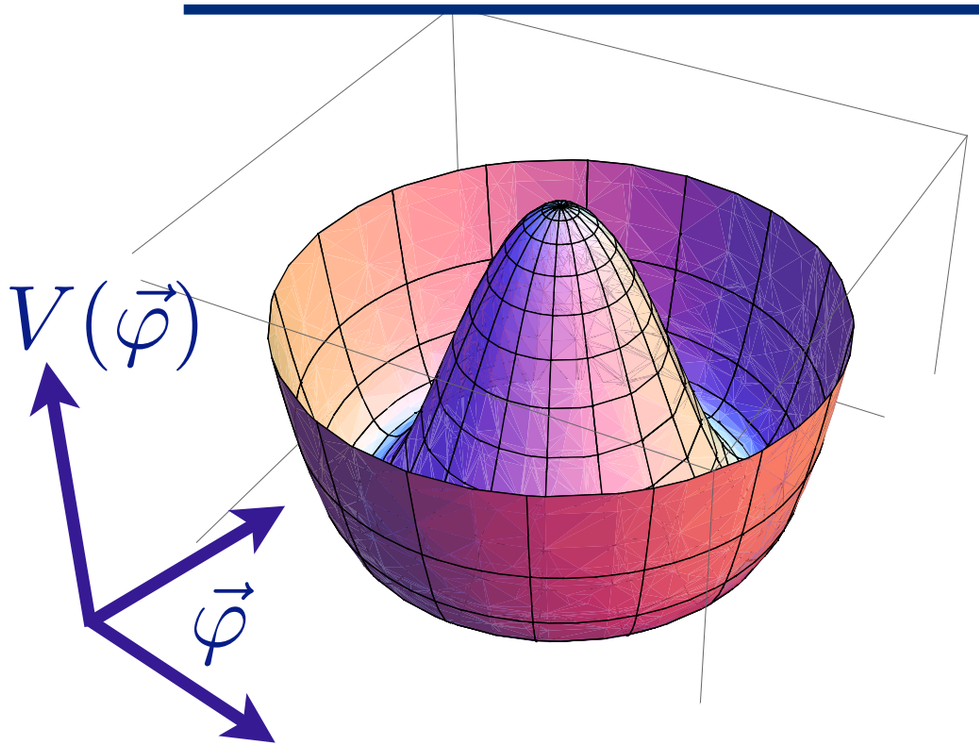

$$V(\vec{\varphi}) = (\lambda - \lambda_c)\vec{\varphi}^2 + u\left(\vec{\varphi}^2\right)^2$$

$$\lambda < \lambda_c$$

Excitation spectrum in the Néel phase

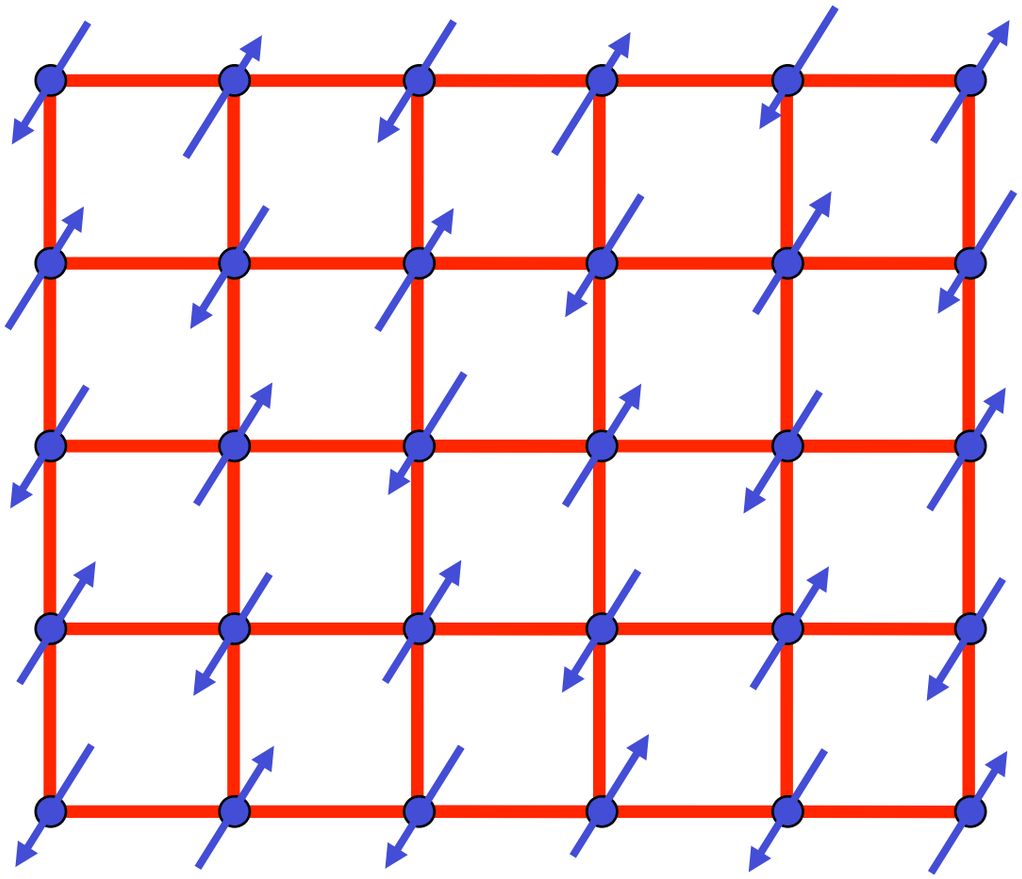

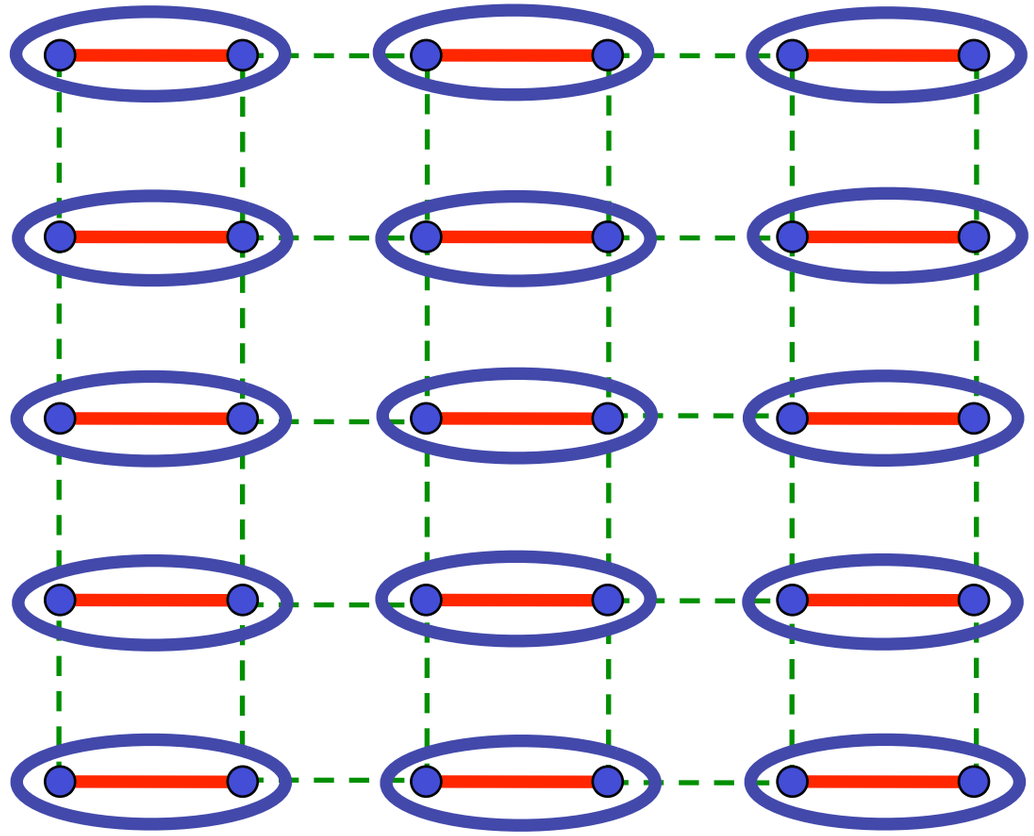

λ

λ_c

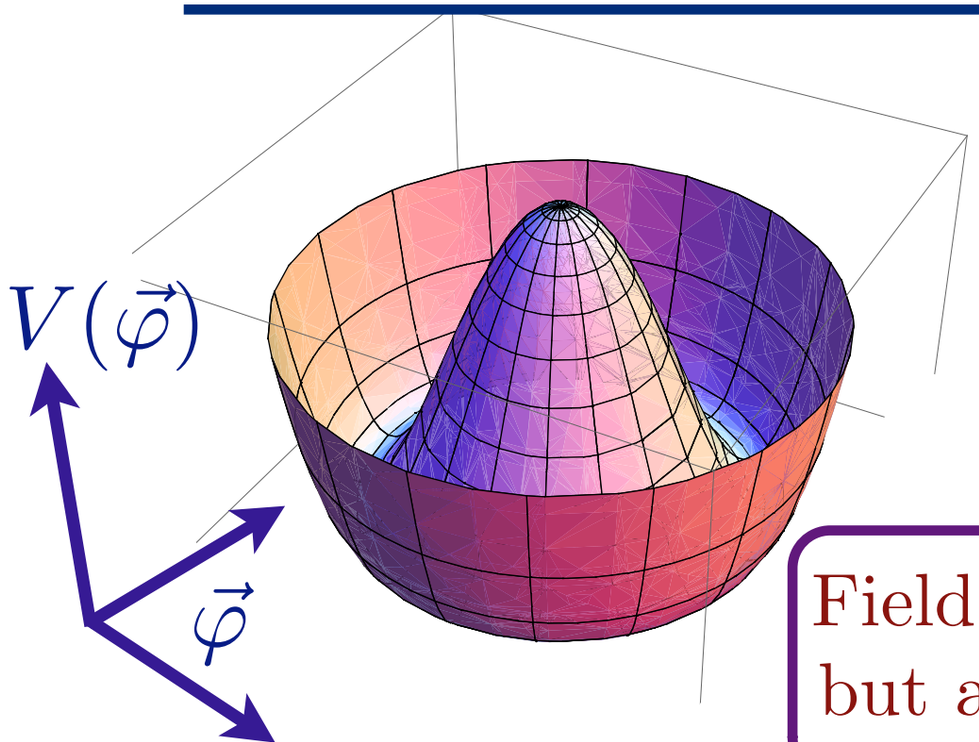

$$V(\vec{\varphi}) = (\lambda - \lambda_c)\vec{\varphi}^2 + u\left(\vec{\varphi}^2\right)^2$$

$$\lambda < \lambda_c$$

Field theory yields spin waves ("Goldstone" modes) but also an additional longitudinal "Higgs" particle

$TlCuCl_3$ with varying pressure

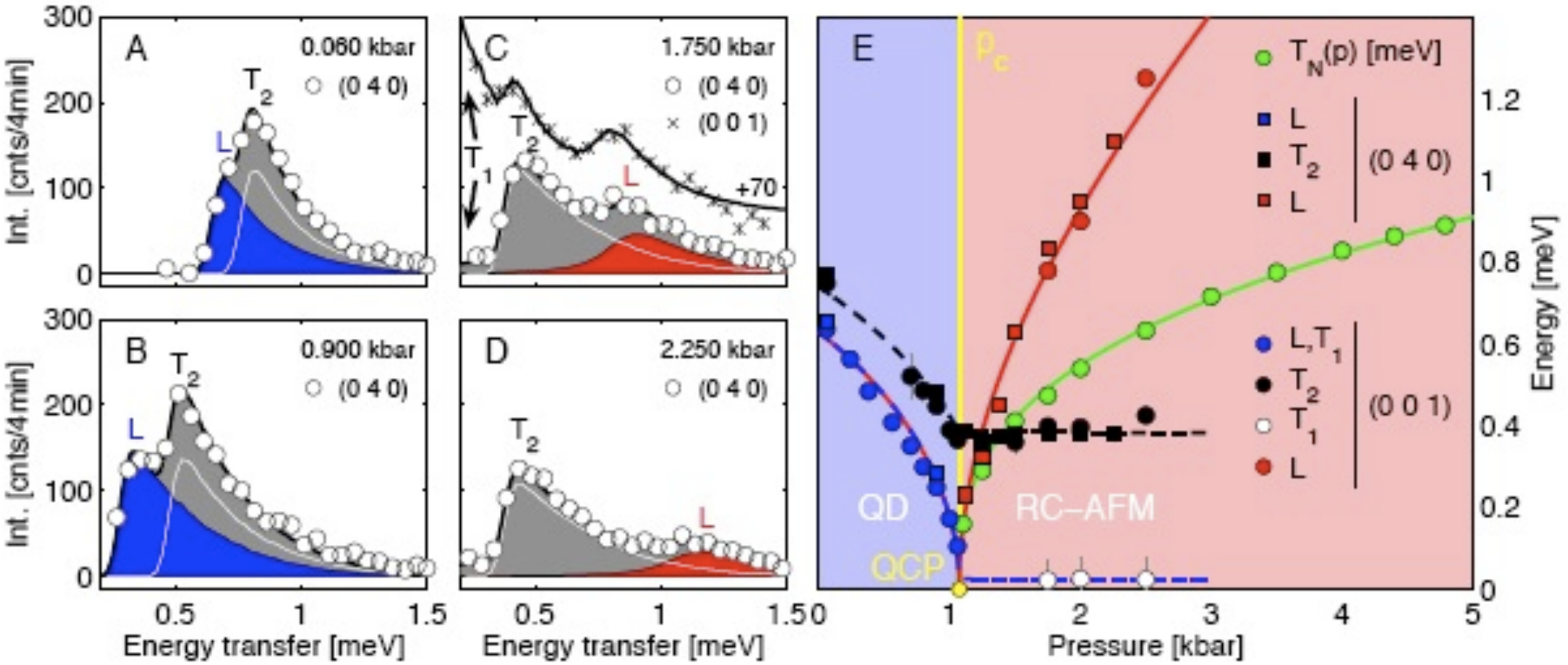

Observation of $3 \rightarrow 2$ low energy modes,
emergence of new Higgs particle in the Néel phase,
and vanishing of Néel temperature at the quantum critical point

Christian Ruegg, Bruce Normand, Masashige Matsumoto, Albert Furrer,
Desmond McMorrow, Karl Kramer, Hans–Ulrich Gudel, Severian Gvasaliya,
Hannu Mutka, and Martin Boehm, *Phys. Rev. Lett.* **100**, 205701 (2008)

Prediction of quantum field theory

Potential for $\vec{\varphi}$ fluctuations: $V(\vec{\varphi}) = (\lambda - \lambda_c)\vec{\varphi}^2 + u\left(\vec{\varphi}^2\right)^2$

Paramagnetic phase, $\lambda > \lambda_c$

Expand about $\vec{\varphi} = 0$:

$$V(\vec{\varphi}) \approx (\lambda - \lambda_c)\vec{\varphi}^2$$

Yields 3 particles with energy gap $\sim \sqrt{(\lambda - \lambda_c)}$

Prediction of quantum field theory

Potential for $\vec{\varphi}$ fluctuations: $V(\vec{\varphi}) = (\lambda - \lambda_c)\vec{\varphi}^2 + u\left(\vec{\varphi}^2\right)^2$

Paramagnetic phase, $\lambda > \lambda_c$

Expand about $\vec{\varphi} = 0$:

$$V(\vec{\varphi}) \approx (\lambda - \lambda_c)\vec{\varphi}^2$$

Yields 3 particles with energy gap $\sim \sqrt{(\lambda - \lambda_c)}$

Néel phase, $\lambda < \lambda_c$

Expand $\vec{\varphi} = \left(0, 0, \sqrt{(\lambda_c - \lambda)/(2u)}\right) + \vec{\varphi}_1$:

$$V(\vec{\varphi}) \approx 2(\lambda_c - \lambda)\varphi_{1z}^2$$

Yields 2 gapless spin waves and one Higgs-Englert-Brout particle with energy gap $\sim \sqrt{2(\lambda_c - \lambda)}$

Prediction of quantum field theory

$$\frac{\text{Energy of Higgs particle}}{\text{Energy of triplon}} = \sqrt{2}$$

$$V(\vec{\varphi}) = (\lambda - \lambda_c)\vec{\varphi}^2 + u\left(\vec{\varphi}^2\right)^2$$

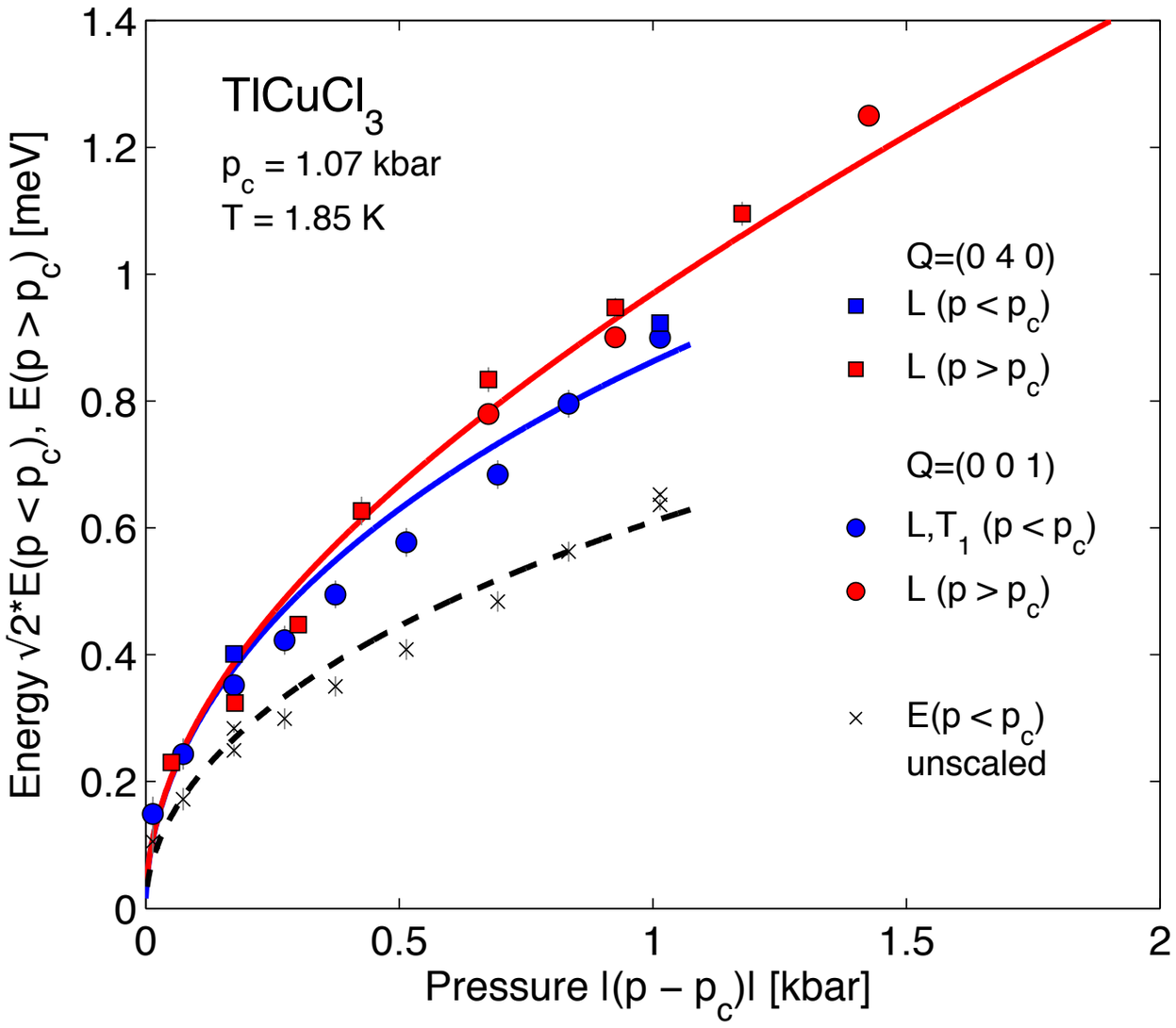

Christian Ruegg, Bruce Normand, Masashige Matsumoto, Albert Furrer, Desmond McMorrow, Karl Kramer, Hans–Ulrich Gudel, Severian Gvasaliya, Hannu Mutka, and Martin Boehm, *Phys. Rev. Lett.* **100**, 205701 (2008)

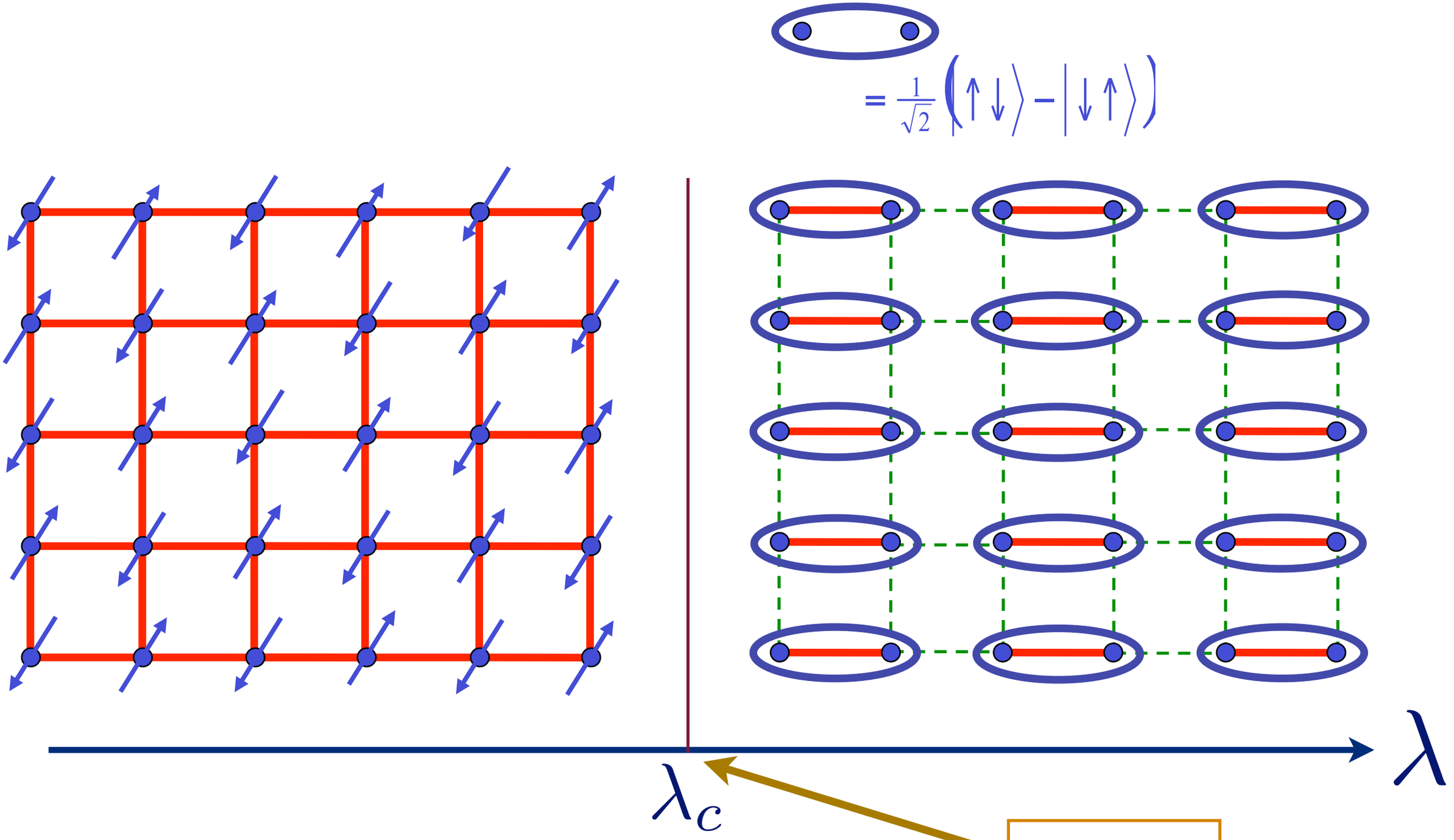

O(3) order parameter $\vec{\varphi}$

$$\mathcal{S} = \int d^2 r d\tau \left[(\partial_\tau \varphi)^2 + c^2 (\nabla_r \vec{\varphi})^2 + s\vec{\varphi}^2 + u\left(\vec{\varphi}^2\right)^2 \right]$$

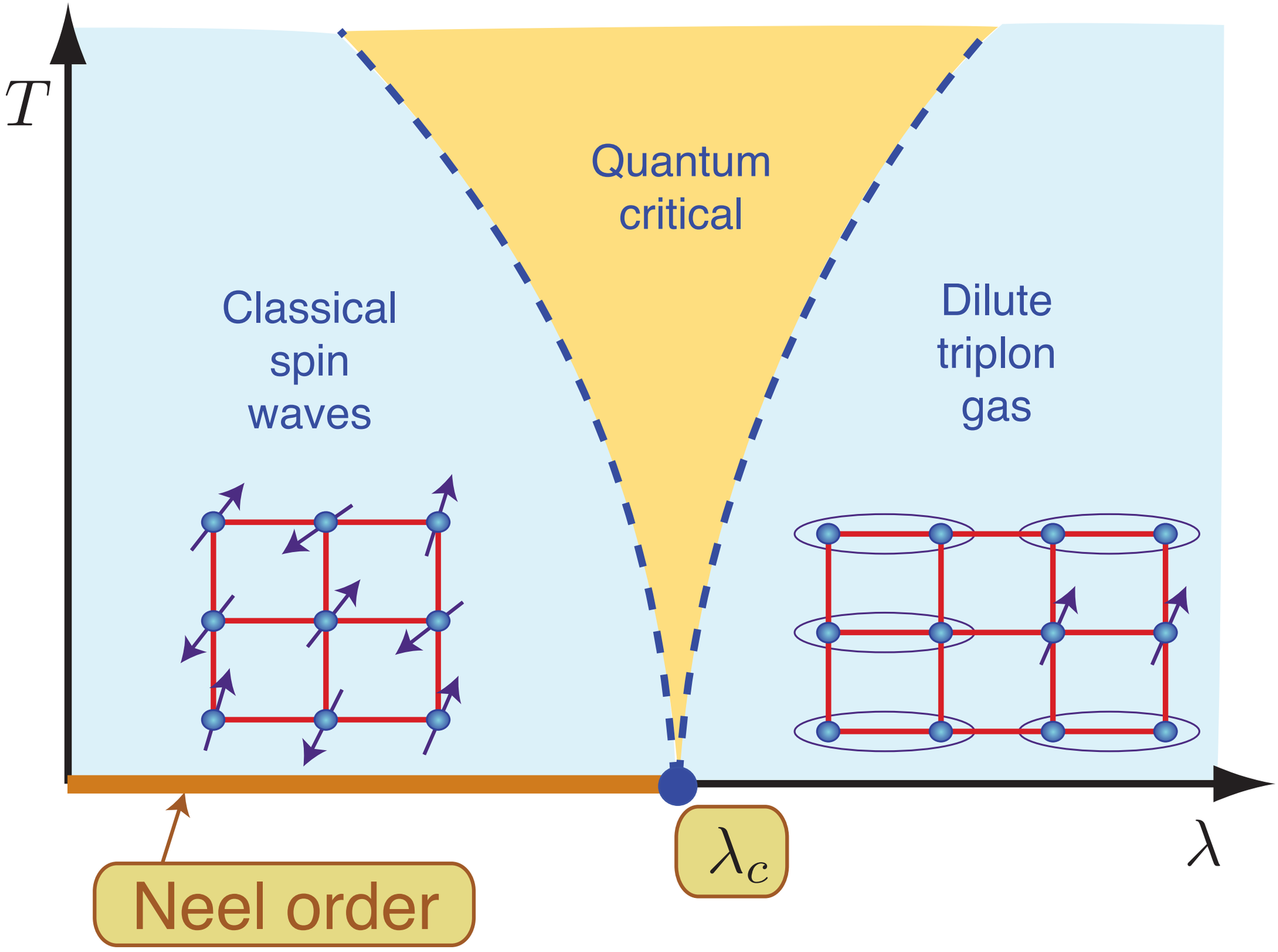
T
Quantum
critical
Classical
spin
waves
Dilute
triplon
gas
Neel order
λ_c
λ

Classical dynamics of spin waves

T

Quantum critical

Classical spin waves

Dilute triplon gas

Neel order

λ_c

λ

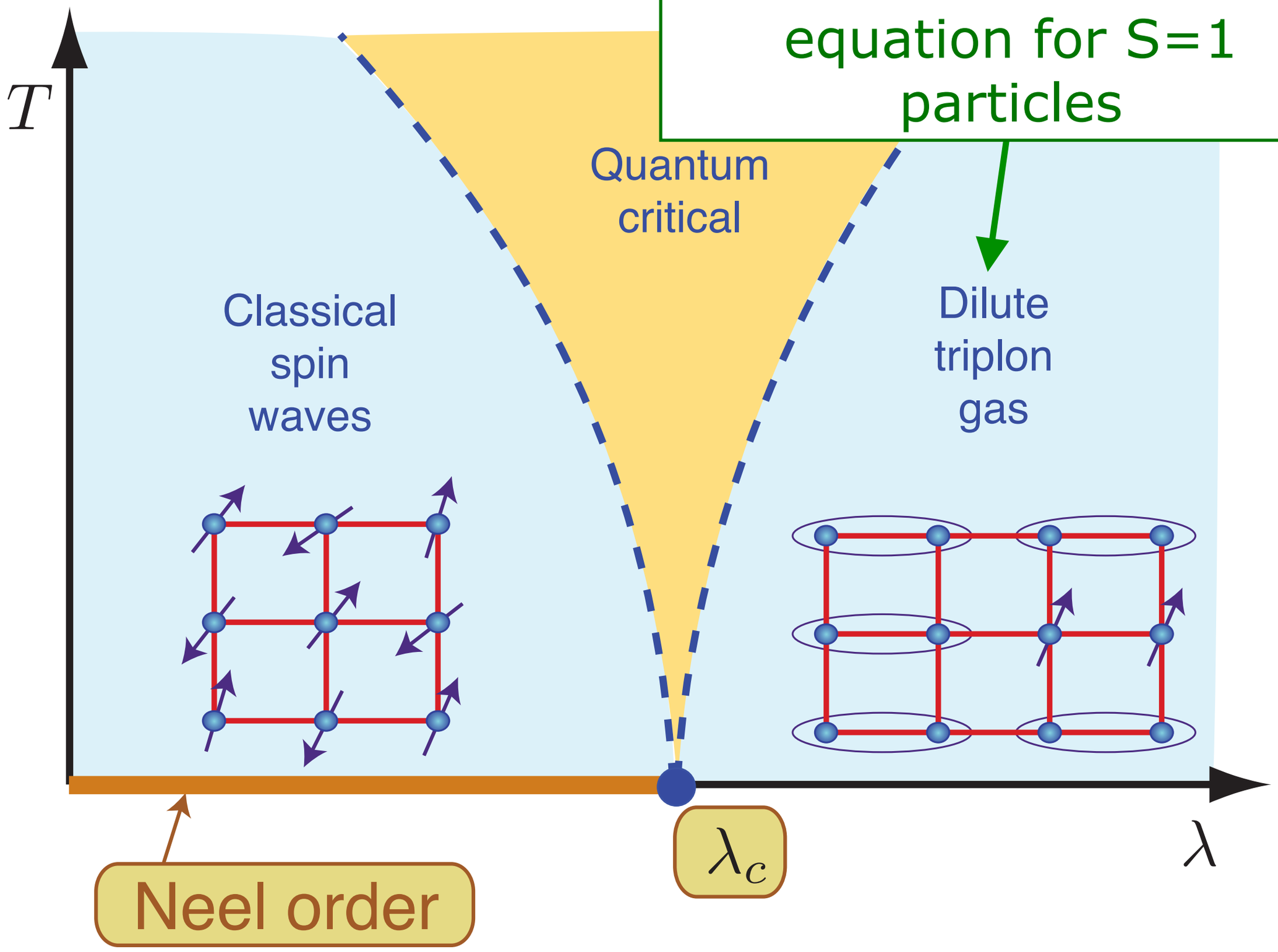
Classical Boltzmann equation for S=1 particles
T
Quantum critical
Classical spin waves
Dilute triplon gas
Neel order
λ_c
λ

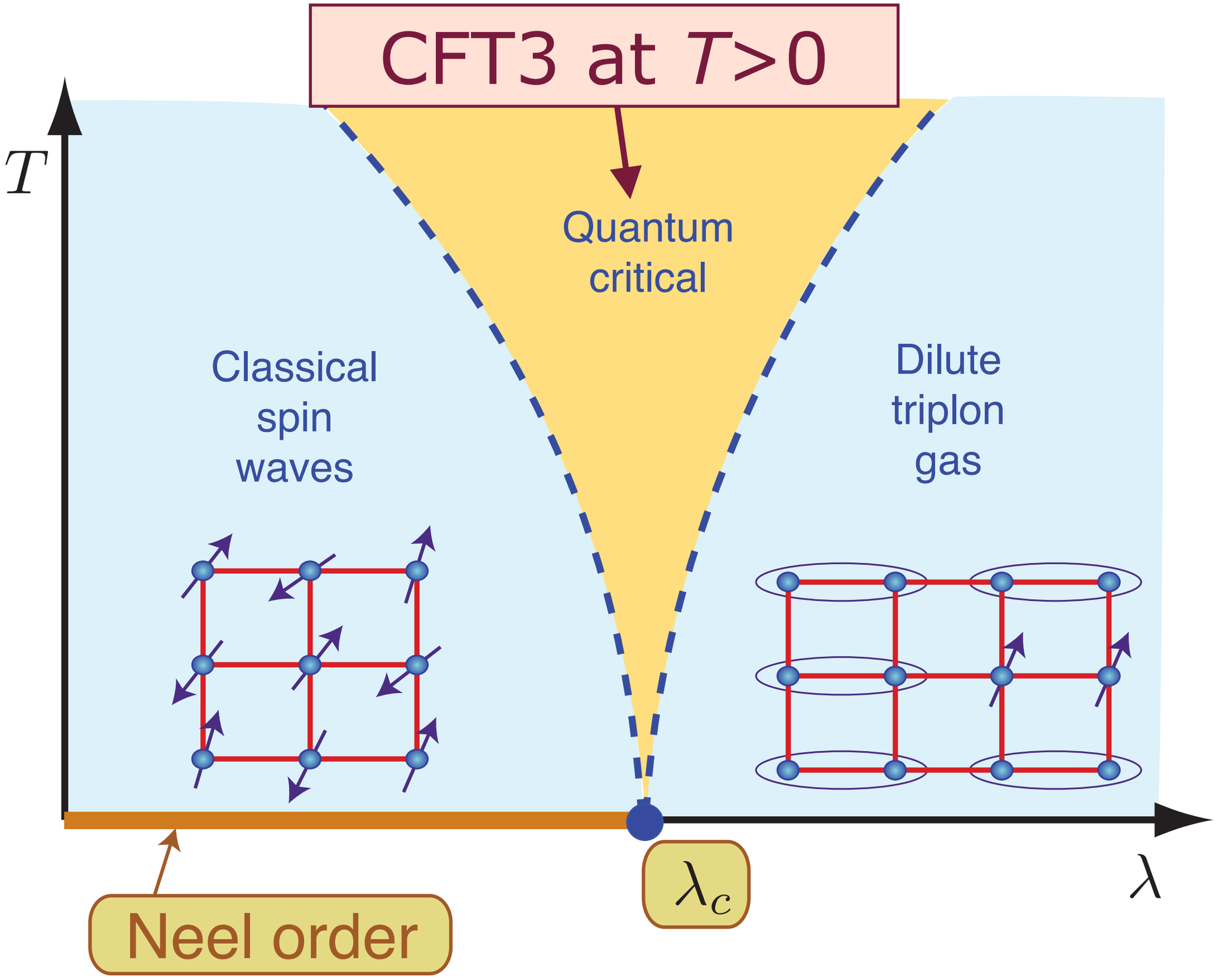
CFT3 at $T>0$
Quantum critical
Classical spin waves
Dilute triplon gas
T
λ
λ_c
Neel order

Outline

1. Coupled dimer antiferromagnets

   Order parameters and Landau-Ginzburg criticality

2. Graphene

   `Topological' Fermi surface transitions

3. Quantum criticality and black holes

   AdS_4 theory of compressible quantum liquids

4. Quantum criticality in the cuprates

   Global phase diagram and the spin density wave transition in metals

Outline

1. Coupled dimer antiferromagnets

   Order parameters and Landau-Ginzburg criticality

2. Graphene

   `Topological' Fermi surface transitions

3. Quantum criticality and black holes

   AdS_4 theory of compressible quantum liquids

4. Quantum criticality in the cuprates

   Global phase diagram and the spin density wave transition in metals

Graphene

Graphene

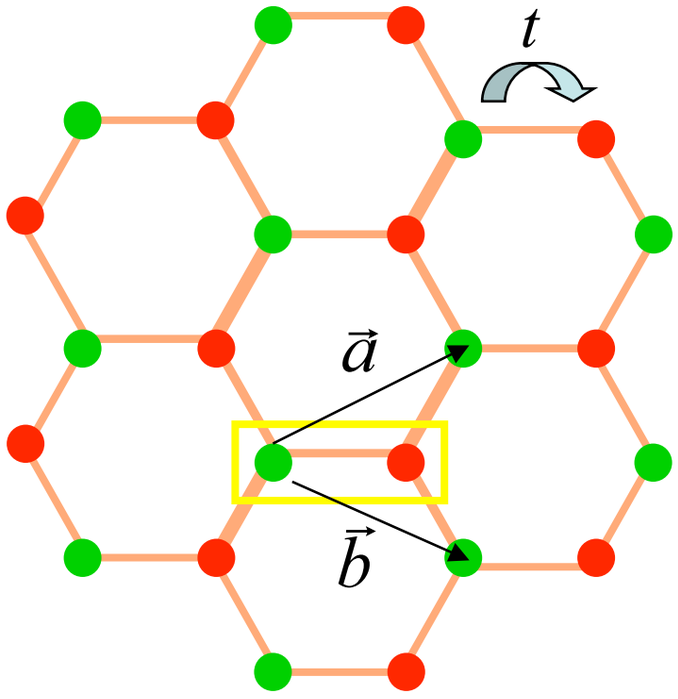

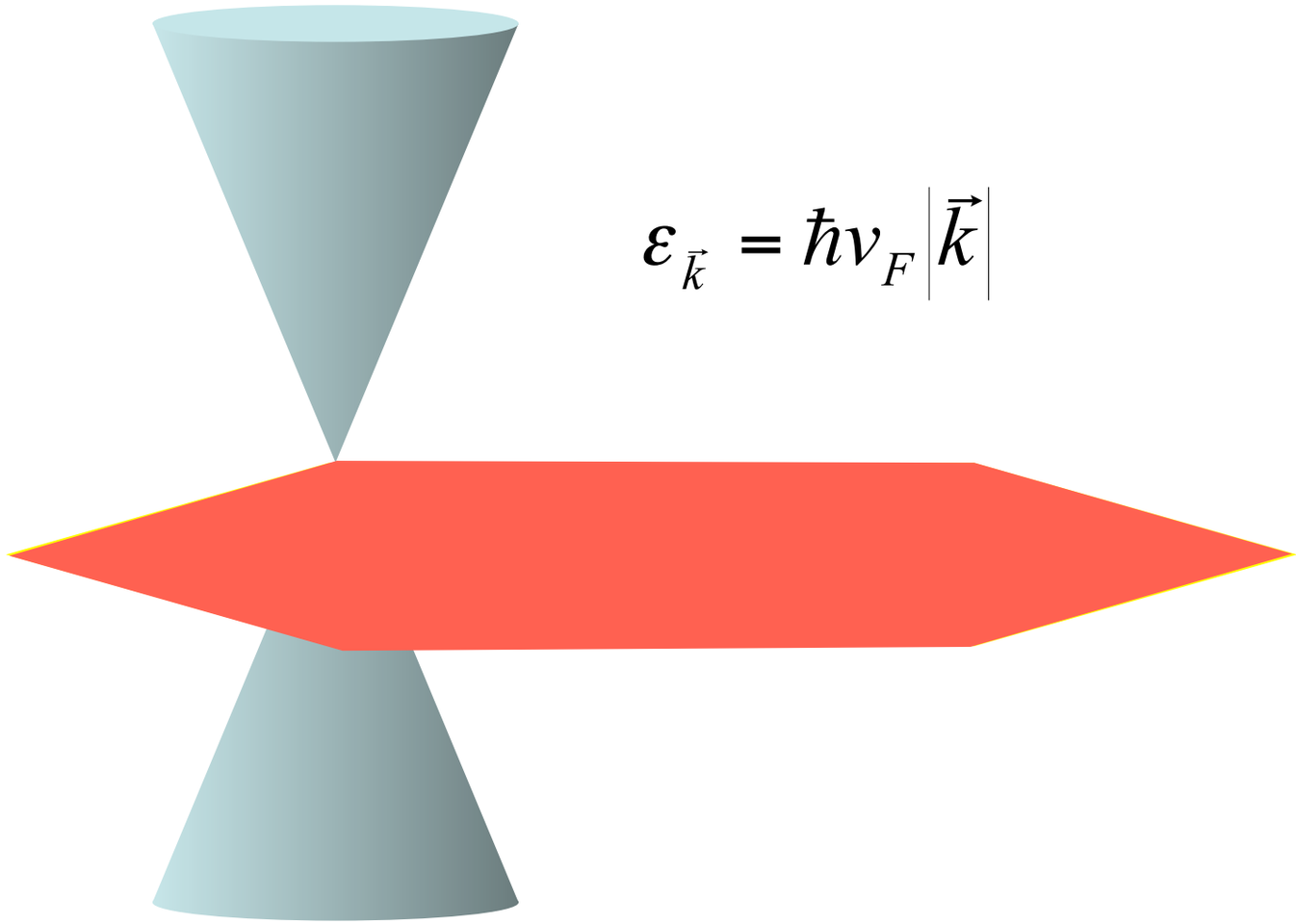

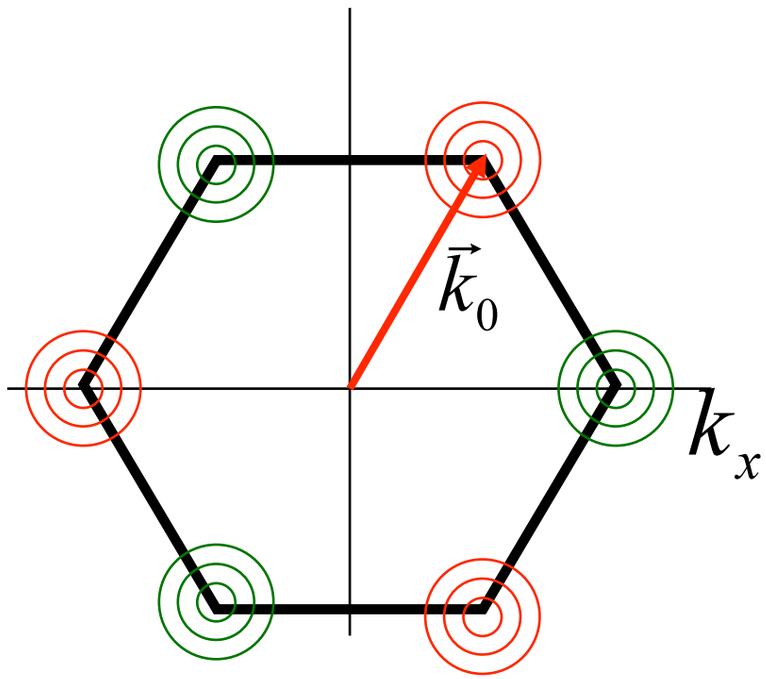

Conical Dirac dispersion

Quantum phase transition in graphene tuned by a gate voltage

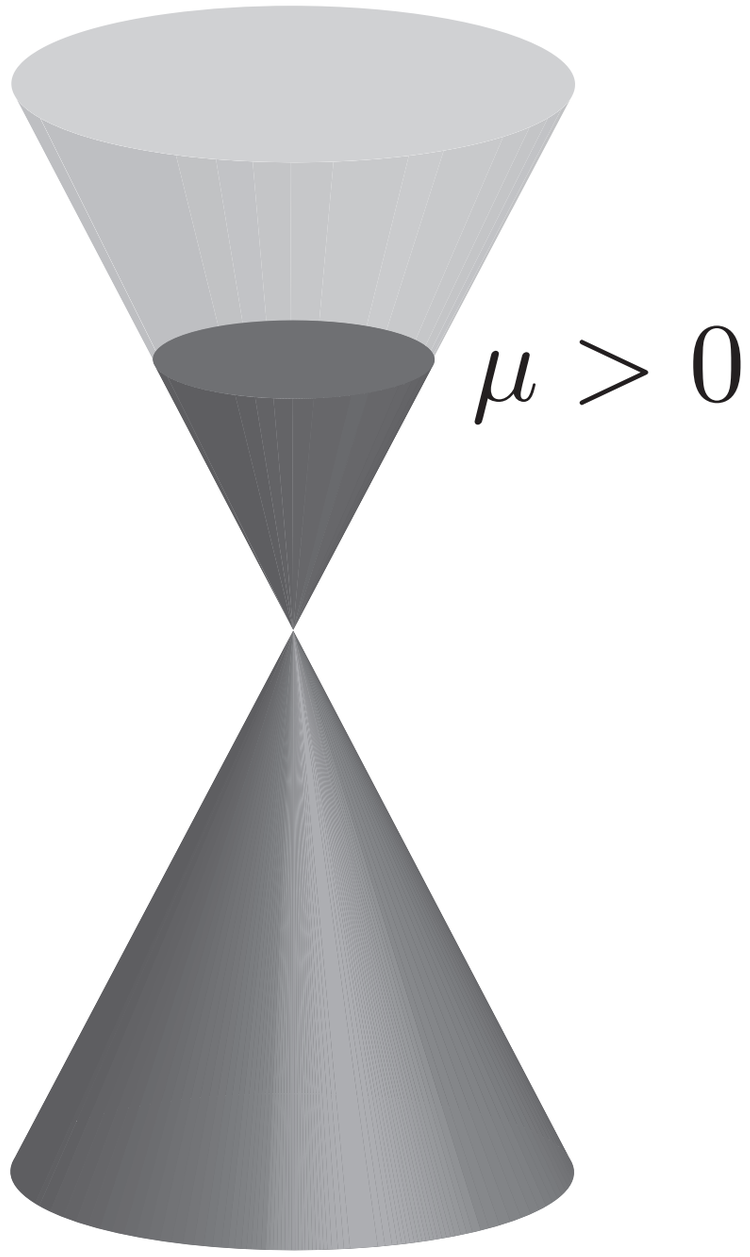

Electron
Fermi surface

Quantum phase transition in graphene tuned by a gate voltage

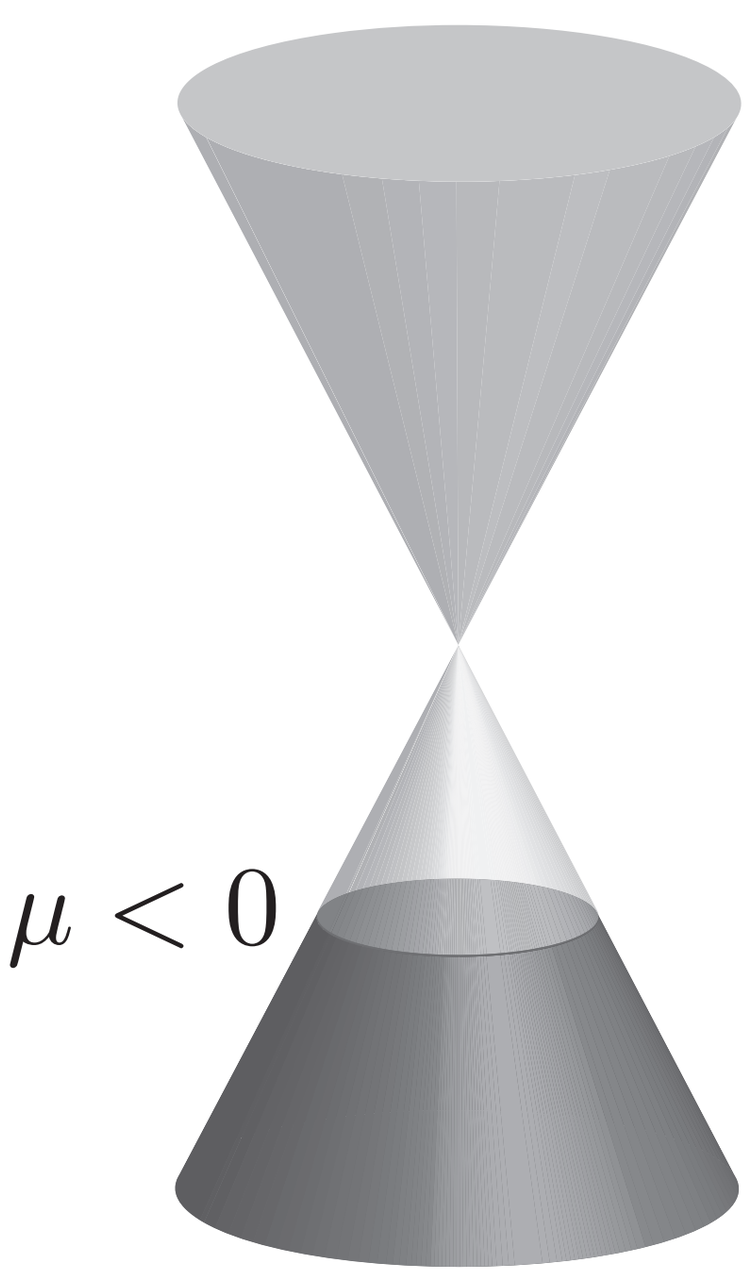

Hole
Fermi surface

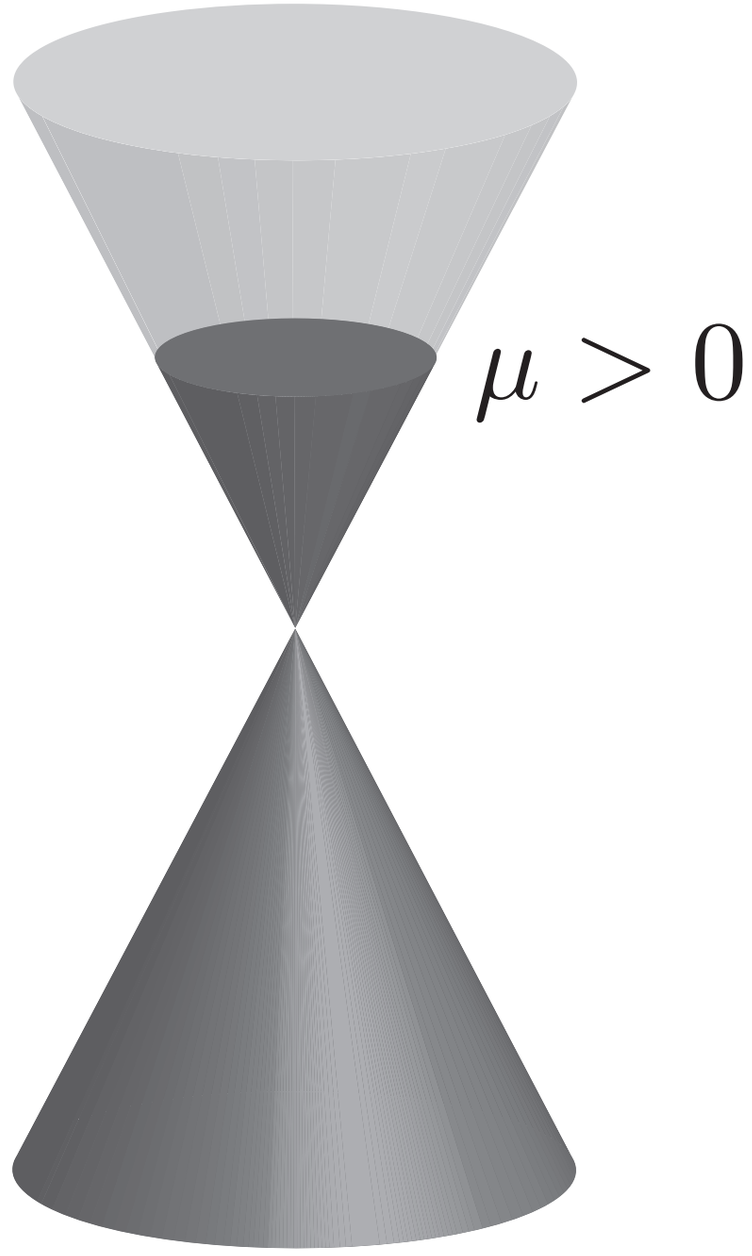

Electron
Fermi surface

Quantum phase transition in graphene tuned by a gate voltage

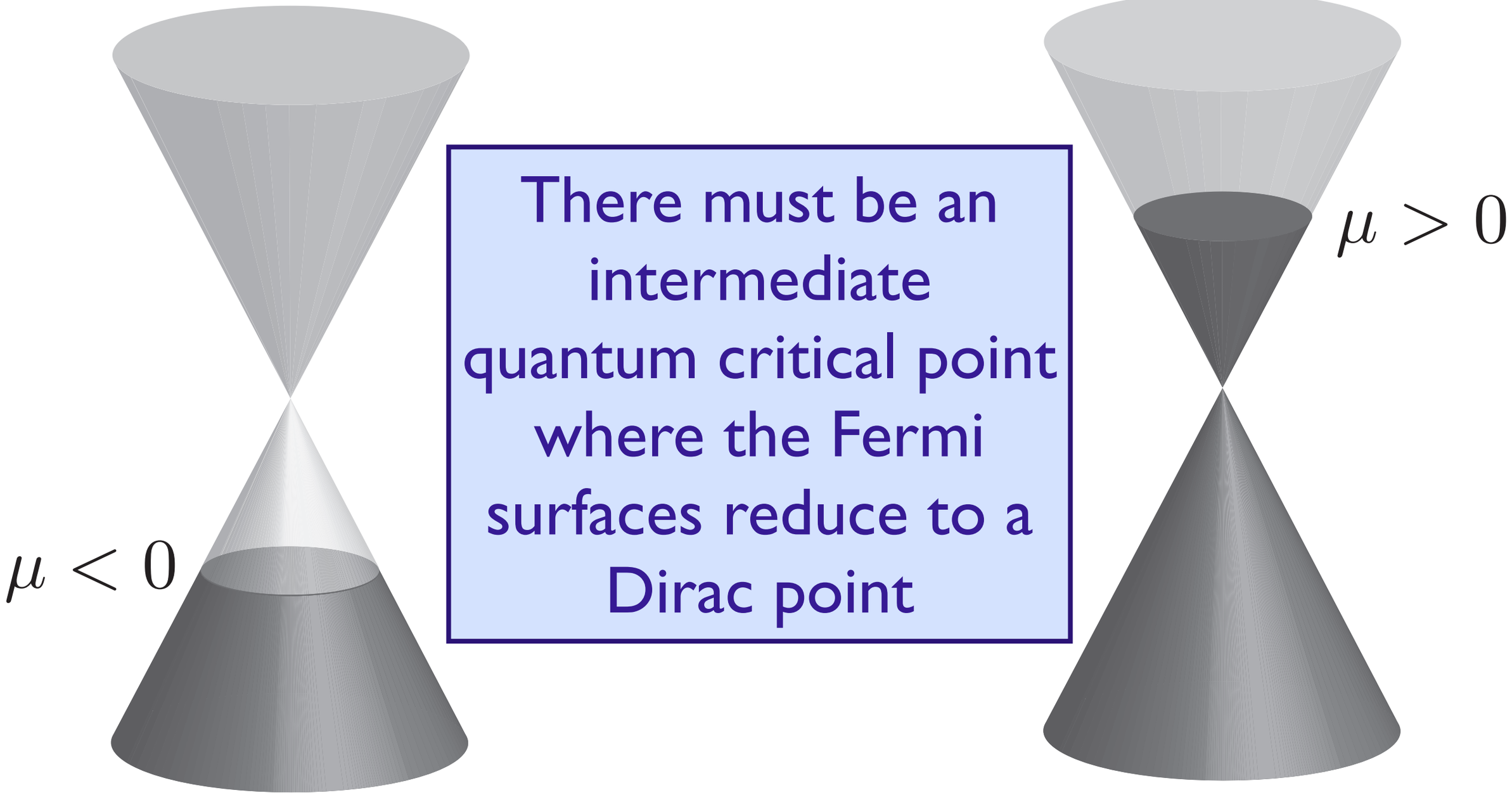

There must be an intermediate quantum critical point where the Fermi surfaces reduce to a Dirac point

Hole Fermi surface

Electron Fermi surface

Quantum critical graphene

Low energy theory has 4 two-component Dirac fermions, ψ_σ, $\sigma = 1 \ldots 4$, interacting with a $1/r$ Coulomb interaction

$$\begin{aligned} \mathcal{S} &= \int d^2 r d\tau \psi_\sigma^\dagger \left(\partial_\tau - i v_F \vec{\sigma} \cdot \vec{\nabla} \right) \psi_\sigma \\ &\quad + \frac{e^2}{2} \int d^2 r d^2 r' d\tau \psi_\sigma^\dagger \psi_\sigma(r) \frac{1}{|r - r'|} \psi_{\sigma'}^\dagger \psi_{\sigma'}(r') \end{aligned}$$

Quantum critical graphene

Low energy theory has 4 two-component Dirac fermions, ψ_σ, $\sigma = 1 \ldots 4$, interacting with a $1/r$ Coulomb interaction

$$\begin{aligned} \mathcal{S} &= \int d^2r d\tau \psi^\dagger_\sigma \left(\partial_\tau - i v_F \vec{\sigma} \cdot \vec{\nabla} \right) \psi_\sigma \\ &\quad + \frac{e^2}{2} \int d^2r d^2r' d\tau \psi^\dagger_\sigma \psi_\sigma(r) \frac{1}{|r - r'|} \psi^\dagger_{\sigma'} \psi_{\sigma'}(r') \end{aligned}$$

Dimensionless "fine-structure" constant $\alpha = e^2/(\hbar v_F)$.
RG flow of α:

$$\frac{d\alpha}{d\ell} = -\alpha^2 + \ldots$$

Behavior is similar to a conformal field theory (CFT) in 2+1 dimensions with $\alpha \sim 1/\ln(\text{scale})$

Quantum phase transition in graphene

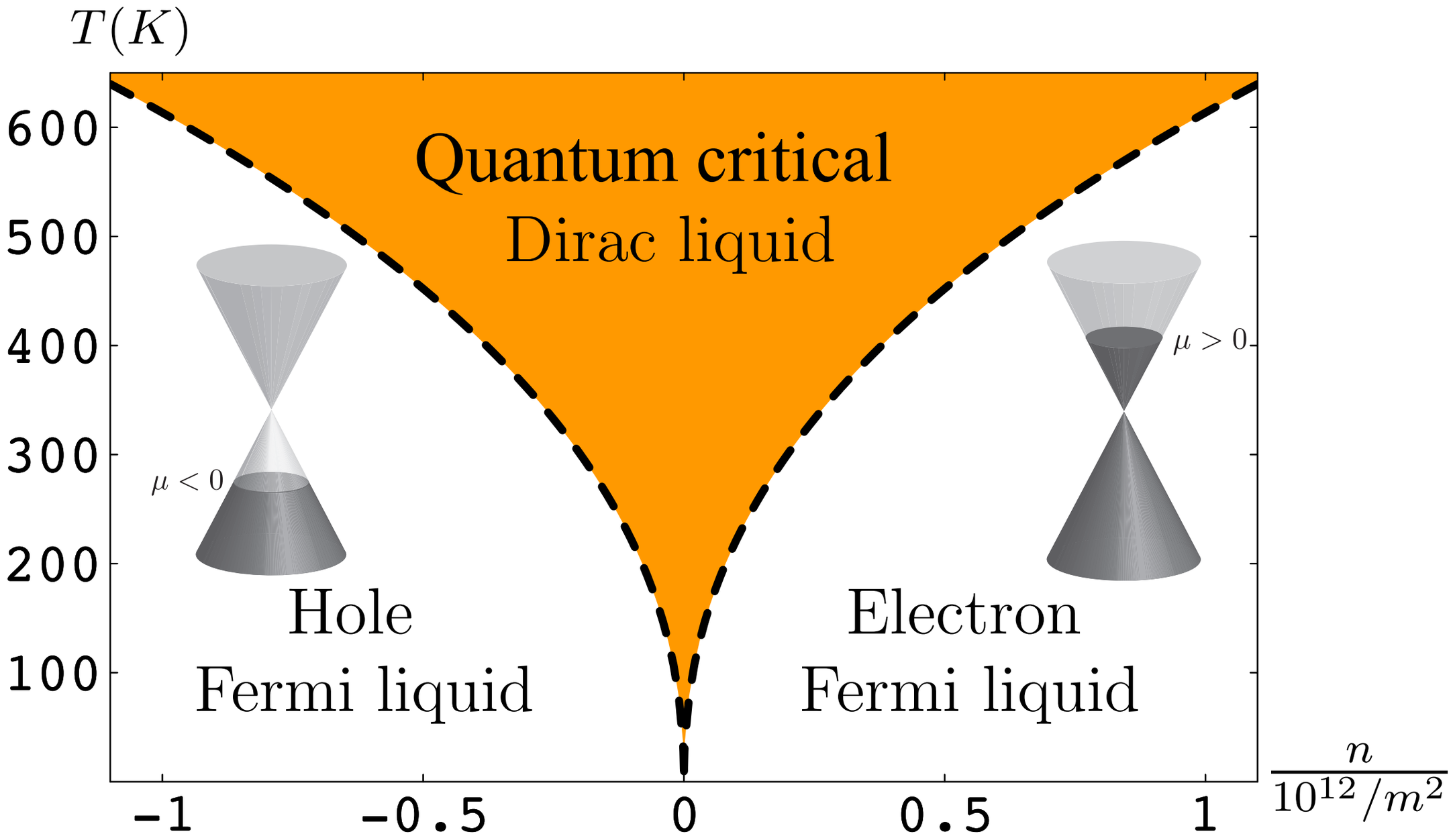

Quantum critical transport

Quantum *"perfect fluid"* with shortest possible relaxation time, τ_R

$$\tau_R \gtrsim \frac{\hbar}{k_B T}$$

S. Sachdev, *Quantum Phase Transitions,* Cambridge (1999).

Quantum critical transport

Transport co-oefficients not determined by collision rate, but by universal constants of nature

Electrical conductivity

$$\sigma = \frac{e^2}{h} \times [\text{Universal constant } \mathcal{O}(1)]$$

M. P. A. Fisher, *Phys. Rev. Lett.* **65**, 923 (1990)
K. Damle and S. Sachdev, *Phys. Rev. B* **56**, 8714 (1997).

Quantum critical transport

Transport co-oefficients not determined by collision rate, but by universal constants of nature

Momentum transport

$$\frac{\eta}{s} \equiv \frac{\text{viscosity}}{\text{entropy density}}$$

$$= \frac{\hbar}{k_B} \times [\text{Universal constant } \mathcal{O}(1)]$$

P. Kovtun, D. T. Son, and A. Starinets, *Phys. Rev. Lett.* **94,** 11601 (2005)

Quantum critical transport in graphene

$$\sigma(\omega) = \begin{cases} \dfrac{e^2}{h}\left[\dfrac{\pi}{2} + \mathcal{O}\left(\dfrac{1}{\ln(\Lambda/\omega)}\right)\right] & , \quad \hbar\omega \gg k_B T \\ \dfrac{e^2}{h\alpha^2(T)}\left[0.760 + \mathcal{O}\left(\dfrac{1}{|\ln(\alpha(T))|}\right)\right] & , \quad \hbar\omega \ll k_B T \alpha^2(T) \end{cases}$$

$$\frac{\eta}{s} = \frac{\hbar}{k_B \alpha^2(T)} \times 0.130$$

where the "fine structure constant" is

$$\alpha(T) = \frac{\alpha}{1 + (\alpha/4)\ln(\Lambda/T)} \overset{T\to 0}{\sim} \frac{4}{\ln(\Lambda/T)}$$

L. Fritz, J. Schmalian, M. Müller and S. Sachdev, *Physical Review B* **78**, 085416 (2008)
M. Müller, J. Schmalian, and L. Fritz, *Physical Review Letters* **103**, 025301 (2009)

Outline

1. Coupled dimer antiferromagnets

   Order parameters and Landau-Ginzburg criticality

2. Graphene

   `Topological' Fermi surface transitions

3. Quantum criticality and black holes

   AdS_4 theory of compressible quantum liquids

4. Quantum criticality in the cuprates

   Global phase diagram and the spin density wave transition in metals

Outline

1. Coupled dimer antiferromagnets

   Order parameters and Landau-Ginzburg criticality

2. Graphene

   `Topological' Fermi surface transitions

3. Quantum criticality and black holes

   AdS_4 theory of compressible quantum liquids

4. Quantum criticality in the cuprates

   Global phase diagram and the spin density wave transition in metals

AdS/CFT correspondence

The quantum theory of a black hole in a 3+1-dimensional negatively curved AdS universe is holographically represented by a CFT (the theory of a quantum critical point) in 2+1 dimensions

3+1 dimensional AdS space

Maldacena, Gubser, Klebanov, Polyakov, Witten

AdS/CFT correspondence

The quantum theory of a black hole in a 3+1-dimensional negatively curved AdS universe is holographically represented by a CFT (the theory of a quantum critical point) in 2+1 dimensions

3+1 dimensional AdS space

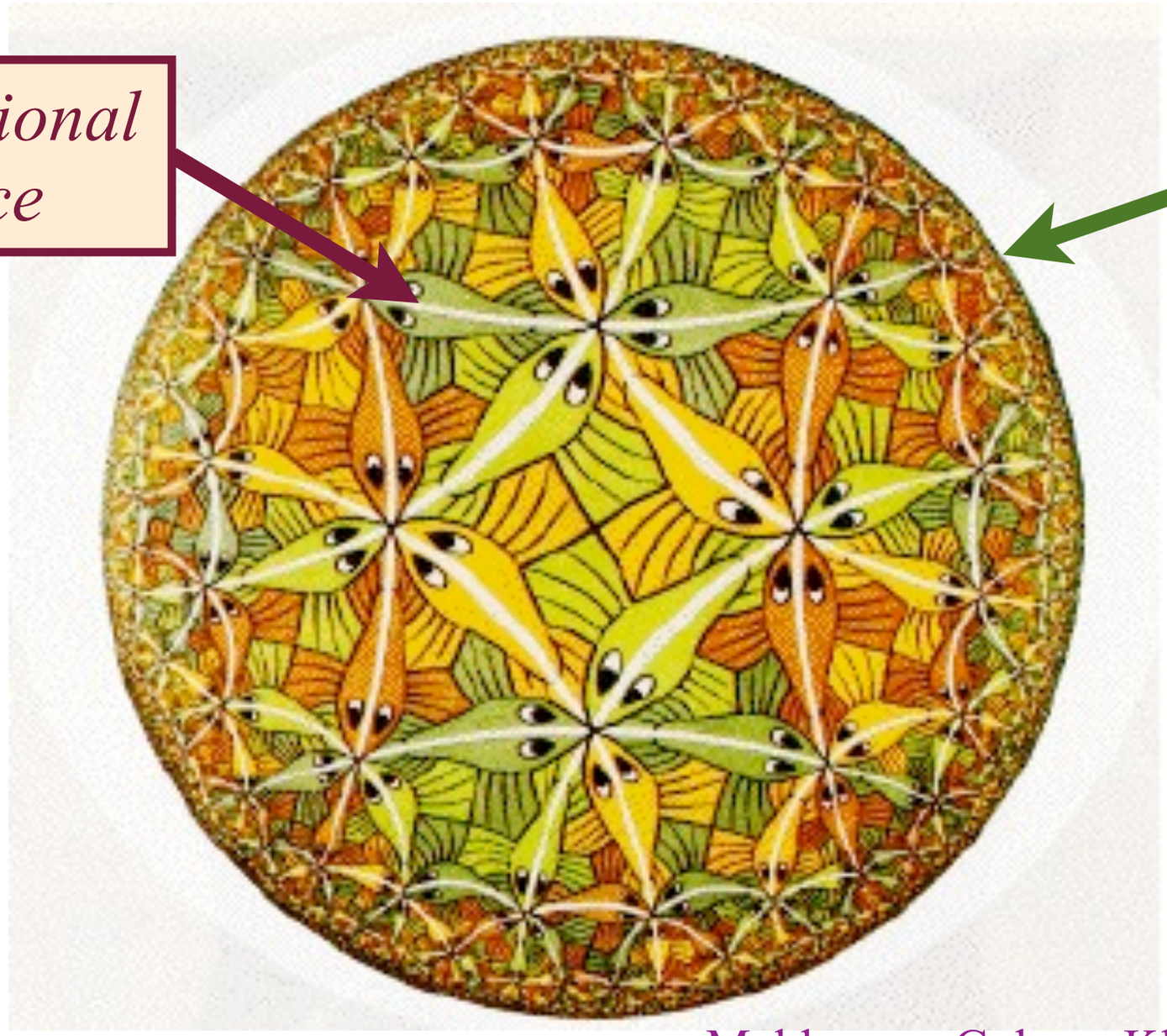

A 2+1 dimensional system at its quantum critical point

Maldacena, Gubser, Klebanov, Polyakov, Witten

AdS/CFT correspondence

The quantum theory of a black hole in a 3+1-dimensional negatively curved AdS universe is holographically represented by a CFT (the theory of a quantum critical point) in 2+1 dimensions

3+1 dimensional AdS space

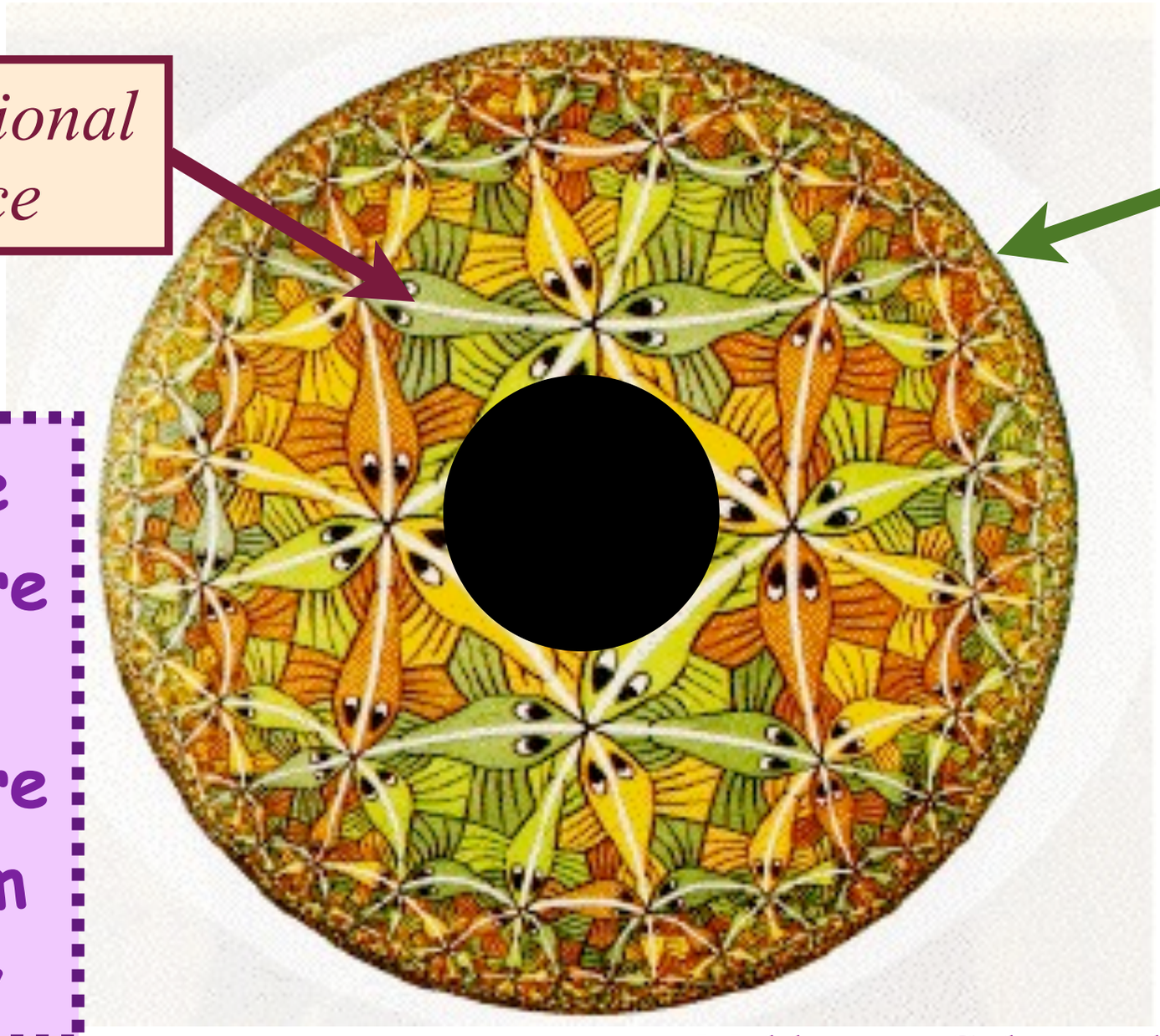

Quantum criticality in 2+1 dimensions

Black hole temperature = temperature of quantum criticality

Maldacena, Gubser, Klebanov, Polyakov, Witten

AdS/CFT correspondence

The quantum theory of a black hole in a 3+1-dimensional negatively curved AdS universe is holographically represented by a CFT (the theory of a quantum critical point) in 2+1 dimensions

3+1 dimensional AdS space

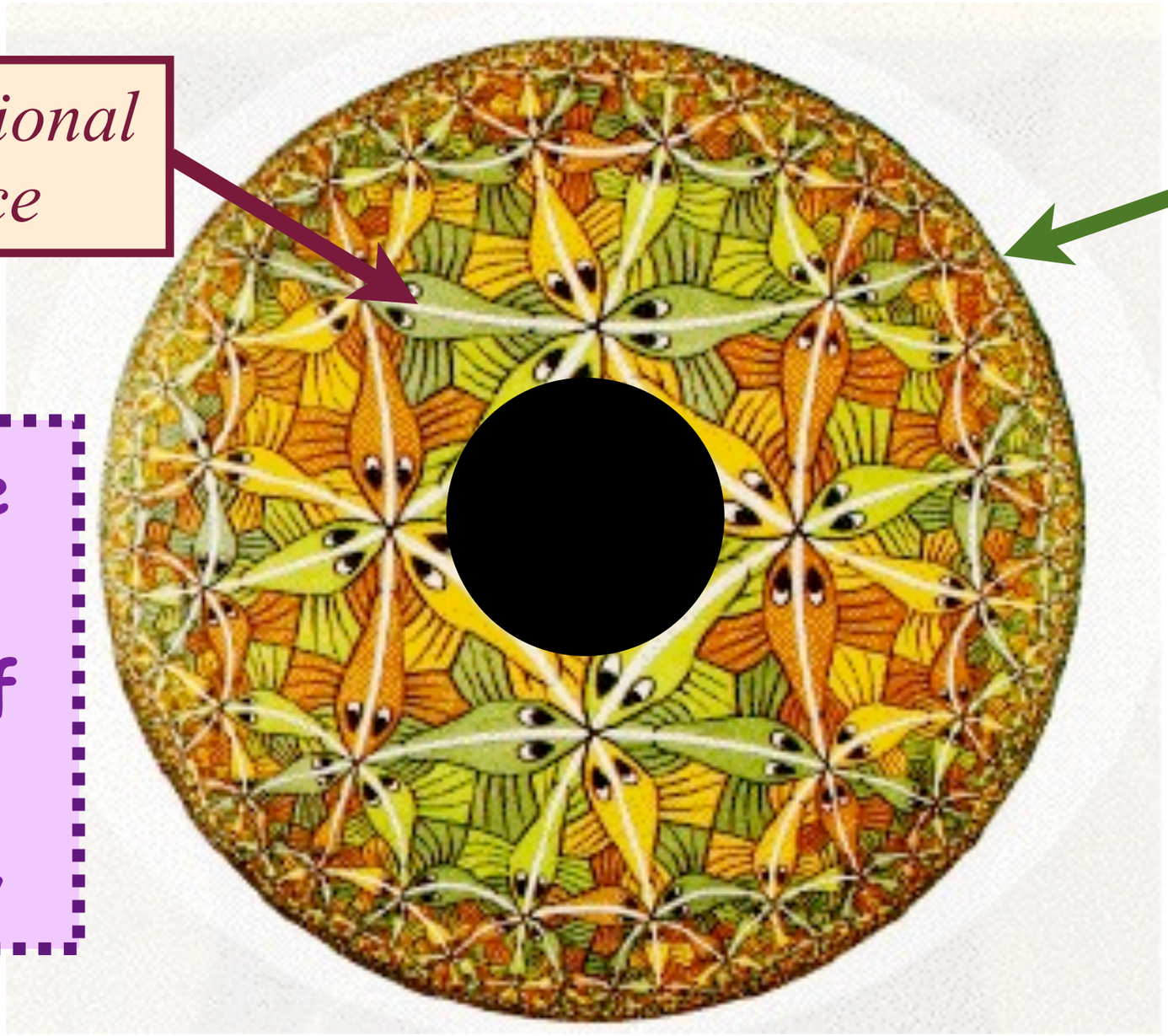

Quantum criticality in 2+1 dimensions

Black hole entropy = entropy of quantum criticality

Strominger, Vafa

AdS/CFT correspondence

The quantum theory of a black hole in a 3+1-dimensional negatively curved AdS universe is holographically represented by a CFT (the theory of a quantum critical point) in 2+1 dimensions

3+1 dimensional AdS space

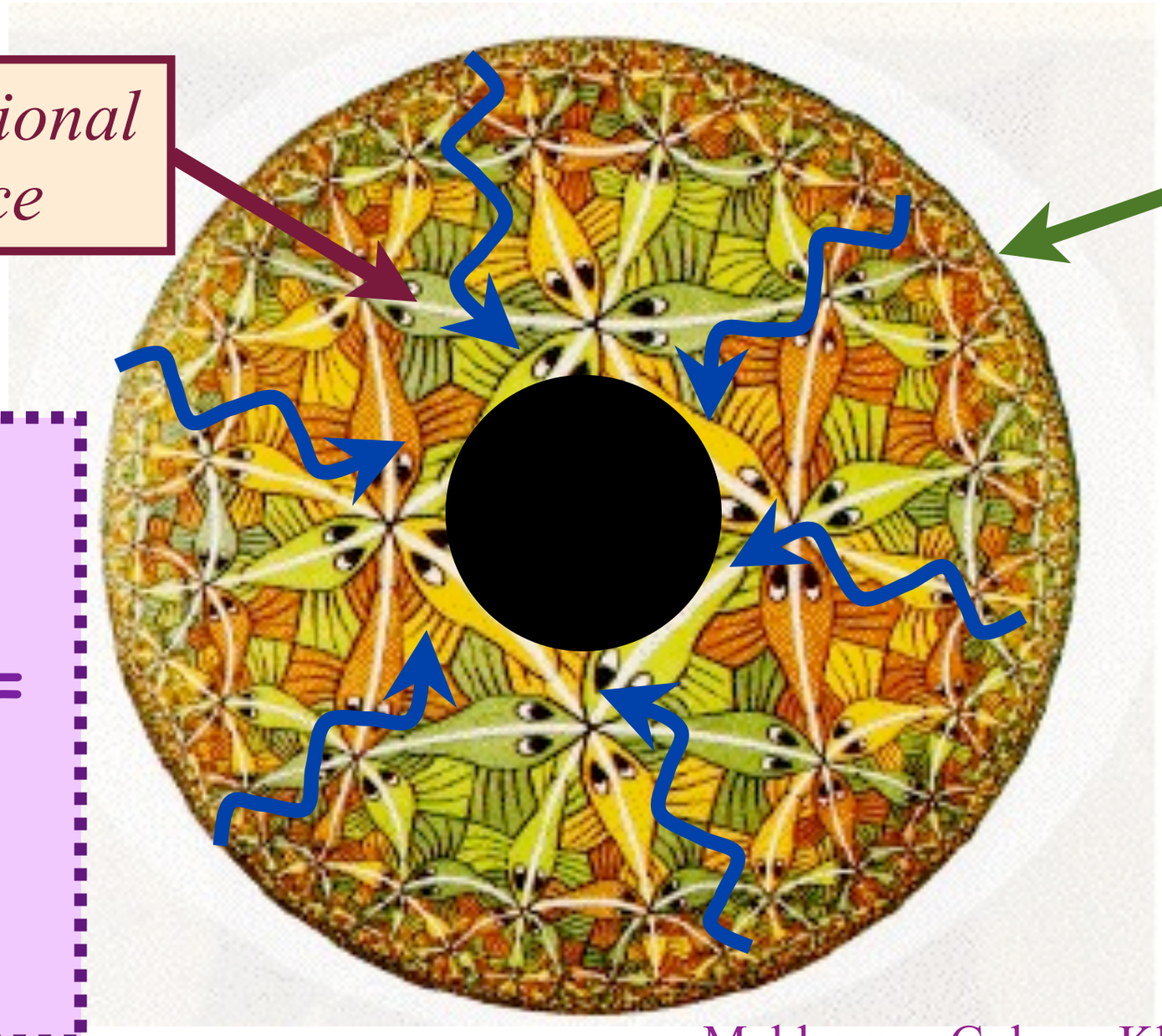

Quantum criticality in 2+1 dimensions

Quantum critical dynamics = waves in curved space

Maldacena, Gubser, Klebanov, Polyakov, Witten

AdS/CFT correspondence

The quantum theory of a black hole in a 3+1-dimensional negatively curved AdS universe is holographically represented by a CFT (the theory of a quantum critical point) in 2+1 dimensions

3+1 dimensional AdS space

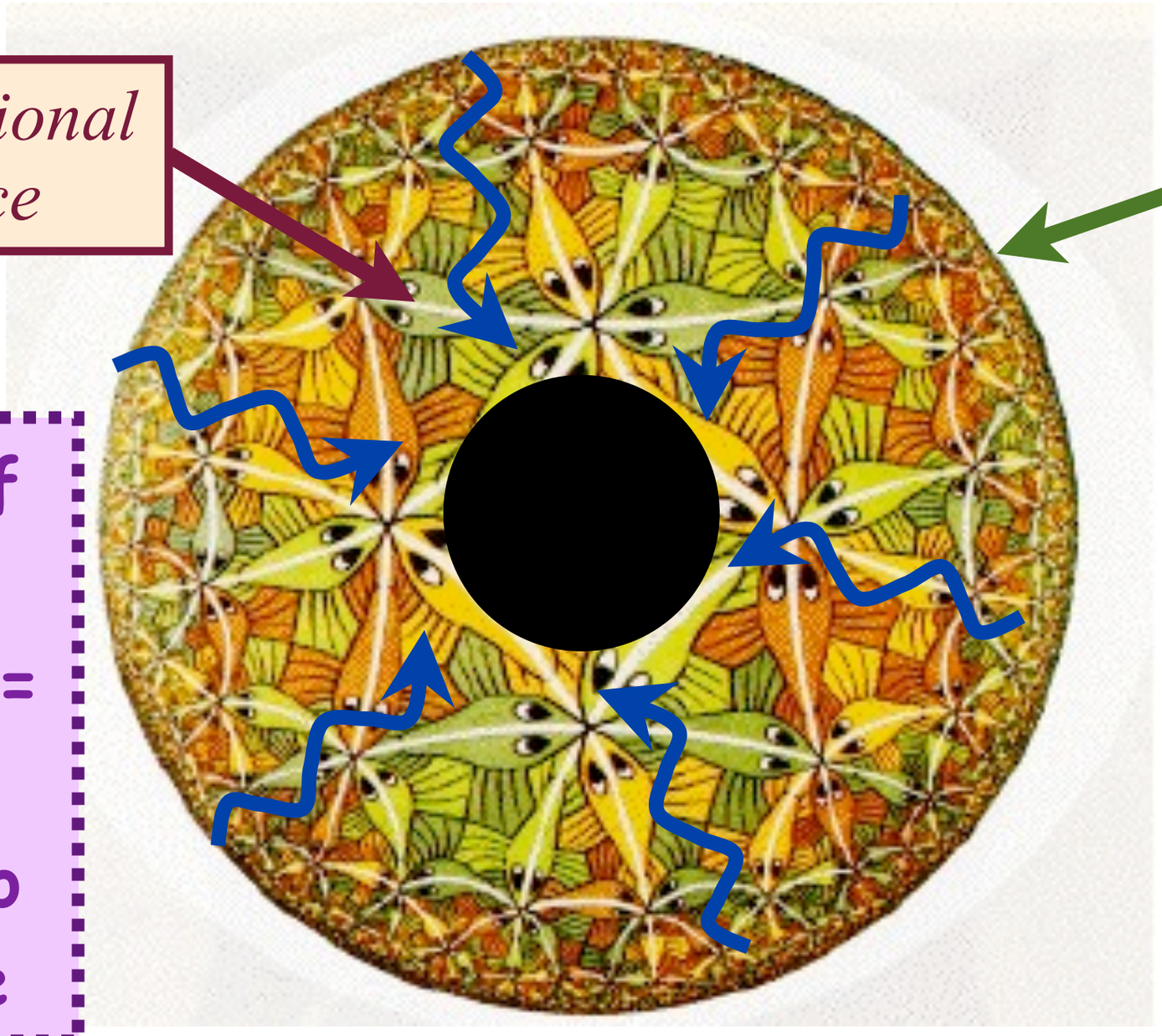

Quantum criticality in 2+1 dimensions

Friction of quantum criticality = waves falling into black hole

Kovtun, Policastro, Son

Conformal field theory
in 2+1 dimensions at $T = 0$

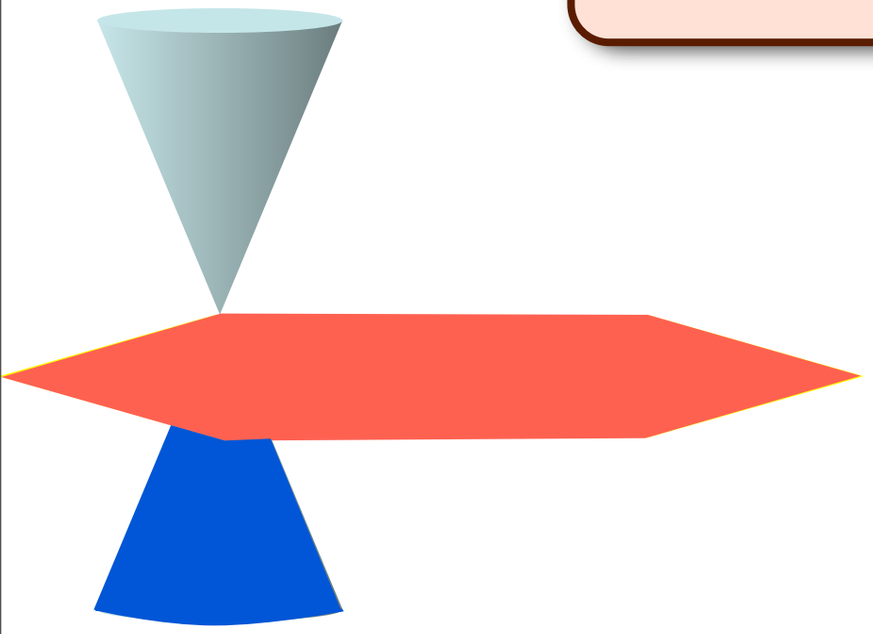

Einstein gravity
on AdS_4

Conformal field theory
in 2+1 dimensions at $T > 0$

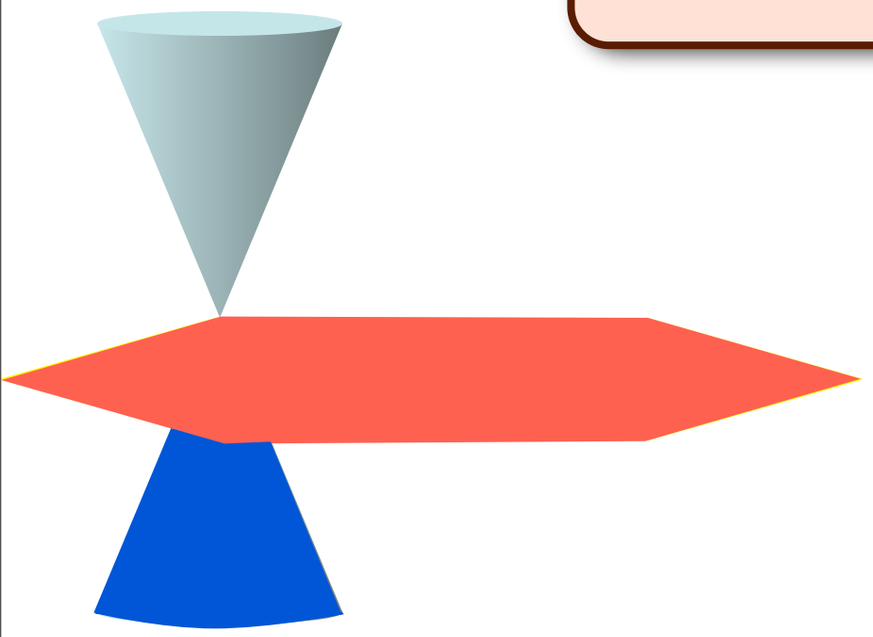

Einstein gravity on AdS_4
with a Schwarzschild
black hole

Conformal field theory
in 2+1 dimensions at $T > 0$,
with a non-zero chemical potential, μ
and applied magnetic field, B

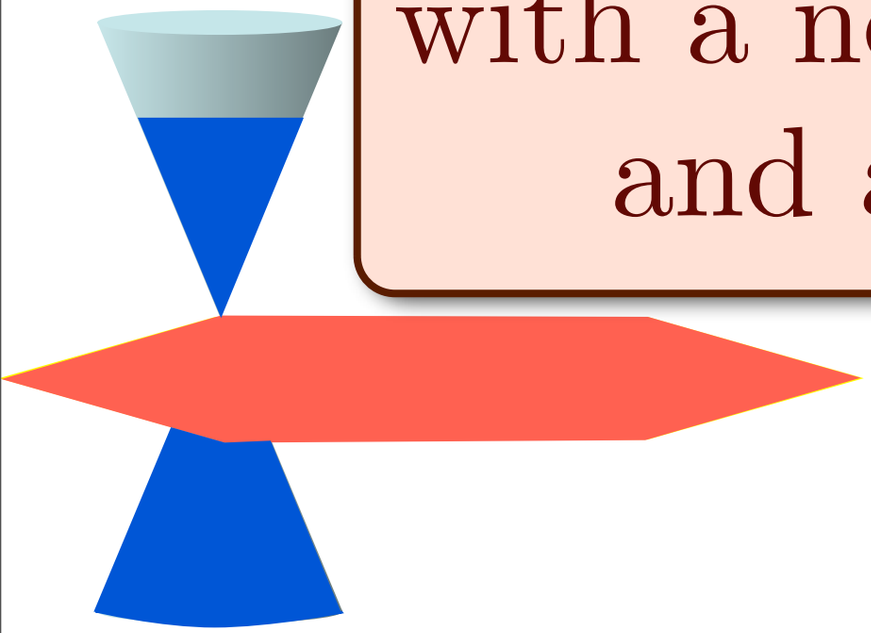

Einstein gravity on AdS_4
with a Reissner-Nordstrom
black hole carrying electric
and magnetic charges

Electrical and thermal dynamics of graphene in quantum critical regime (with $k_B T$ larger than energy scales determined by ω, μ, and B

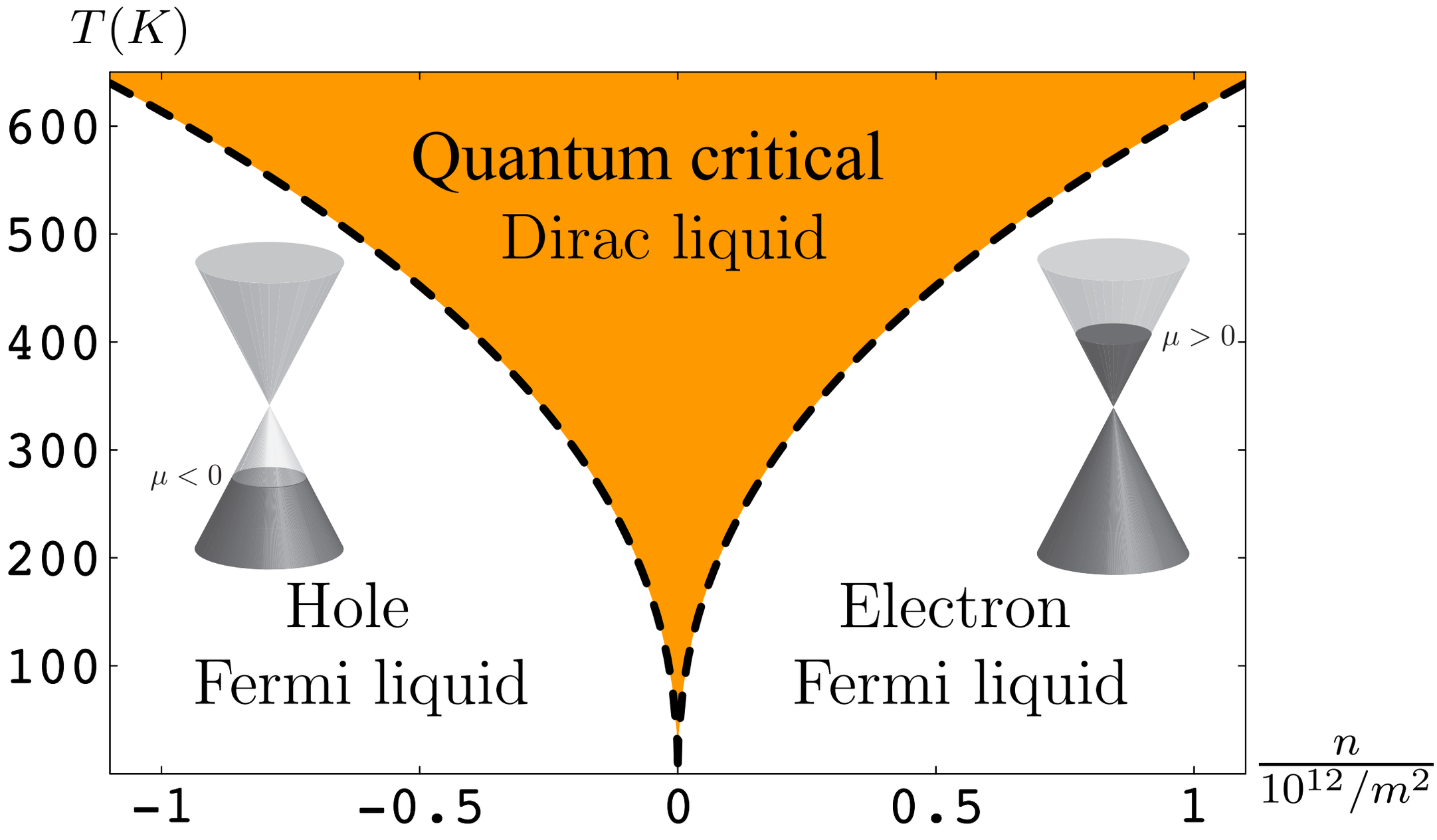

S.A. Hartnoll, P.K. Kovtun, M. Müller, and S. Sachdev, *Phys. Rev.* B **76** 144502 (2007)

Electrical and thermal dynamics of graphene in quantum critical regime (with $k_B T$ larger than energy scales determined by ω, μ, and B

$\Rightarrow$ maps onto quasinormal modes of a Reissner-Nordstorm black hole in AdS_4.

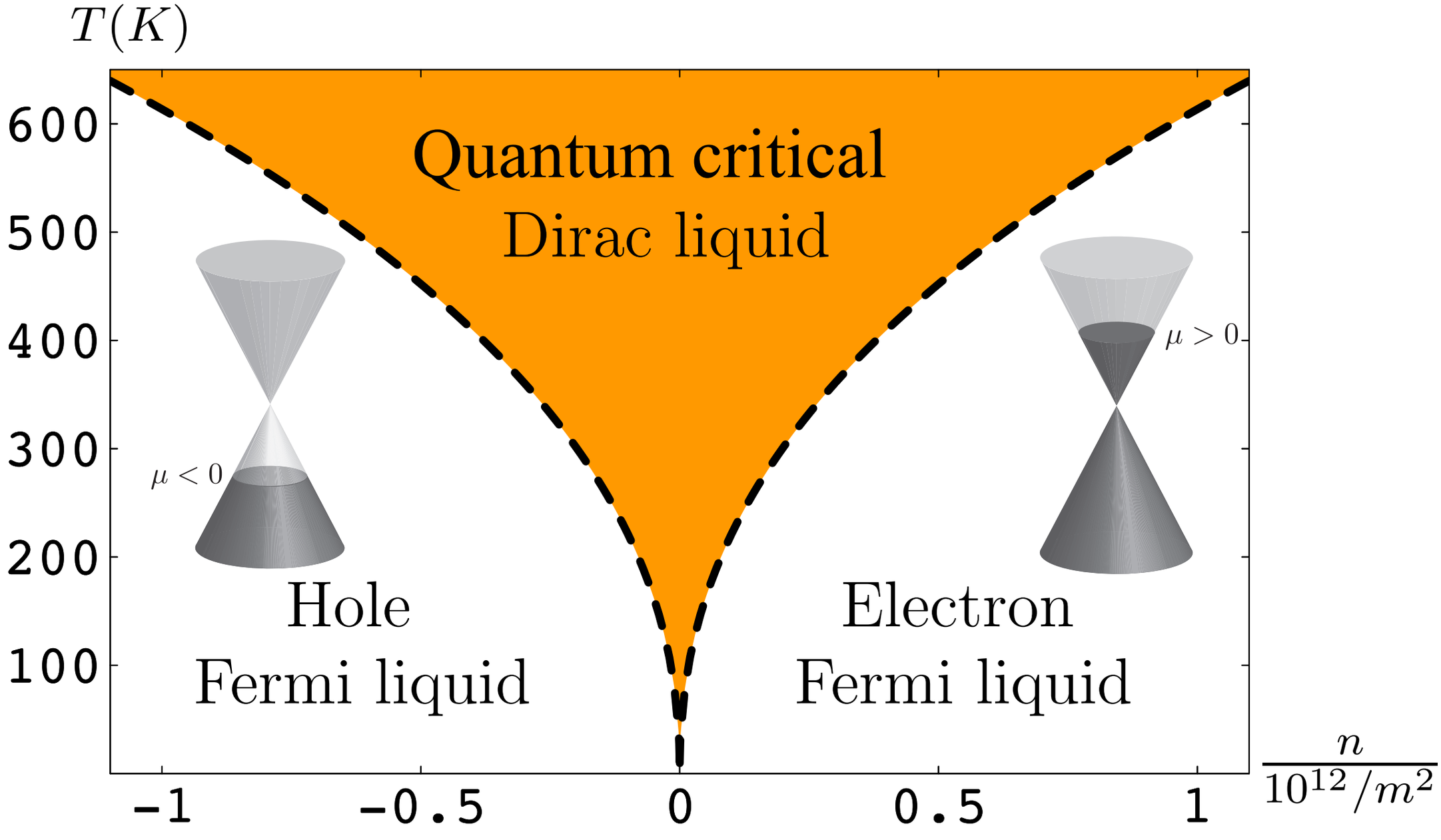

S.A. Hartnoll, P.K. Kovtun, M. Müller, and S. Sachdev, *Phys. Rev.* B **76** 144502 (2007)

Magnetohydrodynamics of quantum criticality

We used the AdS/CFT connection to derive many new relations between thermoelectric transport co-efficients in the quantum critical regime.

S.A. Hartnoll, P.K. Kovtun, M. Müller, and S. Sachdev, *Phys. Rev.* B **76** 144502 (2007)

Magnetohydrodynamics of quantum criticality

We used the AdS/CFT connection to derive many new relations between thermoelectric transport co-efficients in the quantum critical regime.

The **same** results were later obtained from the equations of generalized relativistic magnetohydrodynamics, *and* from a solution of the quantum Boltzmann equation.

So the results apply to experiments on graphene, the cuprates, *and* to the dynamics of black holes.

S.A. Hartnoll, P.K. Kovtun, M. Müller, and S. Sachdev, *Phys. Rev.* B **76** 144502 (2007)

Magnetohydrodynamics of quantum criticality

We used the AdS/CFT connection to derive many new relations between thermoelectric transport co-efficients in the quantum critical regime.

As a simple example, in zero magnetic field, we can write the electrical conductivity as

$$\sigma = \sigma_Q + \frac{e^{*2}\rho^2 v^2}{\varepsilon + P}\pi\delta(\omega)$$

where σ_Q is the universal conductivity of the CFT, ρ is the charge density, ε is the energy density and P is the pressure.

Magnetohydrodynamics of quantum criticality

We used the AdS/CFT connection to derive many new relations between thermoelectric transport co-efficients in the quantum critical regime.

The same quantities also determine a "Wiedemann-Franz"-like relation for thermal conductivity, κ at $B = 0$

$$\kappa = \sigma_Q \left(\frac{k_B^2 T}{e^{*2}}\right) \left(\frac{\varepsilon + P}{k_B T \rho}\right)^2 .$$

At $B \neq 0$ and $\rho = 0$ we have a "Wiedemann-Franz" relation for "vortices"

$$\kappa = \frac{1}{\sigma_Q} k_B^2 T \left(\frac{v(\varepsilon + P)}{k_B T B}\right)^2 .$$

Magnetohydrodynamics of quantum criticality

We used the AdS/CFT connection to derive many new relations between thermoelectric transport co-efficients in the quantum critical regime.

A second example: In an applied magnetic field B, the dynamic transport co-efficients exhibit a **hydrodynamic cyclotron resonance** at a frequency ω_c

$$\omega_c = \frac{e^* B \rho v^2}{c(\varepsilon + P)}$$

and damping constant γ

$$\gamma = \sigma_Q \frac{B^2 v^2}{c^2(\varepsilon + P)}.$$

The same constants determine the **quasinormal frequency** of the Reissner-Nordstrom black hole.

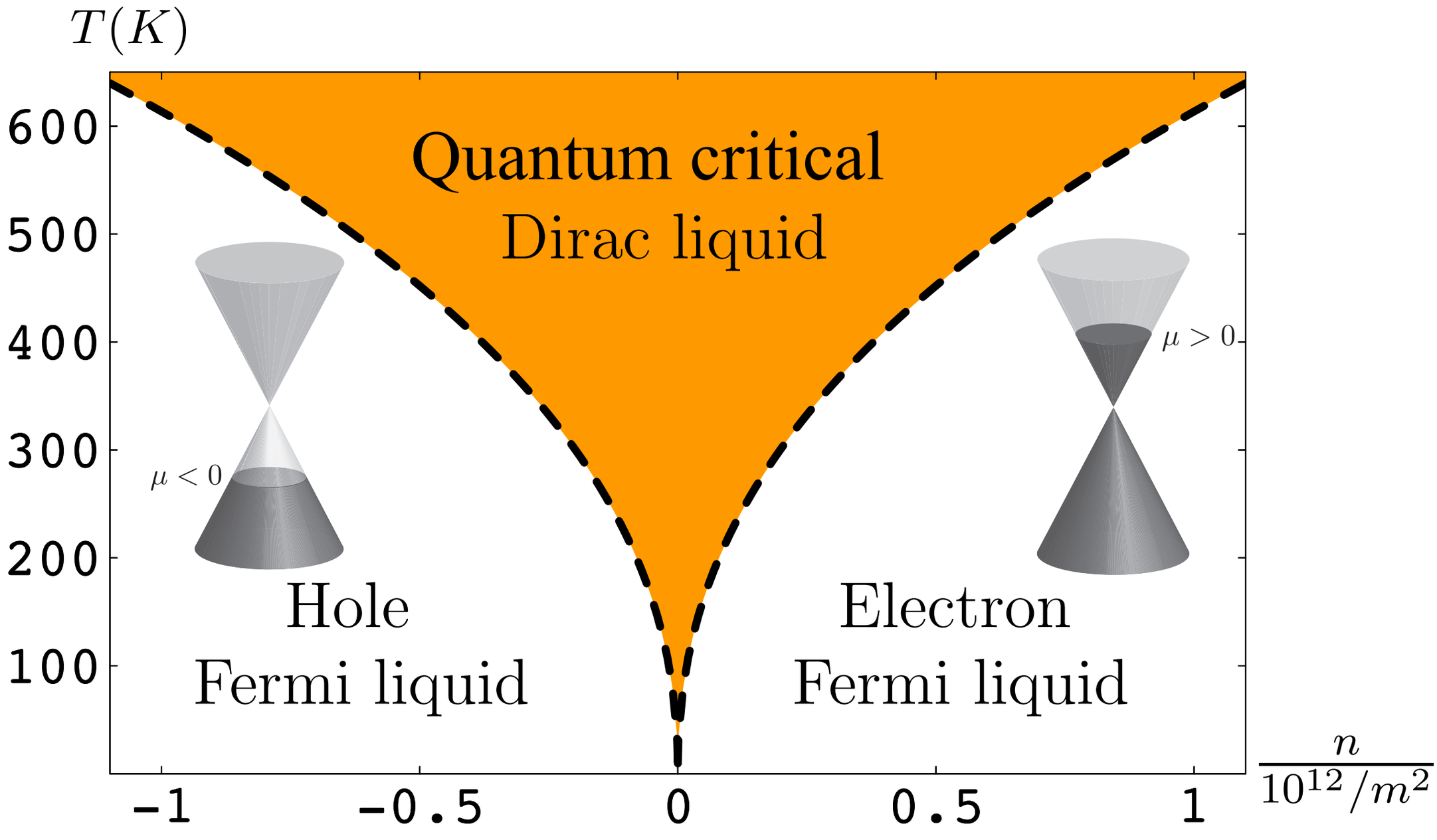

S.A. Hartnoll, P.K. Kovtun, M. Müller, and S. Sachdev, *Phys. Rev.* B **76** 144502 (2007)

At low T graphene is a Fermi liquid

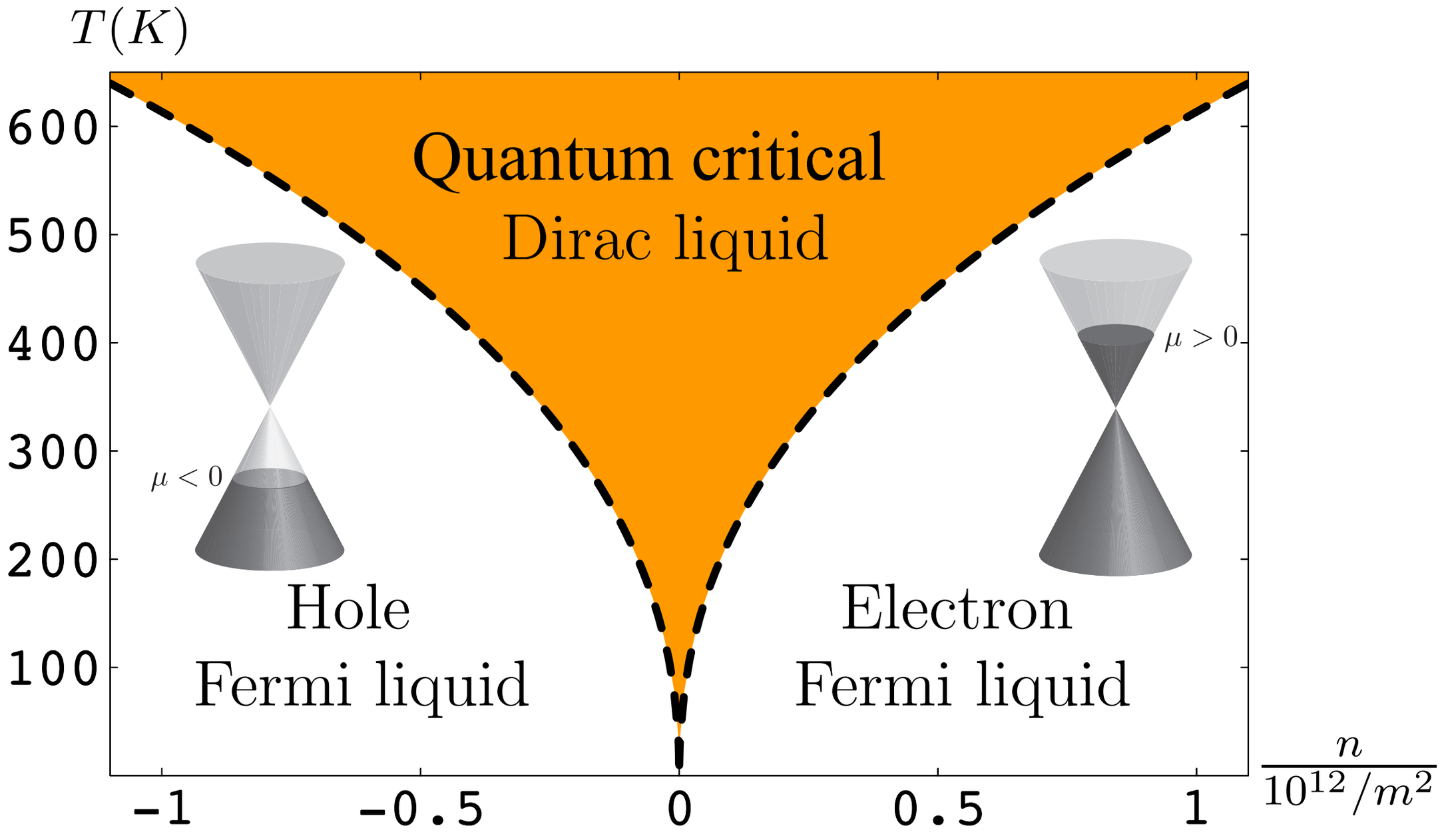

S.A. Hartnoll, P.K. Kovtun, M. Müller, and S. Sachdev, *Phys. Rev.* B **76** 144502 (2007)

At low T graphene is a Fermi liquid

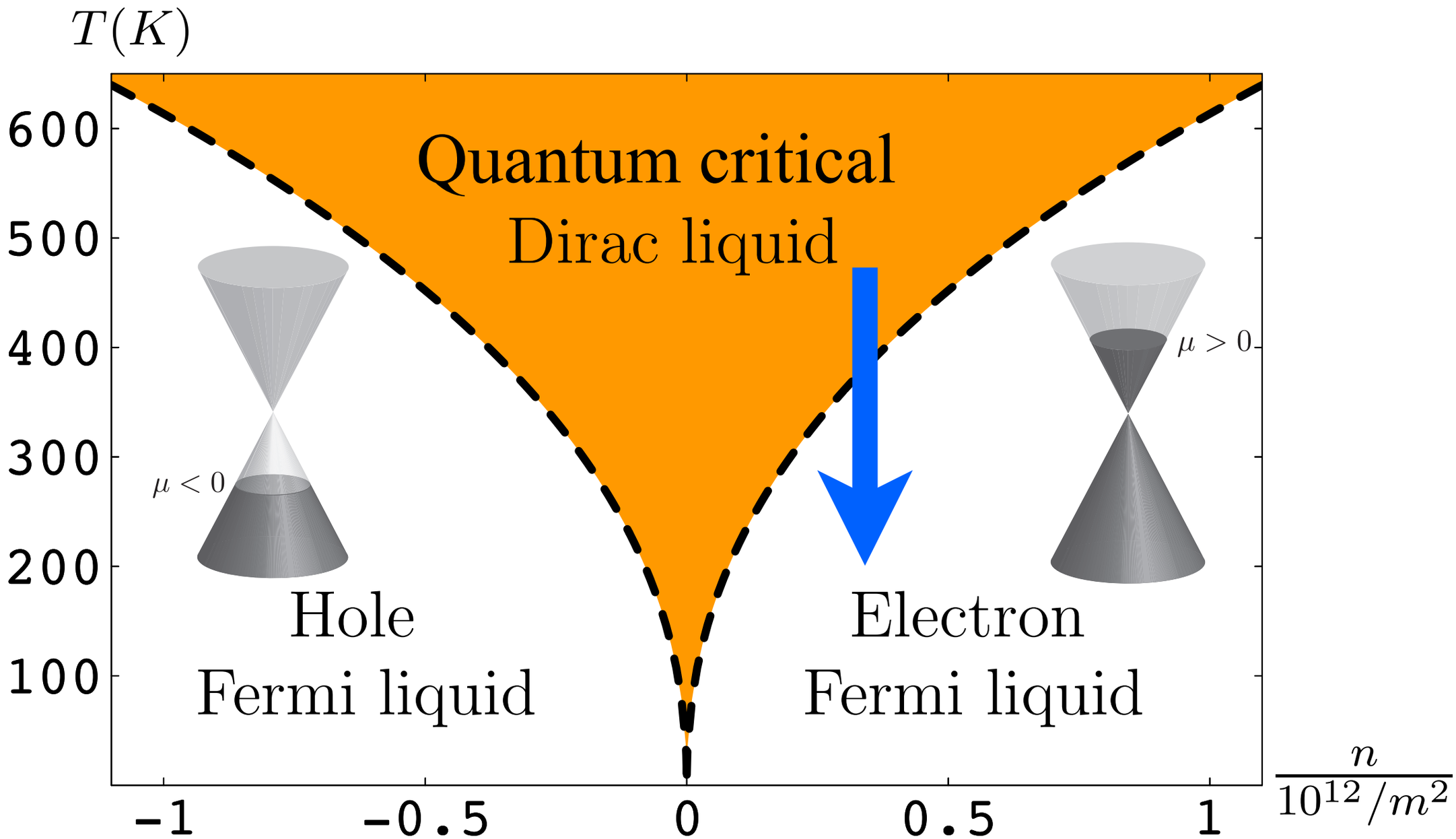

S.A. Hartnoll, P.K. Kovtun, M. Müller, and S. Sachdev, *Phys. Rev.* B **76** 144502 (2007)

At low T graphene is a Fermi liquid

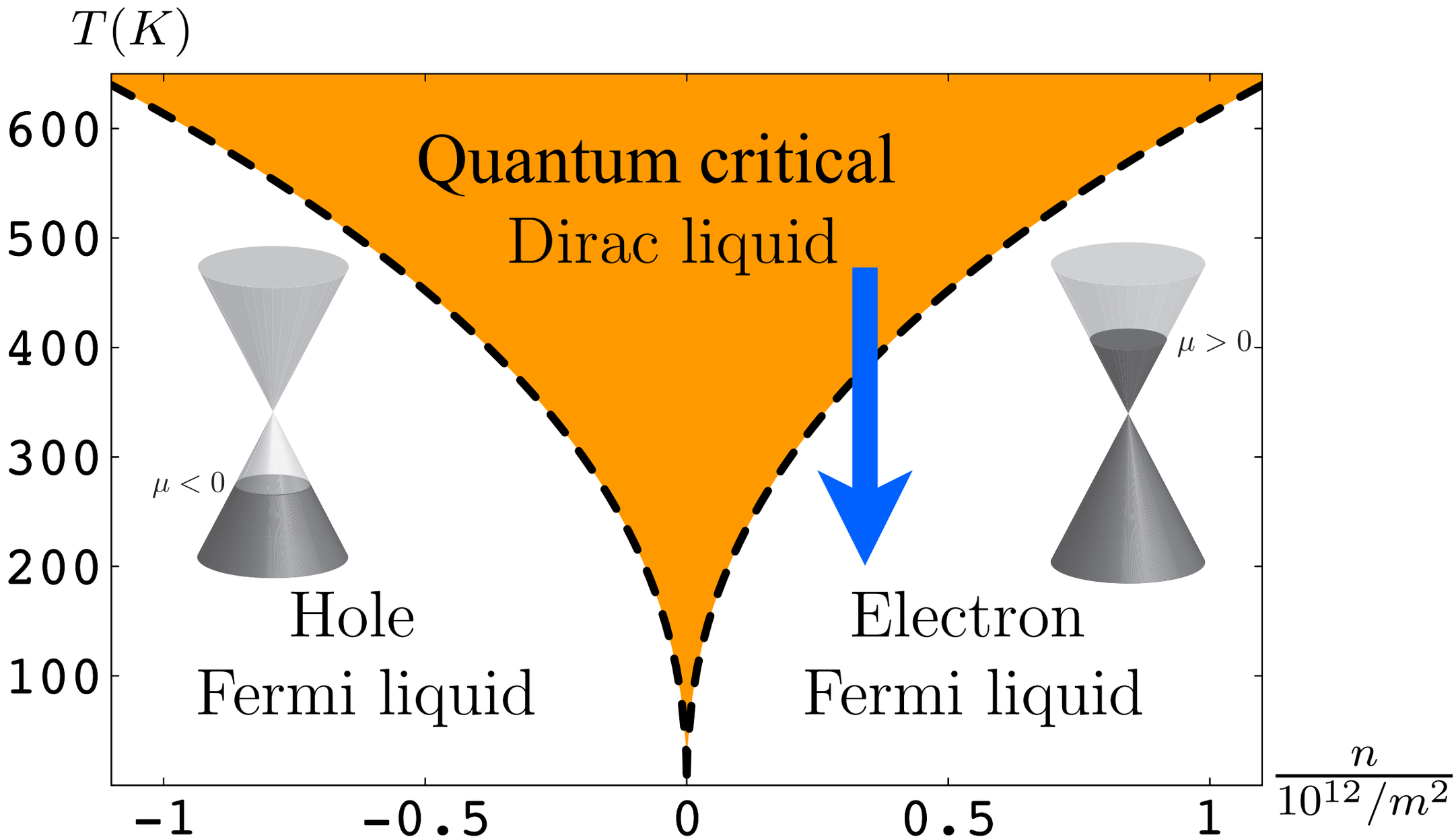

S.A. Hartnoll, P.K. Kovtun, M. Müller, and S. Sachdev, *Phys. Rev.* B **76** 144502 (2007)

At low T graphene is a Fermi liquid

What is the dual of the black hole theory at low T ?

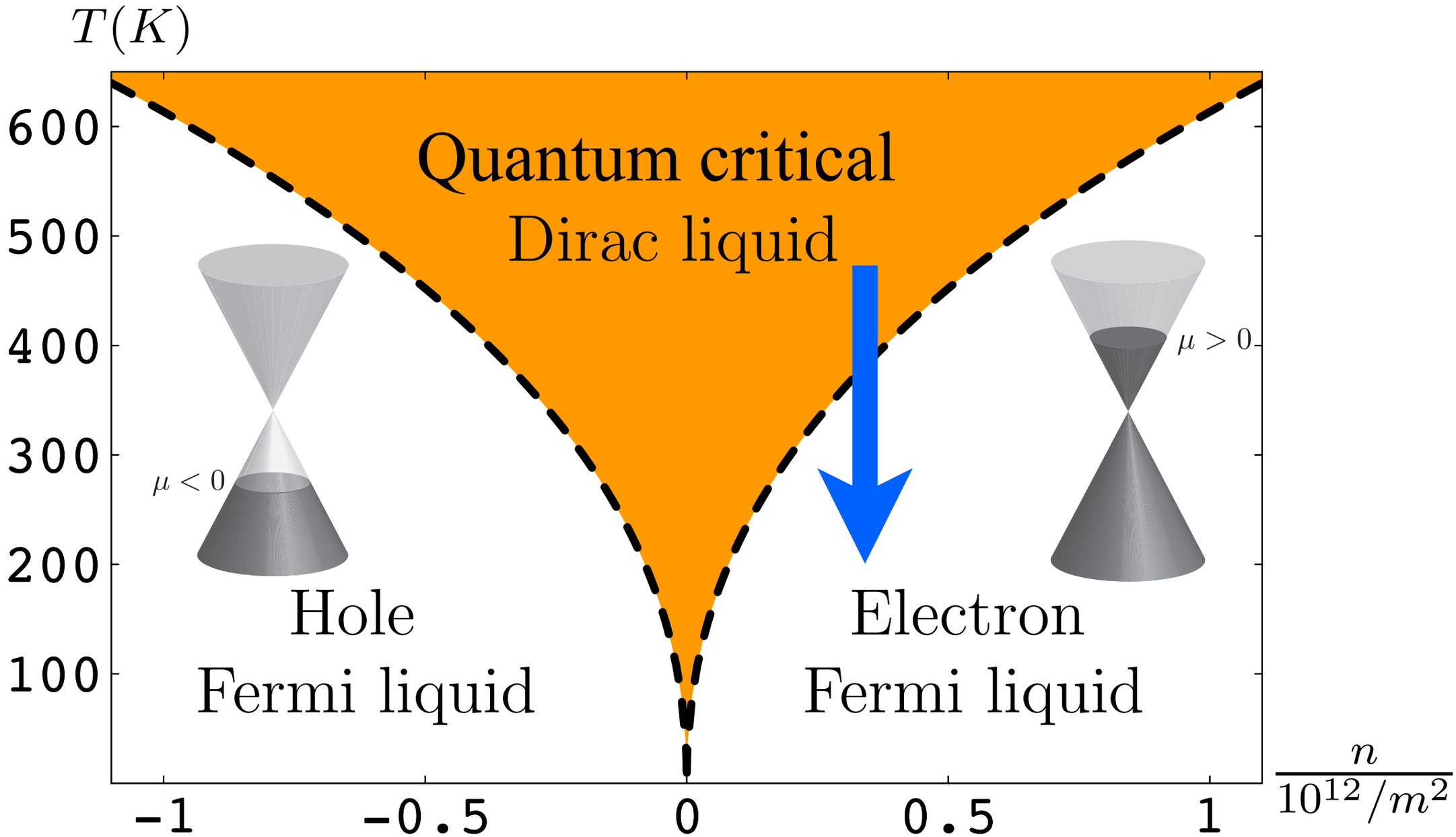

S.A. Hartnoll, P.K. Kovtun, M. Müller, and S. Sachdev, *Phys. Rev.* B **76** 144502 (2007)

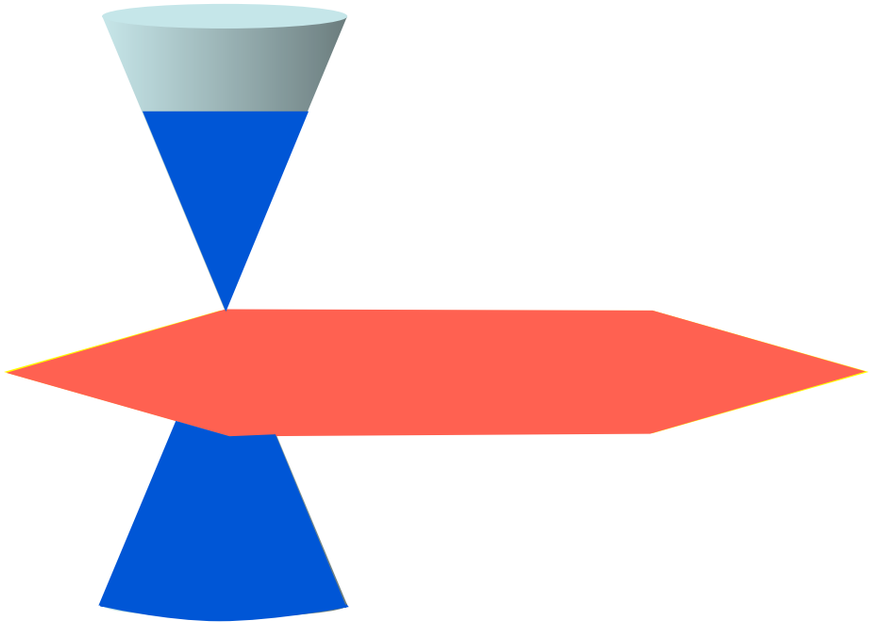

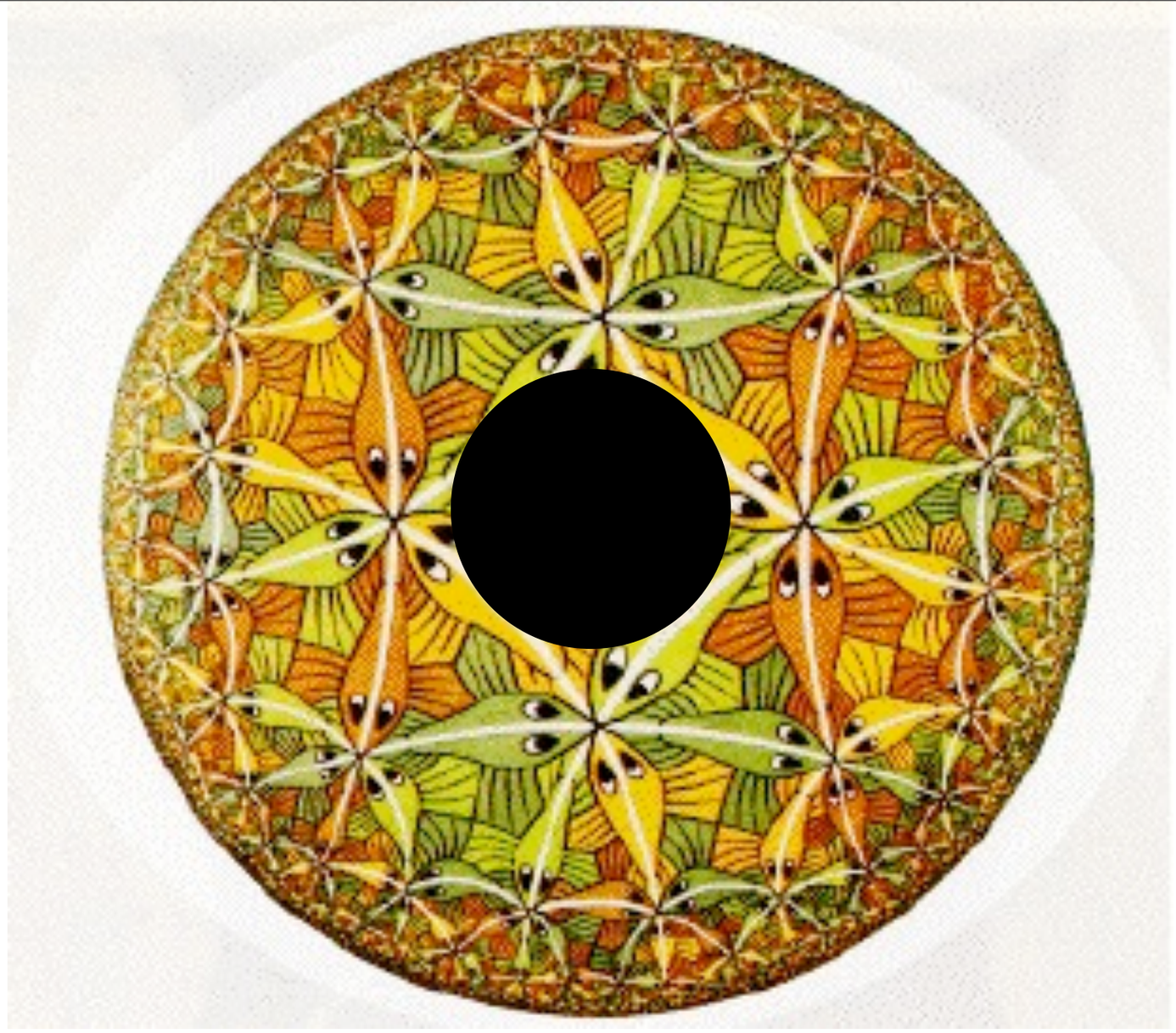

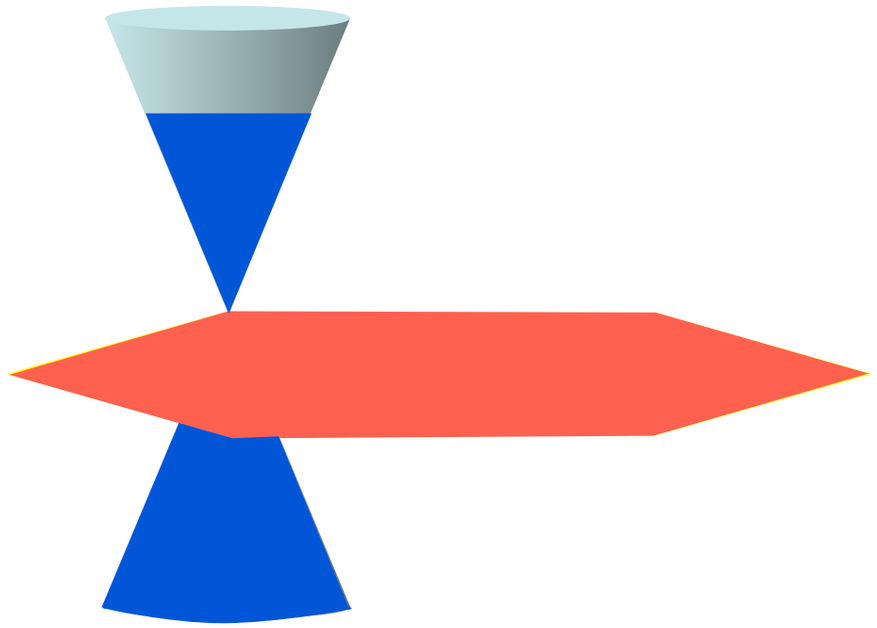

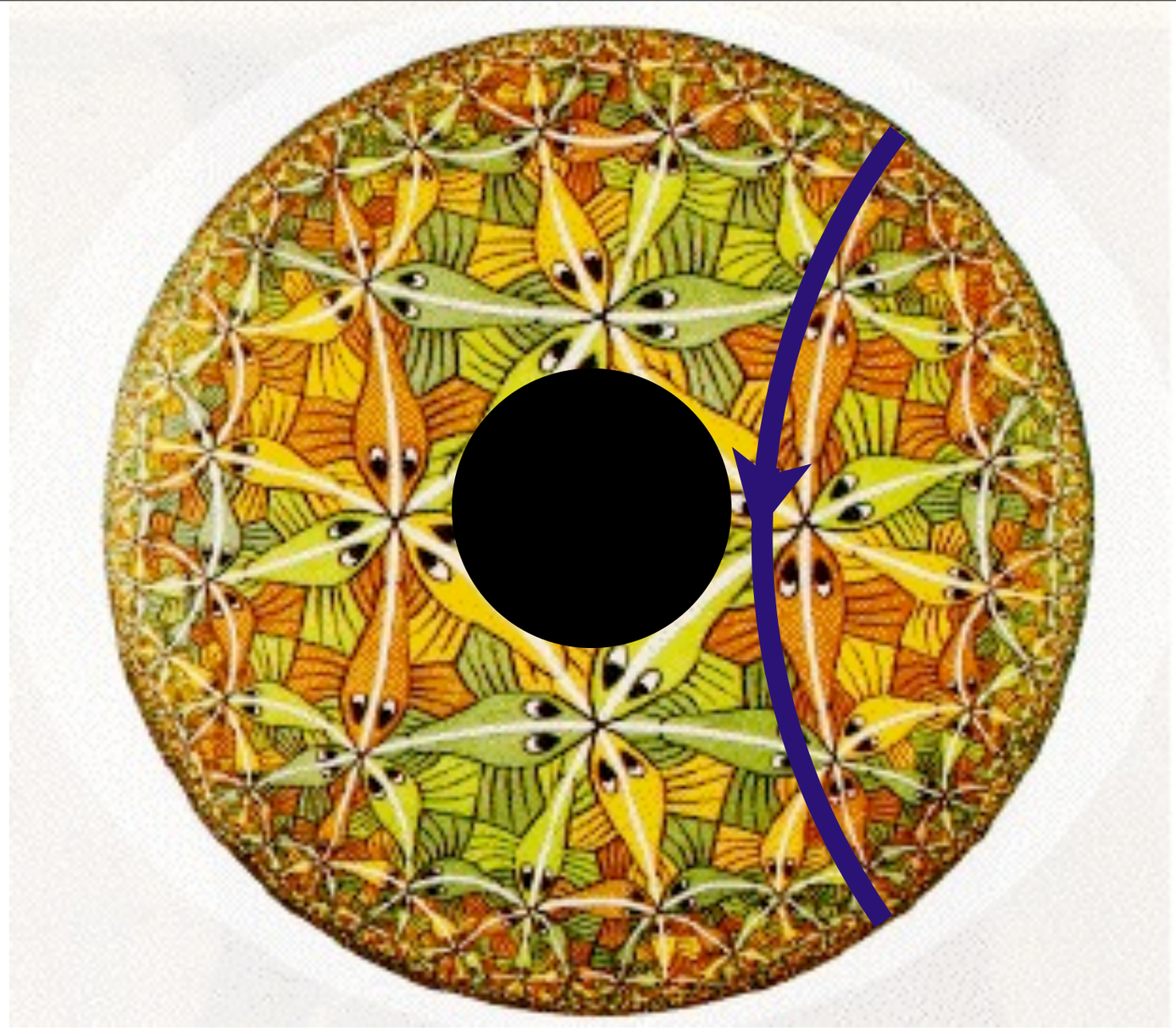

Examine free energy and Green's function of a probe particle

T. Faulkner, H. Liu, J. McGreevy, and D. Vegh, arXiv:0907.2694
F. Denef, S. Hartnoll, and S. Sachdev, arXiv:0908.1788

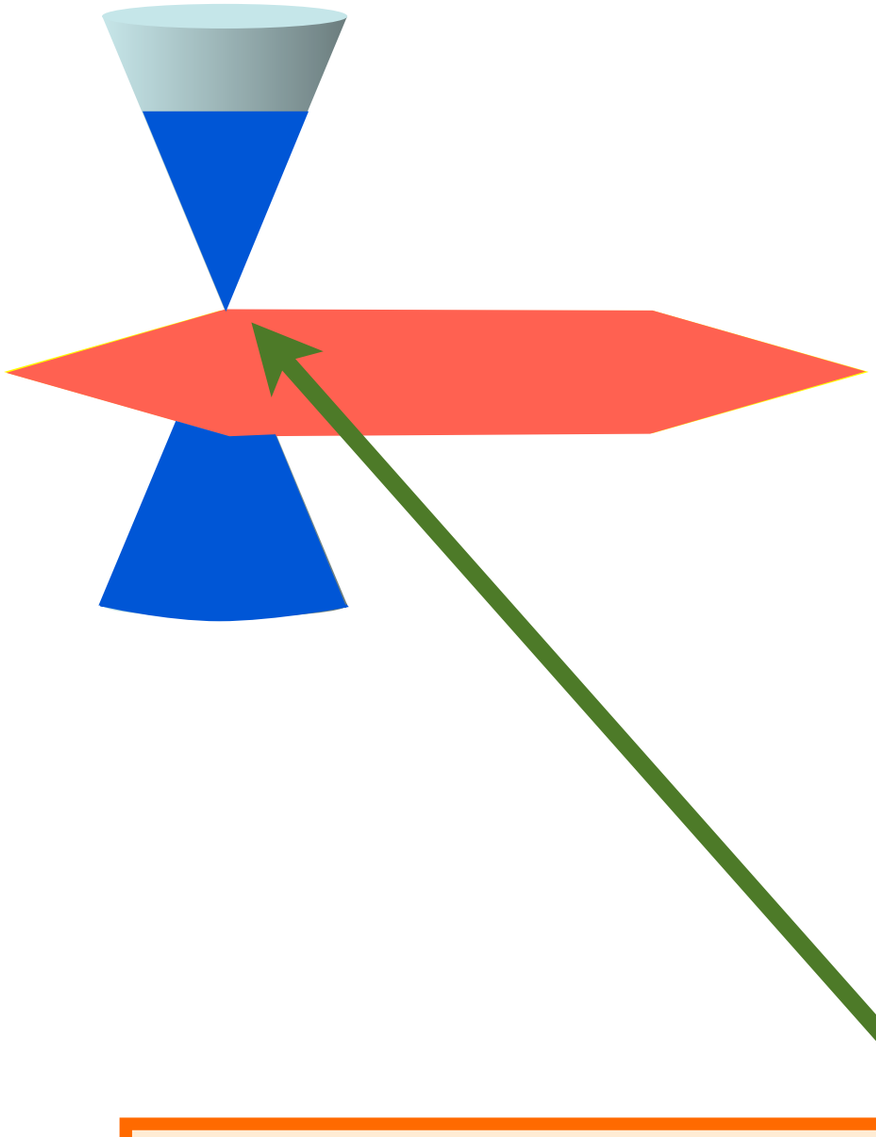

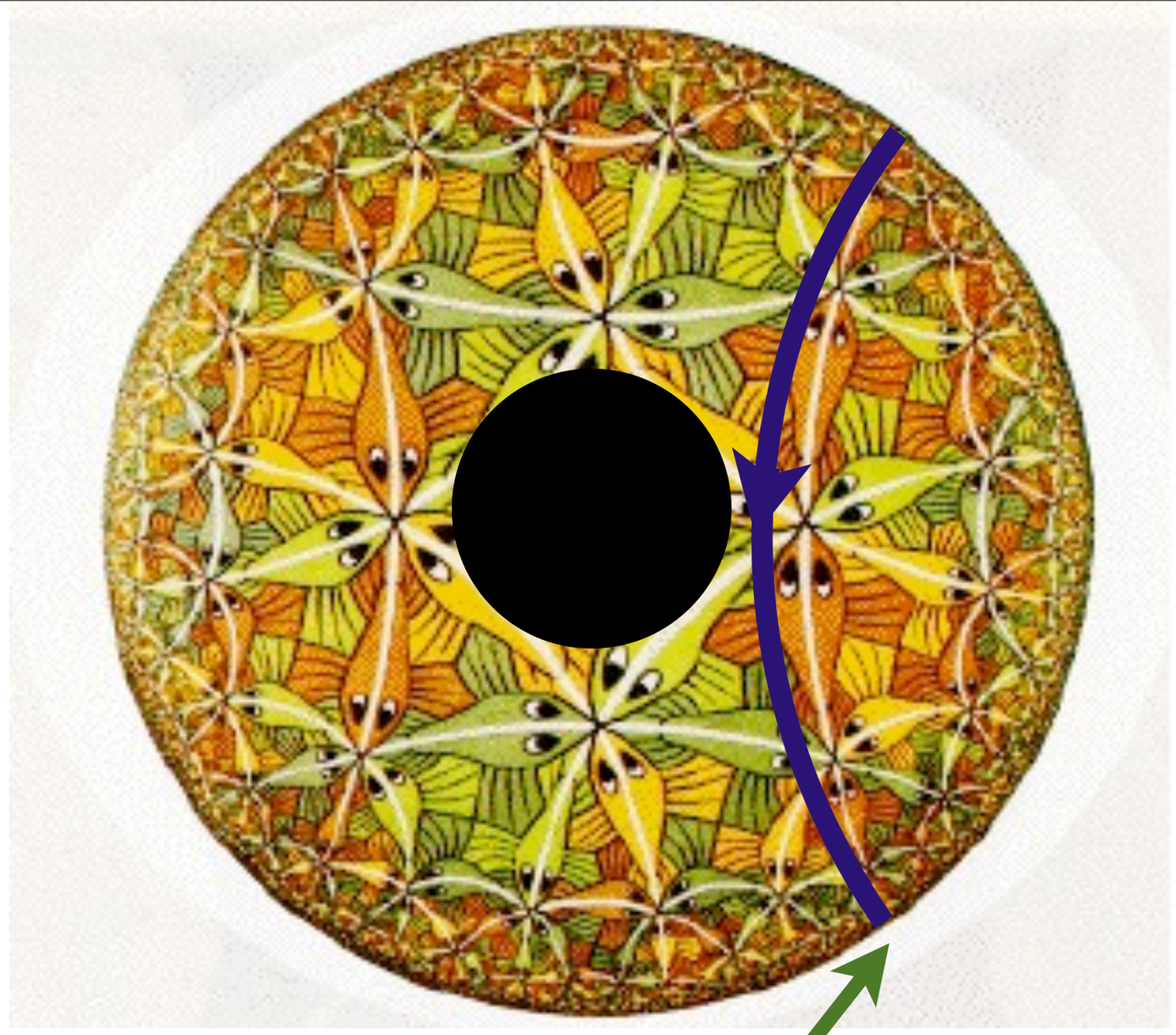

Short time behavior depends upon conformal AdS_4 geometry near boundary

T. Faulkner, H. Liu, J. McGreevy, and D. Vegh, arXiv:0907.2694
F. Denef, S. Hartnoll, and S. Sachdev, arXiv:0908.1788

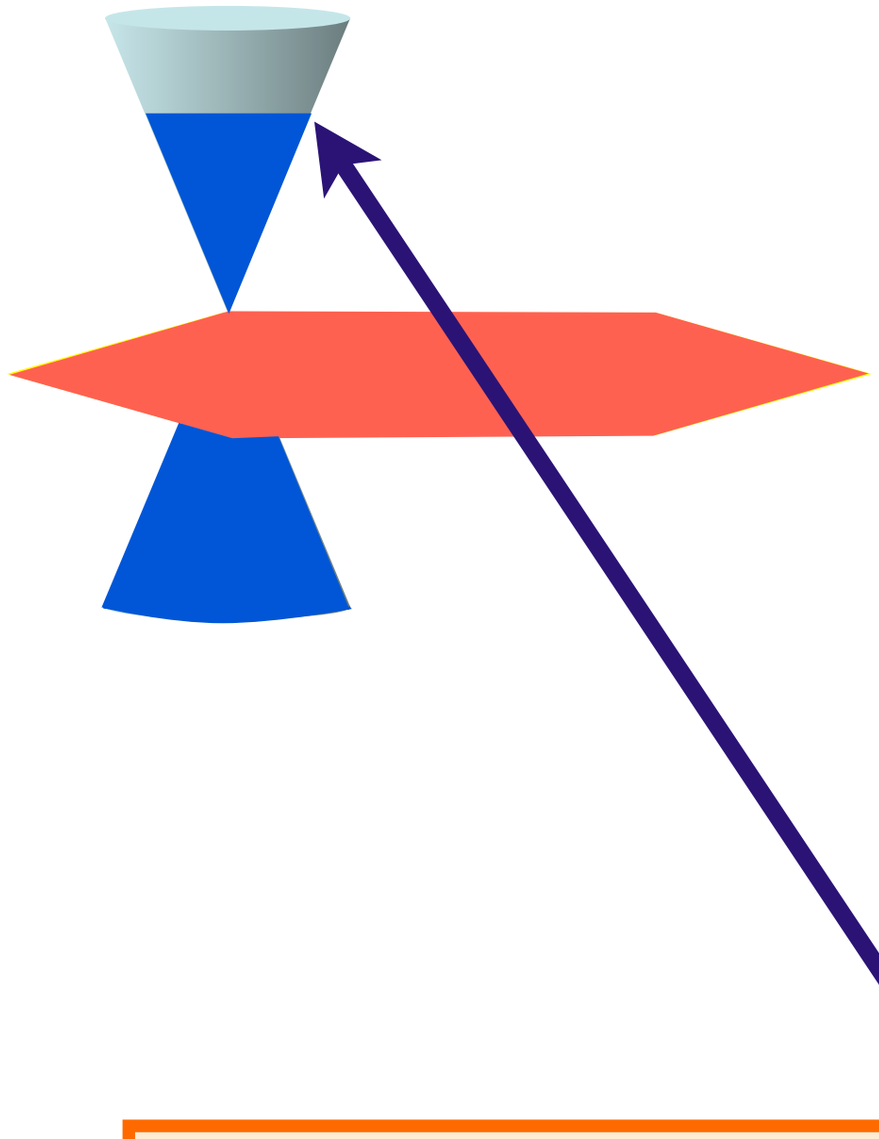

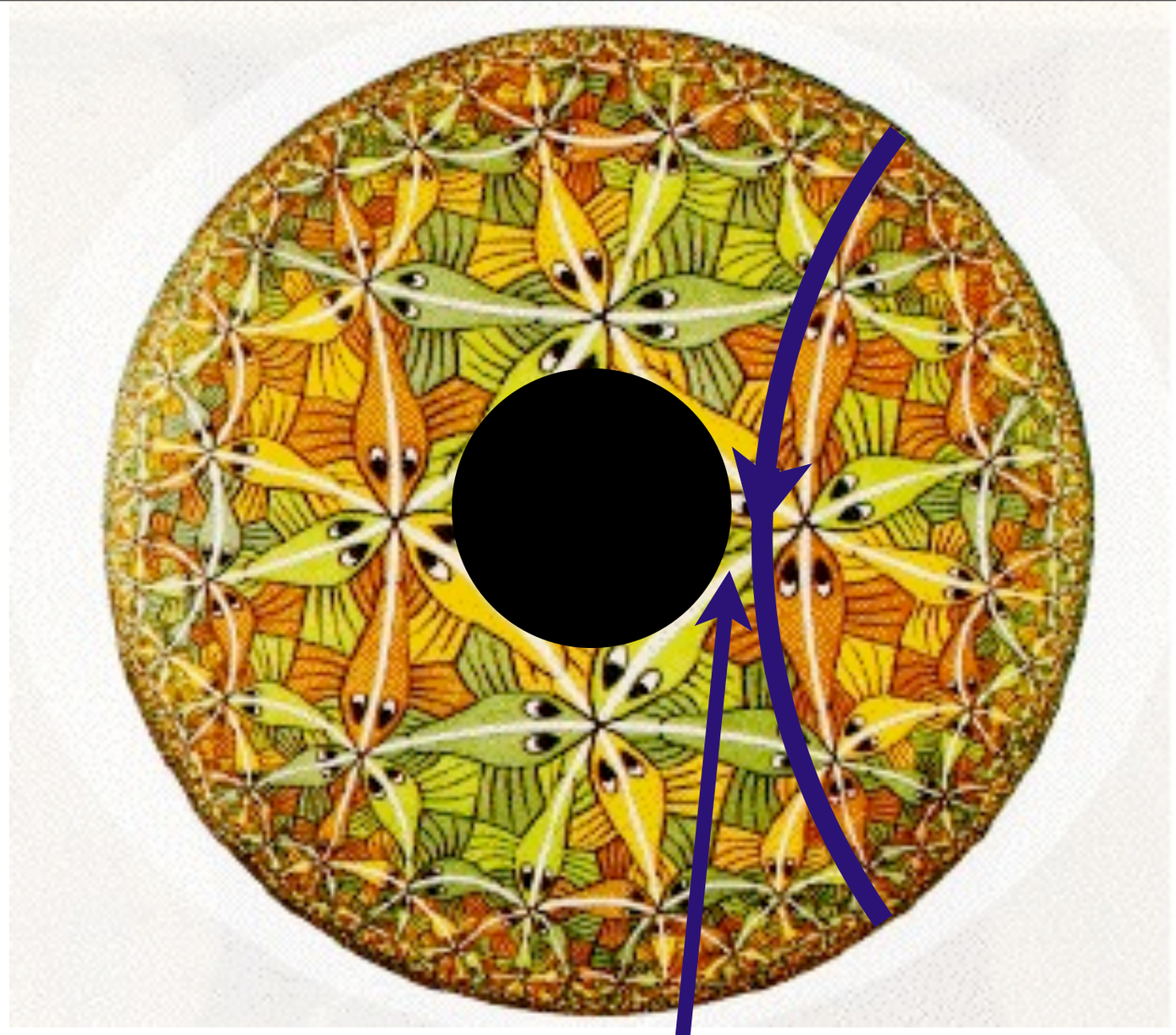

Long time behavior depends upon
near-horizon geometry of black hole

T. Faulkner, H. Liu, J. McGreevy, and D. Vegh, arXiv:0907.2694
F. Denef, S. Hartnoll, and S. Sachdev, arXiv:0908.1788

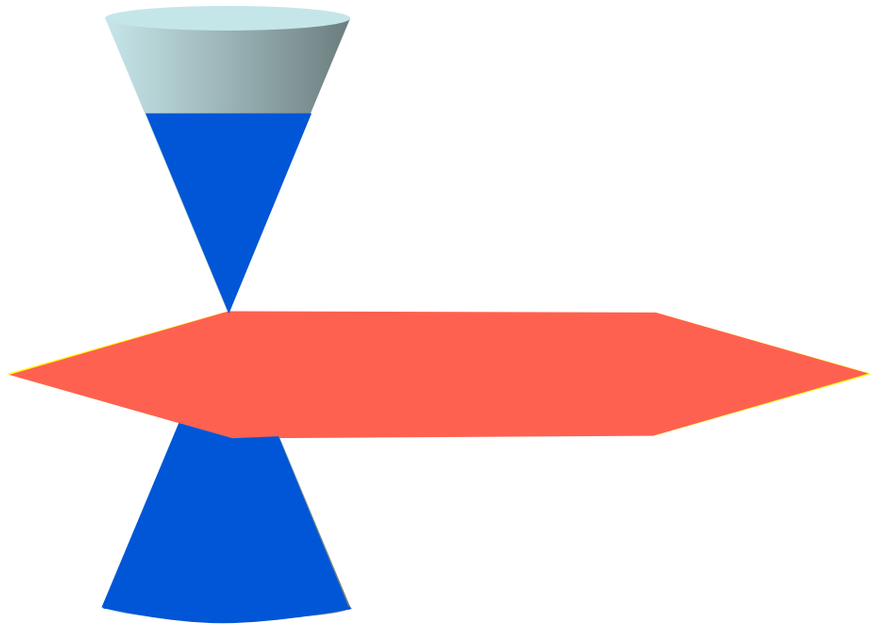

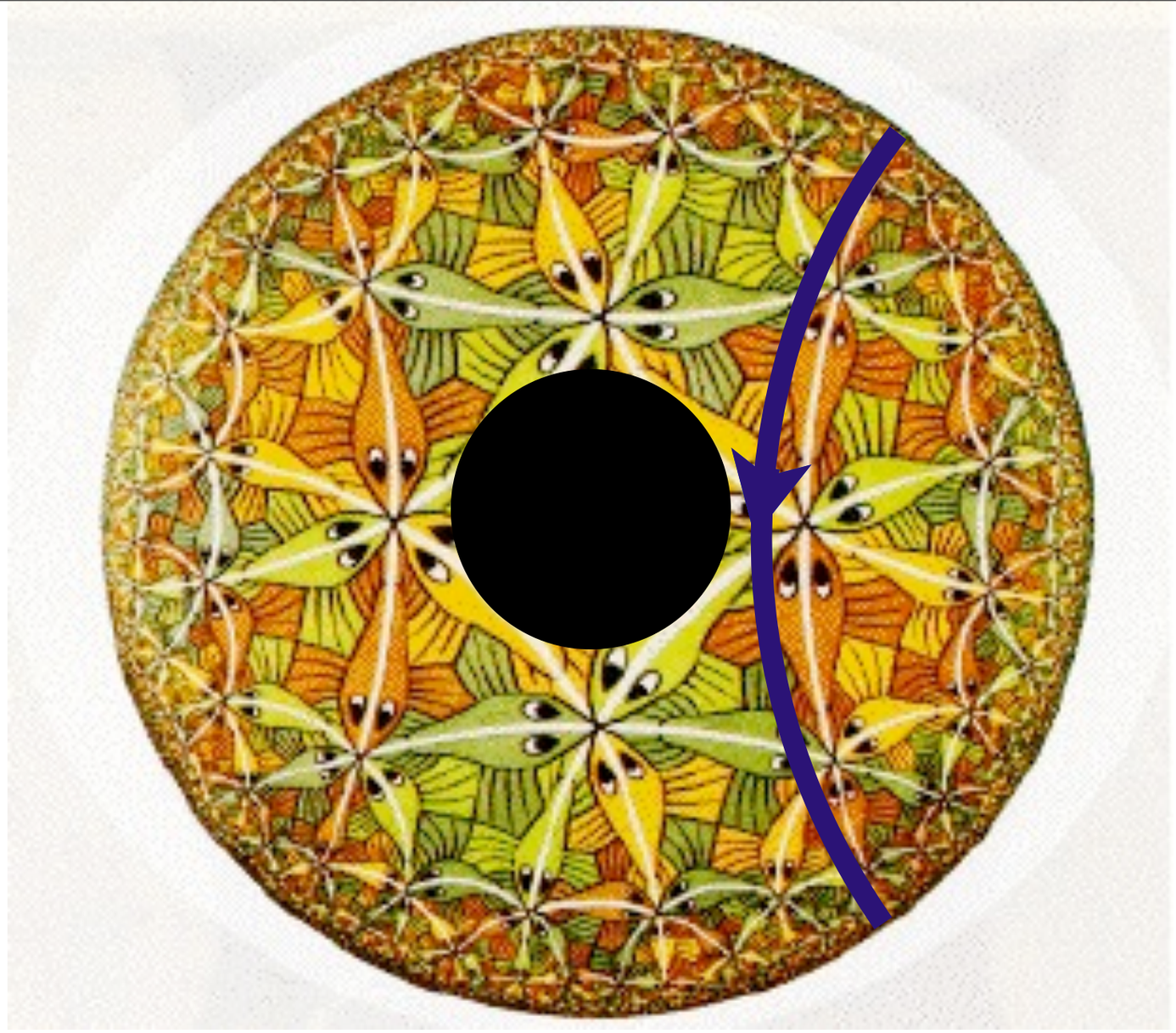

Radial direction of gravity theory is measure of energy scale in CFT

T. Faulkner, H. Liu, J. McGreevy, and D. Vegh, arXiv:0907.2694
F. Denef, S. Hartnoll, and S. Sachdev, arXiv:0908.1788

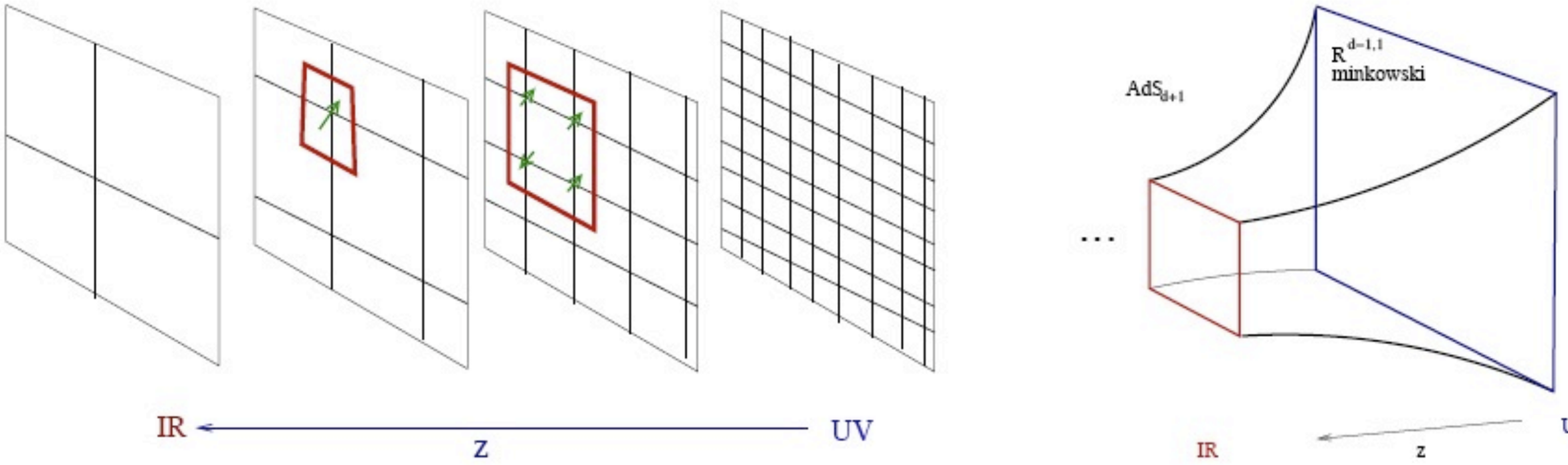

Figure 1: The extra ('radial') dimension of the bulk is the resolution scale of the field theory. The left figure indicates a series of block spin transformations labelled by a parameter z. The right figure is a cartoon of AdS space, which organizes the field theory information in the same way. In this sense, the bulk picture is a hologram: excitations with different wavelengths get put in different places in the bulk image.

J. McGreevy, arXiv0909.0518

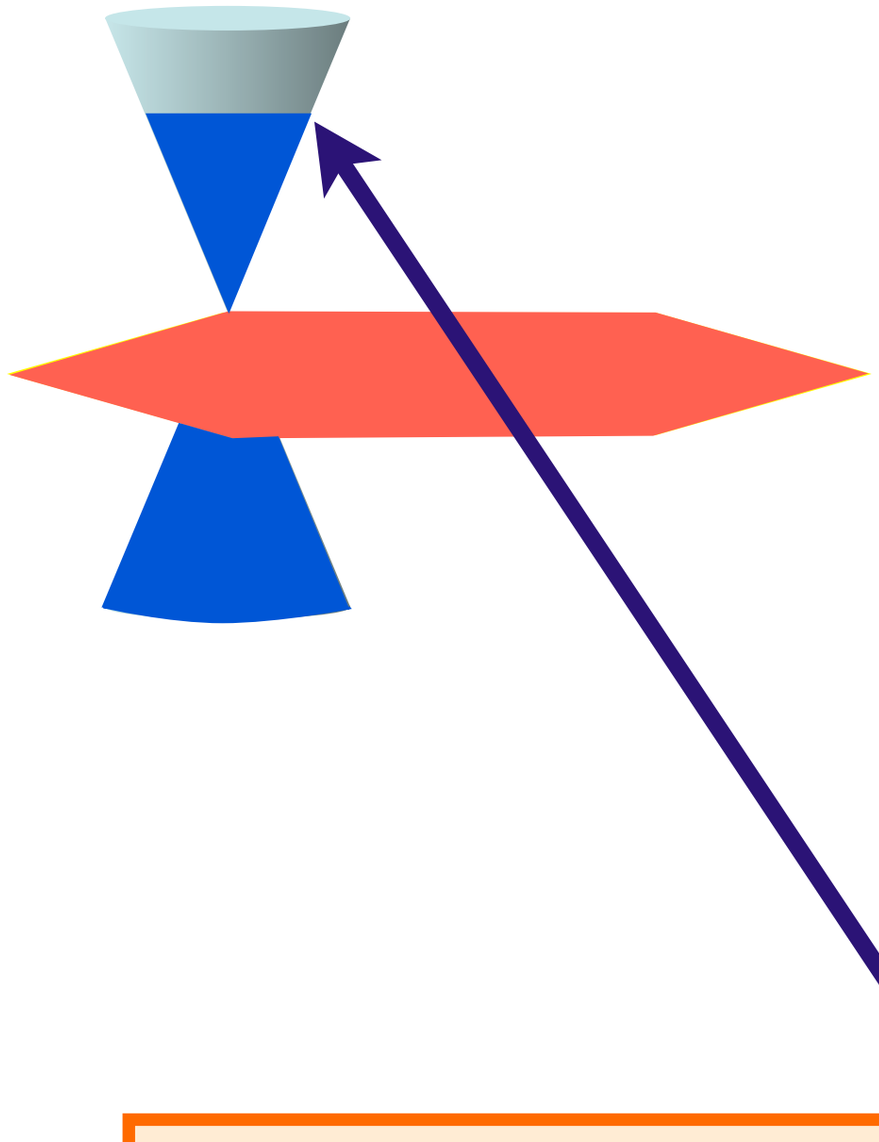

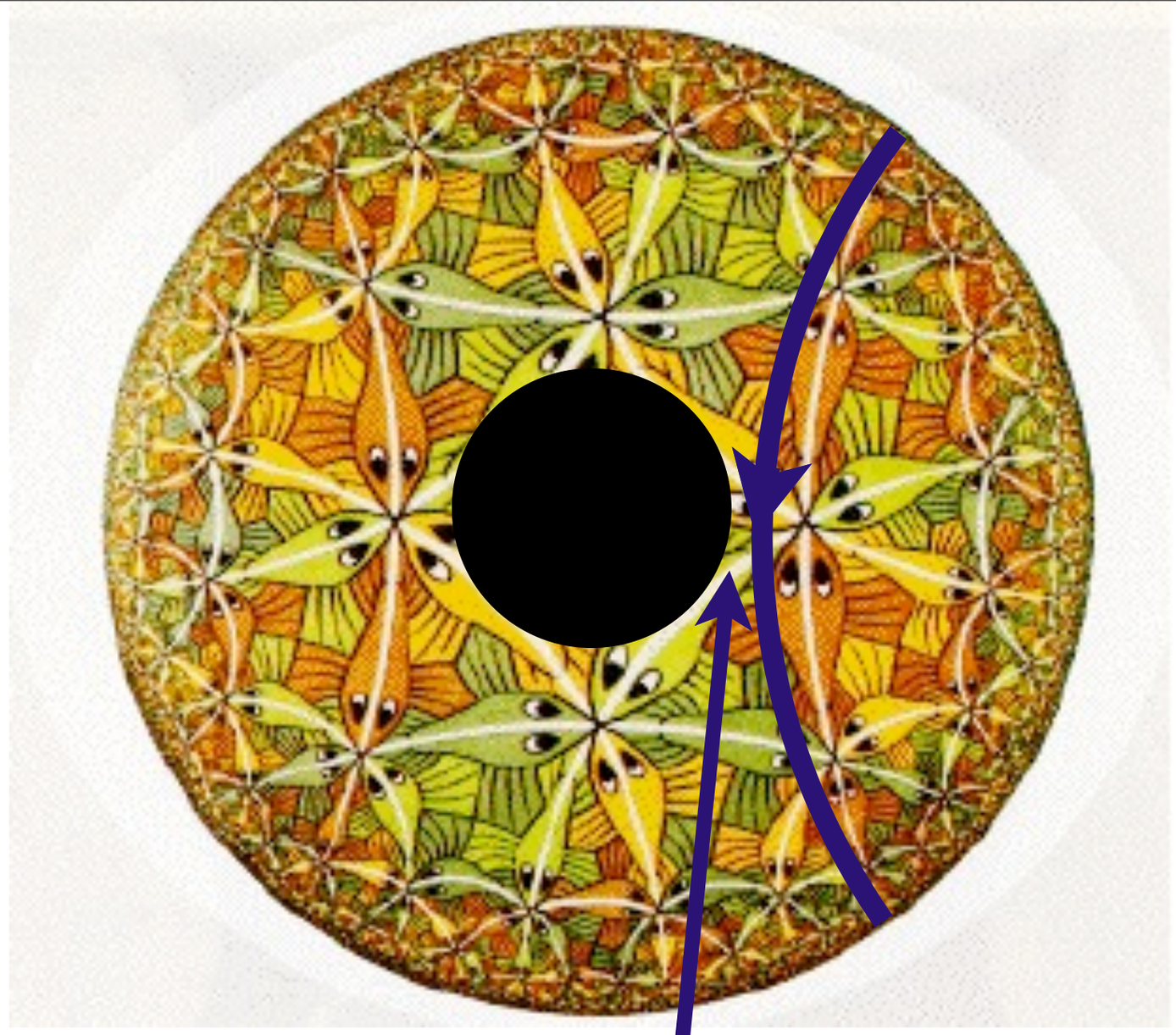

Infrared physics of Fermi surface is linked to the near horizon AdS_2 geometry of Reissner-Nordstrom black hole

T. Faulkner, H. Liu, J. McGreevy, and D. Vegh, arXiv:0907.2694

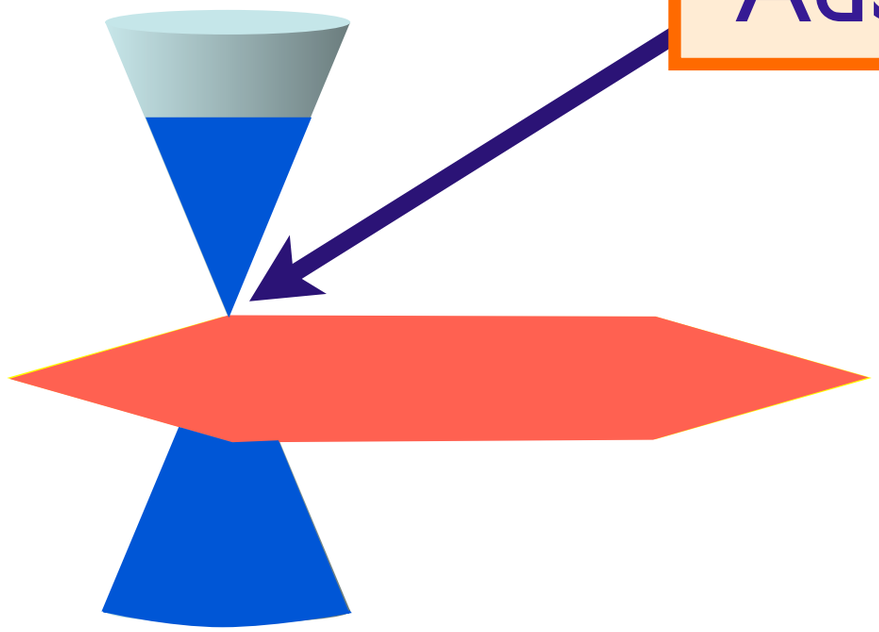

AdS_4

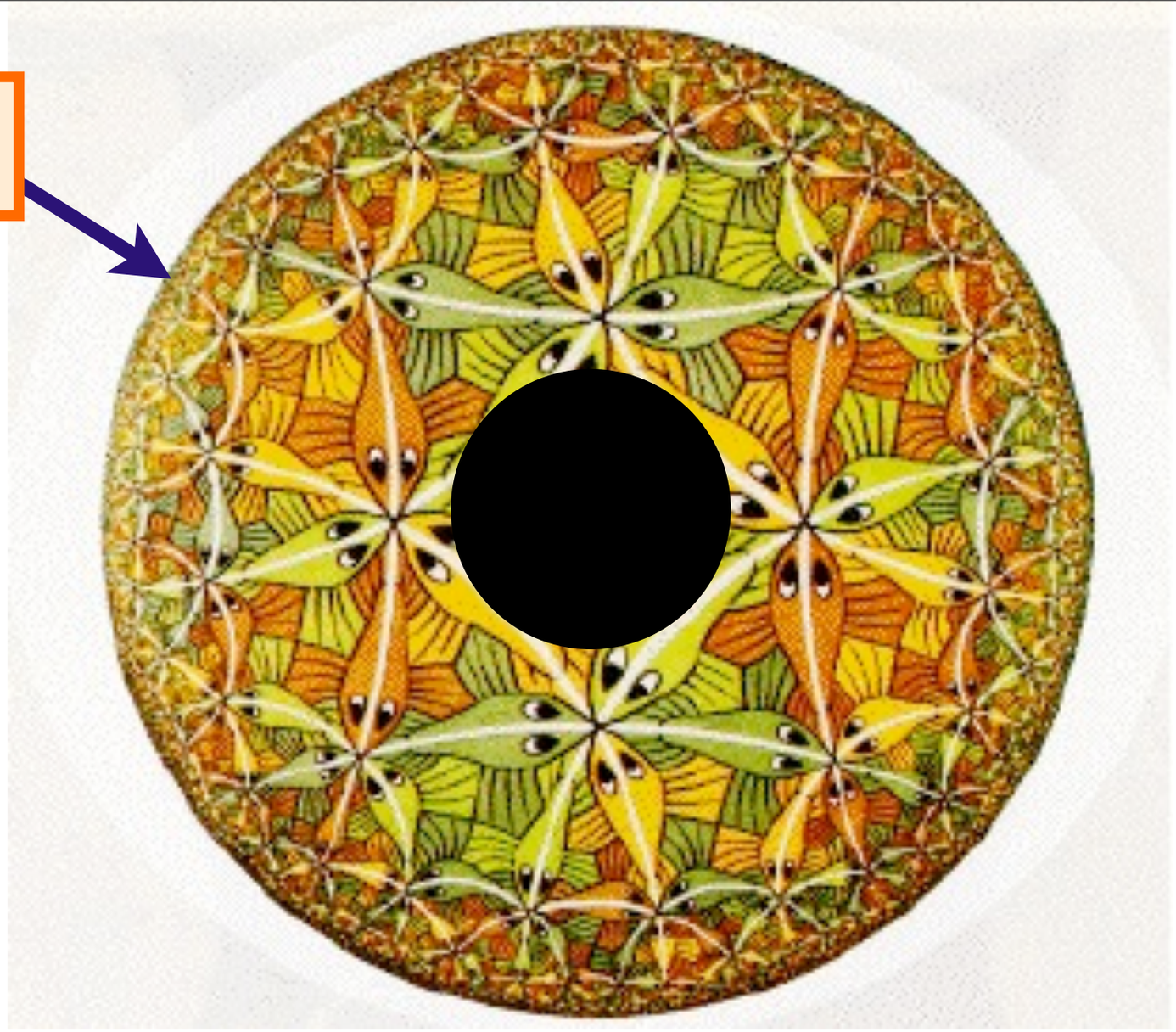

Geometric interpretation of RG flow

T. Faulkner, H. Liu, J. McGreevy, and D. Vegh, arXiv:0907.2694

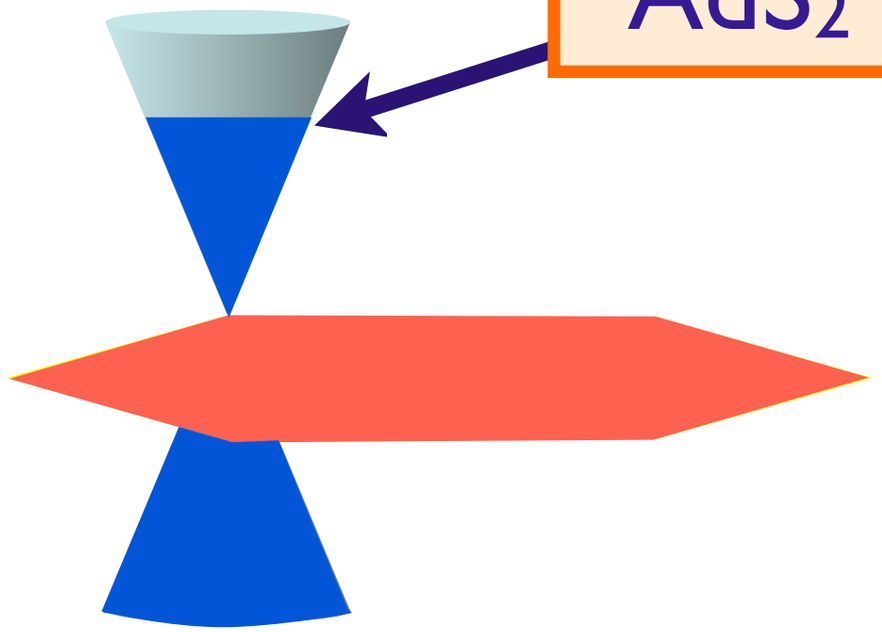

$AdS_2 \times R_2$

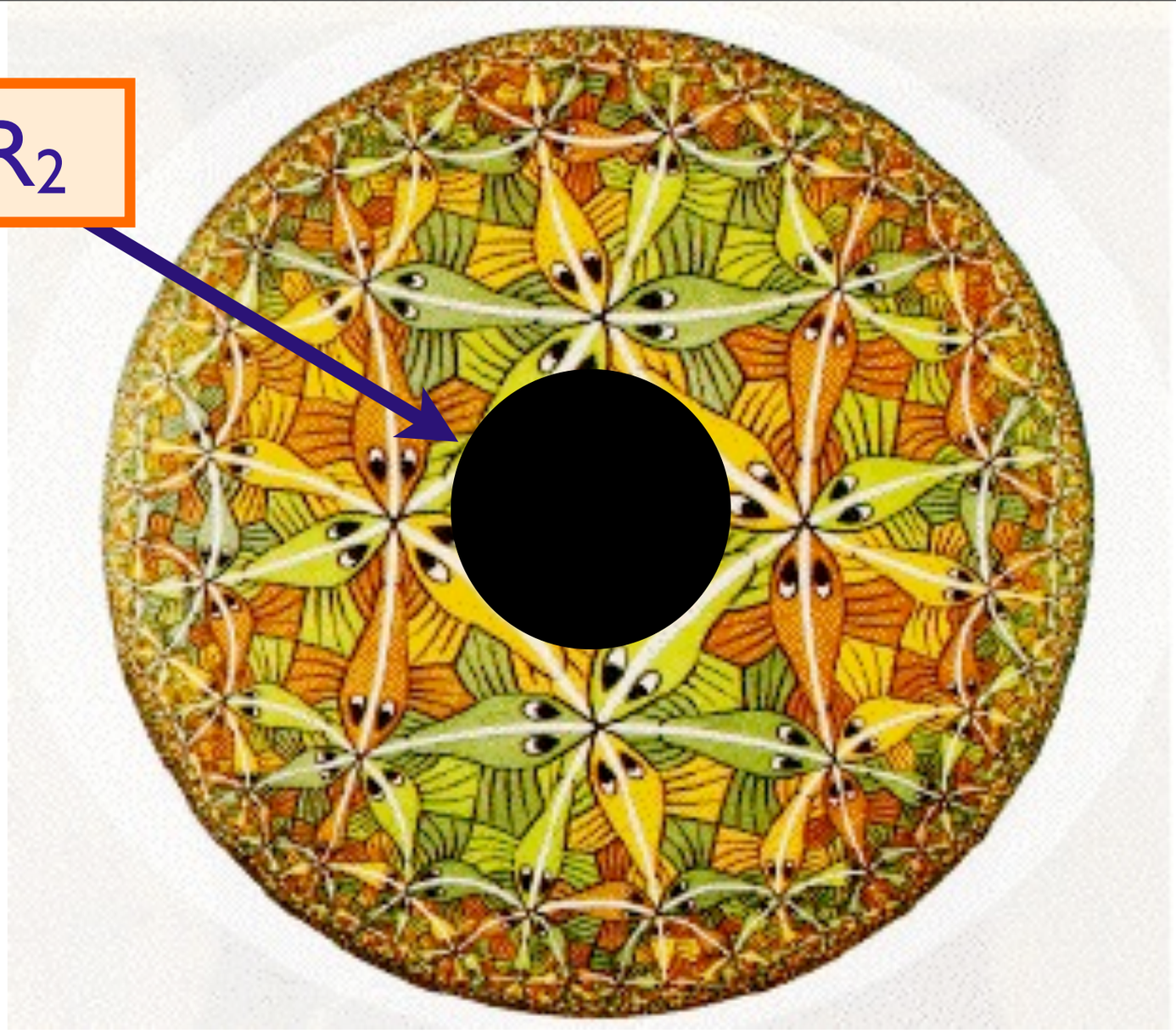

Geometric interpretation of RG flow

T. Faulkner, H. Liu, J. McGreevy, and D. Vegh, arXiv:0907.2694

Green's function of a fermion

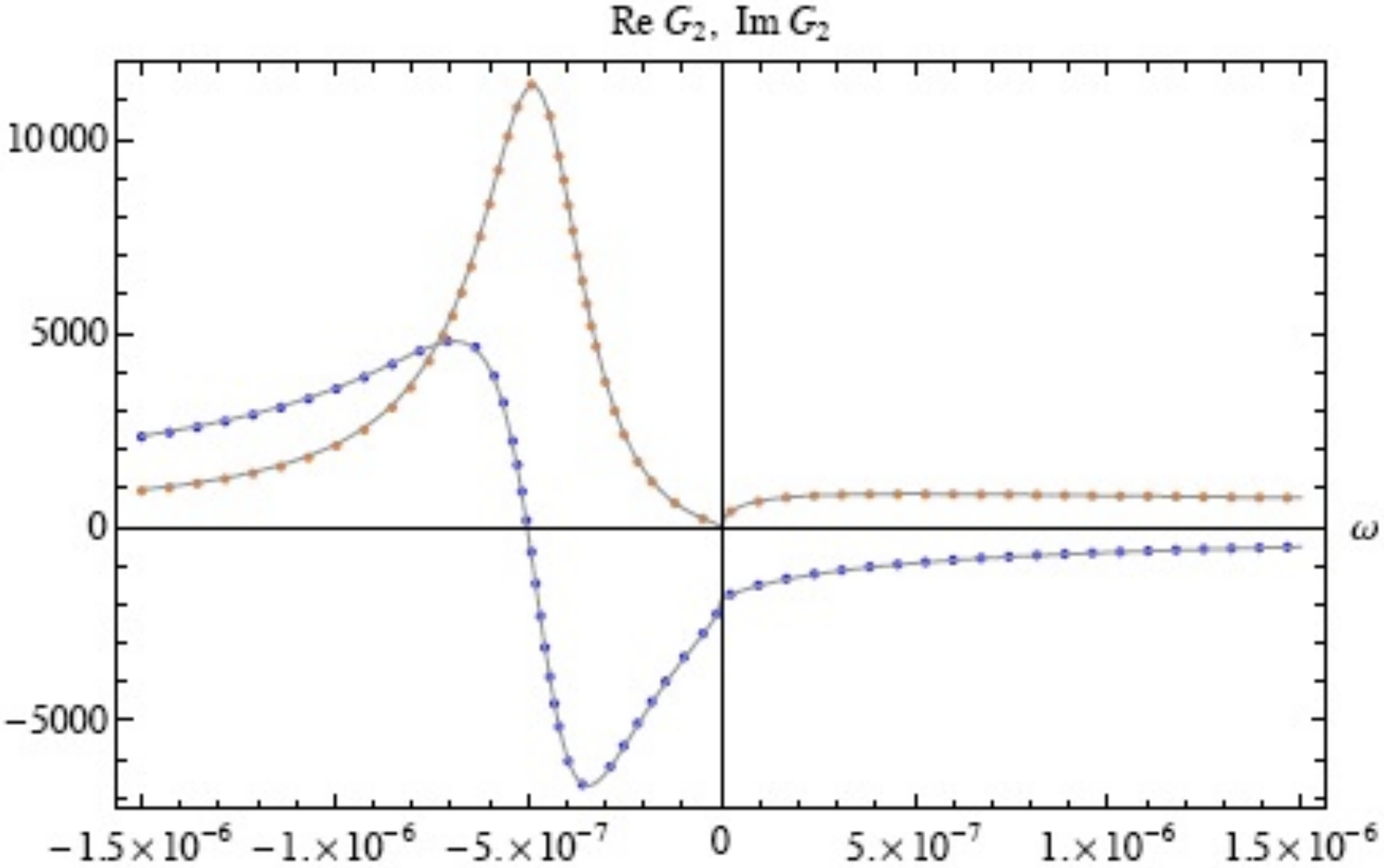

T. Faulkner, H. Liu, J. McGreevy, and D. Vegh, arXiv:0907.2694

$$G(k,\omega) \approx \frac{1}{\omega - v_F(k-k_F) - i\omega^{\theta(k)}}$$

See also M. Cubrovic, J. Zaanen, and K. Schalm, arXiv:0904.1993

Green's function of a fermion

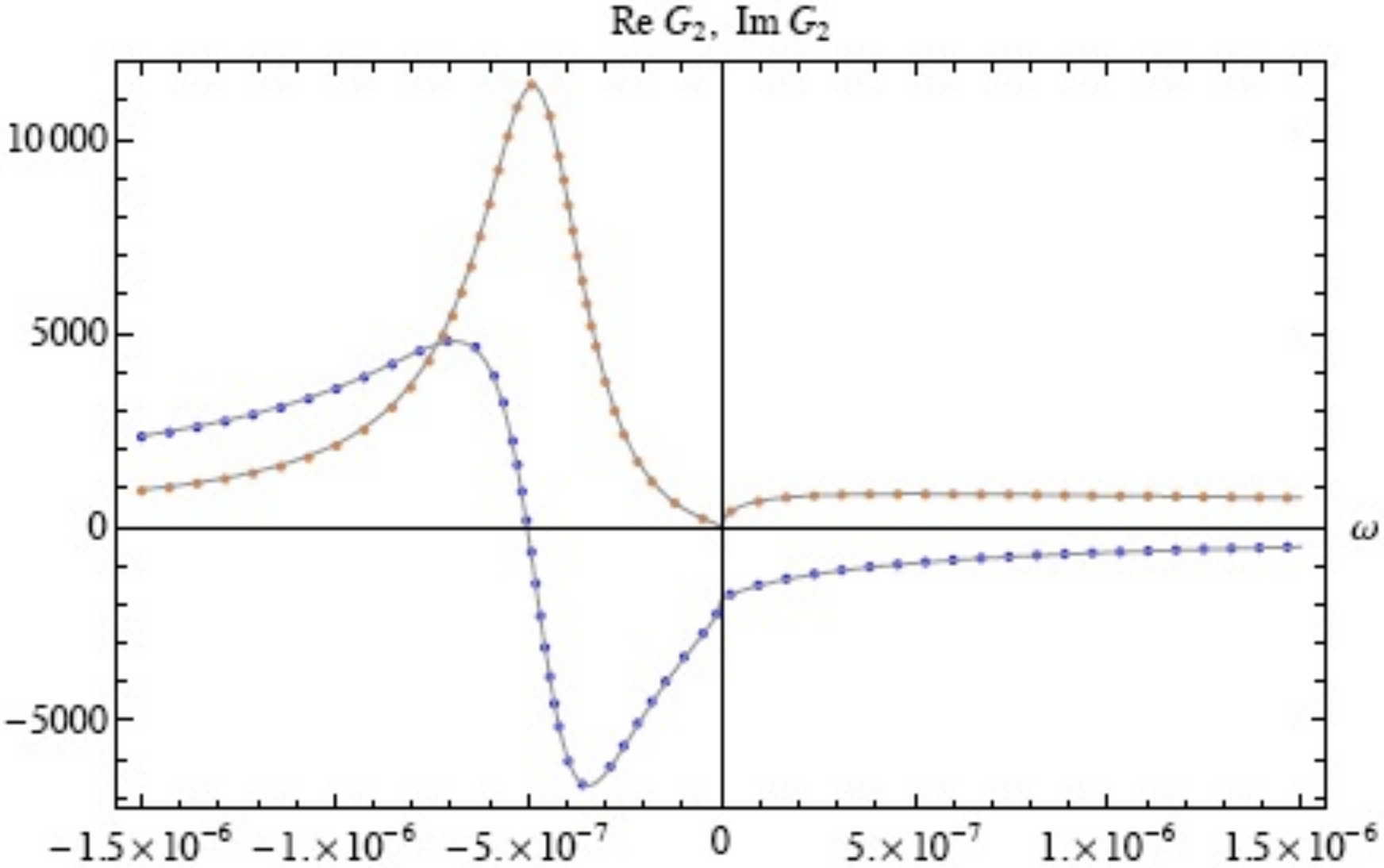

T. Faulkner, H. Liu, J. McGreevy, and D. Vegh, arXiv:0907.2694

$$G(k,\omega) \approx \frac{1}{\omega - v_F(k-k_F) - i\omega^{\theta(k)}}$$

Similar to non-Fermi liquid theories of Fermi surfaces coupled to gauge fields, and at quantum critical points

Free energy from gravity theory

The free energy is expressed as a sum over the "quasinormal frequencies", z_ℓ, of the black hole. Here ℓ represents any set of quantum numbers:

$$\mathcal{F}_{\text{fermion}} = T\sum_\ell \ln\left(\left|\Gamma\left(\frac{iz_\ell}{2\pi T}+\frac{1}{2}\right)\right|^2\right)$$

Application of this formula shows that the fermions exhibit the dHvA quantum oscillations with expected period $(2\pi/(\text{Fermi surface ares}))$ in $1/B$, but with an amplitude corrected from the Fermi liquid formula.

F. Denef, S. Hartnoll, and S. Sachdev, arXiv:0908.1788
S. Hartnoll and D. M. Hofman, arXiv:0912.0008

Outline

1. Coupled dimer antiferromagnets

   Order parameters and Landau-Ginzburg criticality

2. Graphene

   `Topological' Fermi surface transitions

3. Quantum criticality and black holes

   AdS_4 theory of compressible quantum liquids

4. Quantum criticality in the cuprates

   Global phase diagram and the spin density wave transition in metals

Outline

1. Coupled dimer antiferromagnets

   Order parameters and Landau-Ginzburg criticality

2. Graphene

   `Topological' Fermi surface transitions

3. Quantum criticality and black holes

   AdS_4 theory of compressible quantum liquids

4. Quantum criticality in the cuprates

   Global phase diagram and the spin density wave transition in metals

The cuprate superconductors

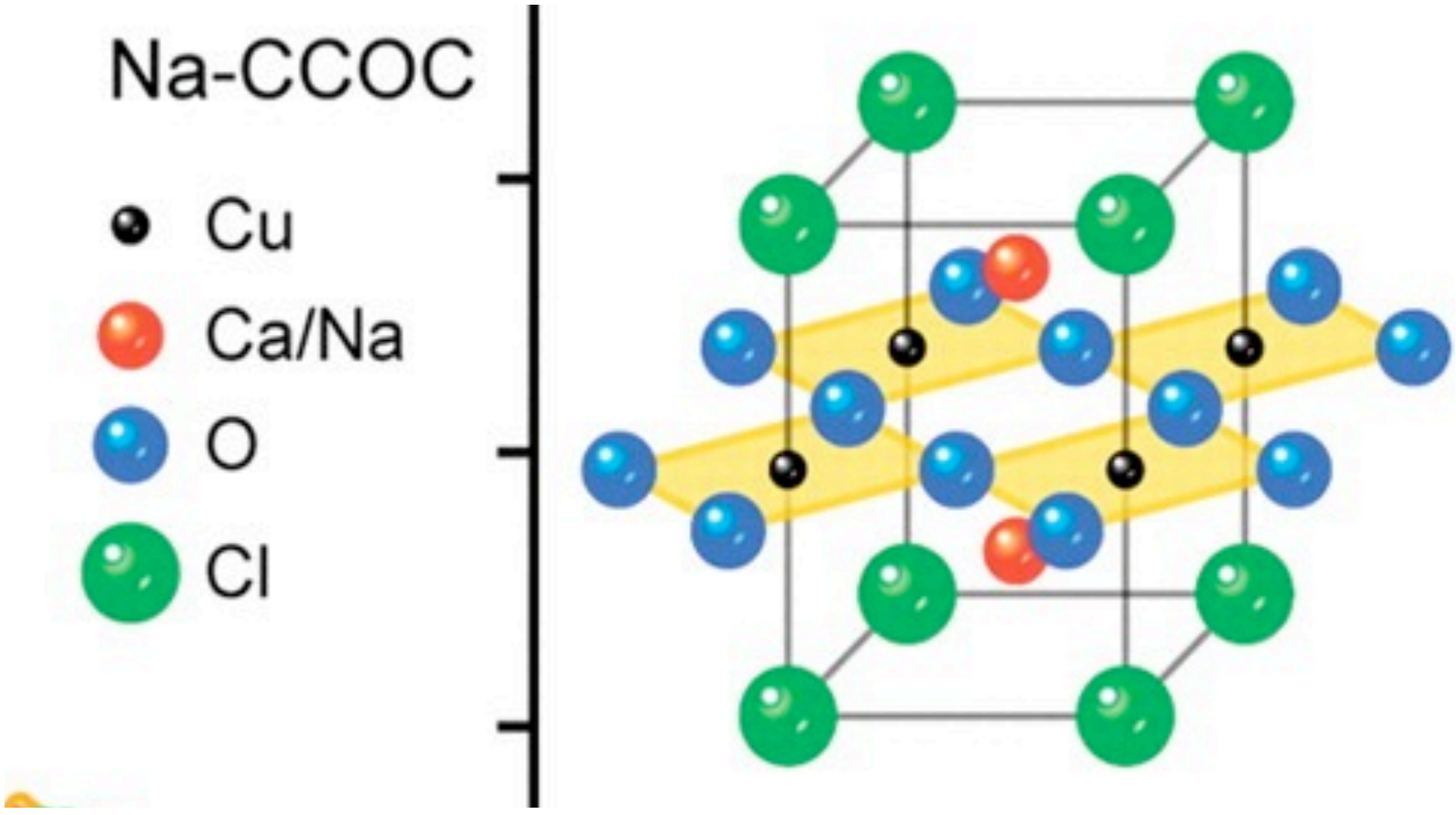

Square lattice antiferromagnet

$$H = \sum_{\langle ij \rangle} J_{ij} \vec{S}_i \cdot \vec{S}_j$$

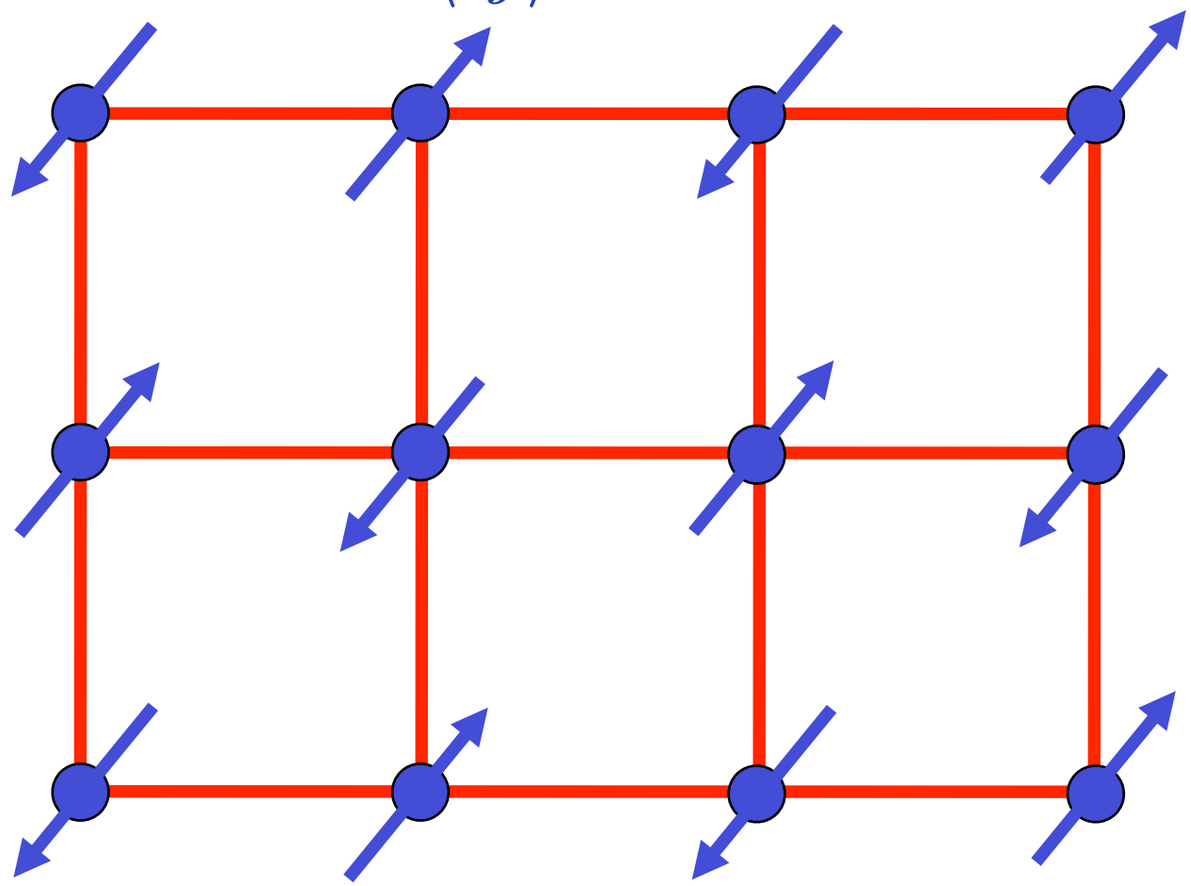

Ground state has long-range Néel order

Order parameter is a single vector field $\vec{\varphi} = \eta_i \vec{S}_i$

$\eta_i = \pm 1$ on two sublattices

$\langle \vec{\varphi} \rangle \neq 0$ in Néel state.

Central ingredients in cuprate phase diagram: antiferromagnetism, superconductivity, and change in Fermi surface

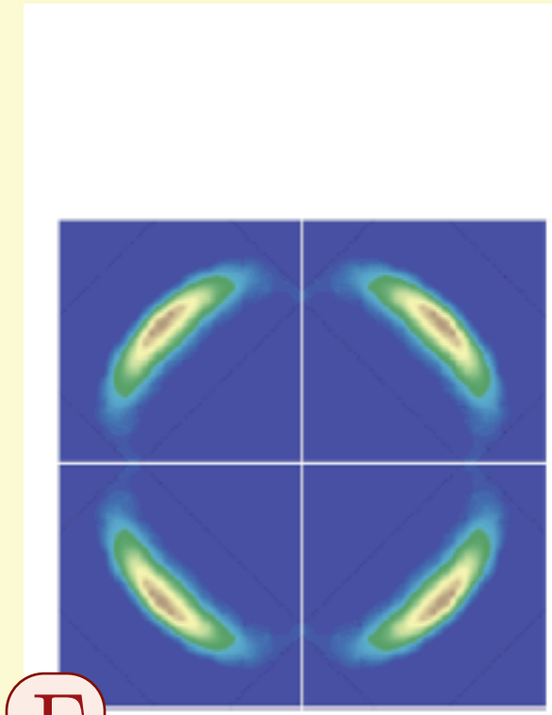

K.M. Shen et al., Science 2005

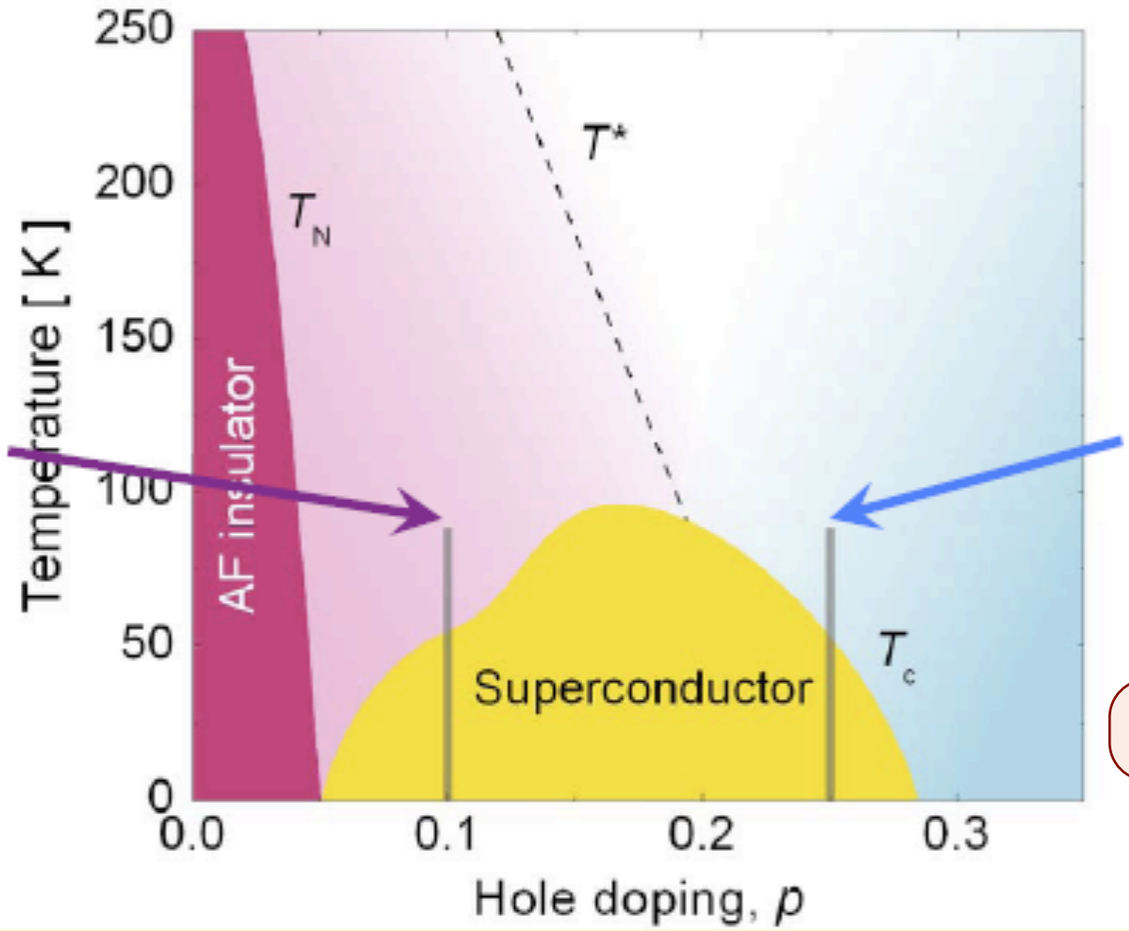

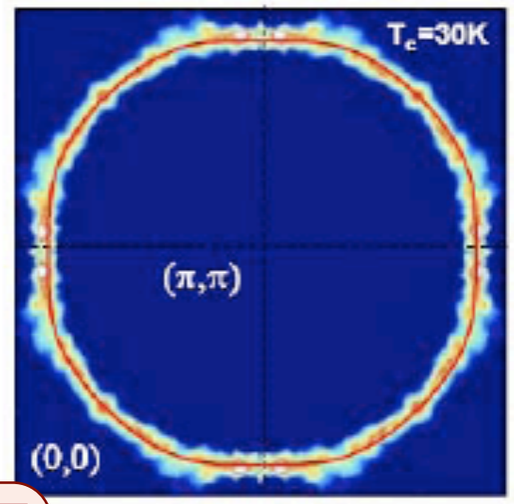

M. Platé et al., PRL 2005

Smaller hole Fermi-pockets

Large hole Fermi surface

Central ingredients in cuprate phase diagram: antiferromagnetism, superconductivity, and change in Fermi surface

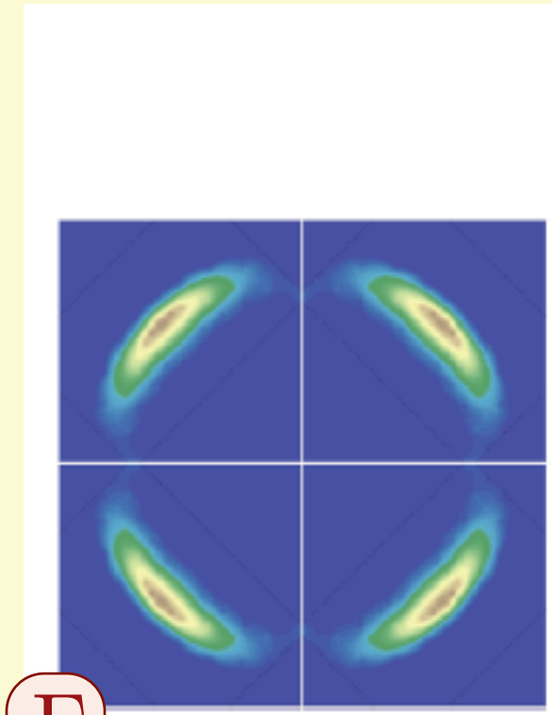

K.M. Shen et al., Science 2005

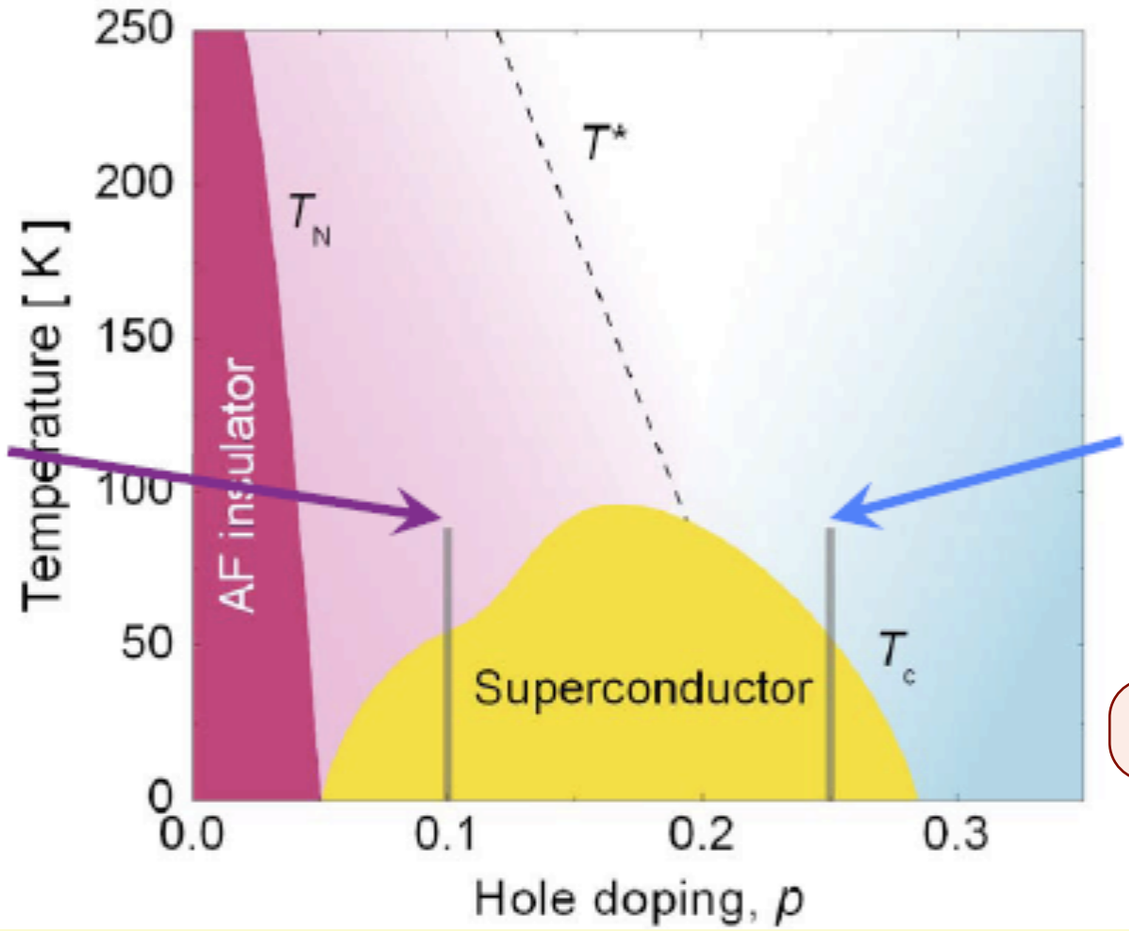

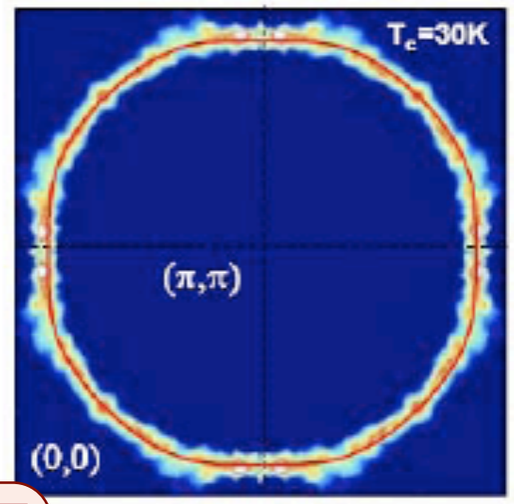

M. Platé et al., PRL 2005

Smaller hole Fermi-pockets

Large hole Fermi surface

Central ingredients in cuprate phase diagram: antiferromagnetism, superconductivity, and change in Fermi surface

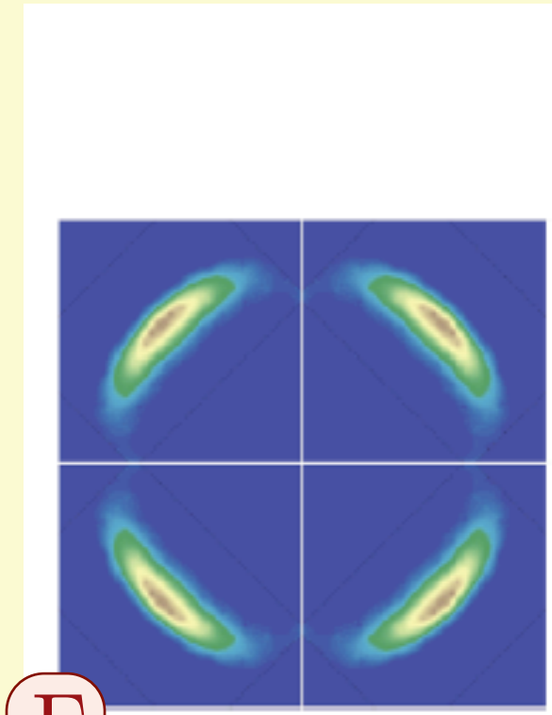

K.M. Shen et al., Science 2005

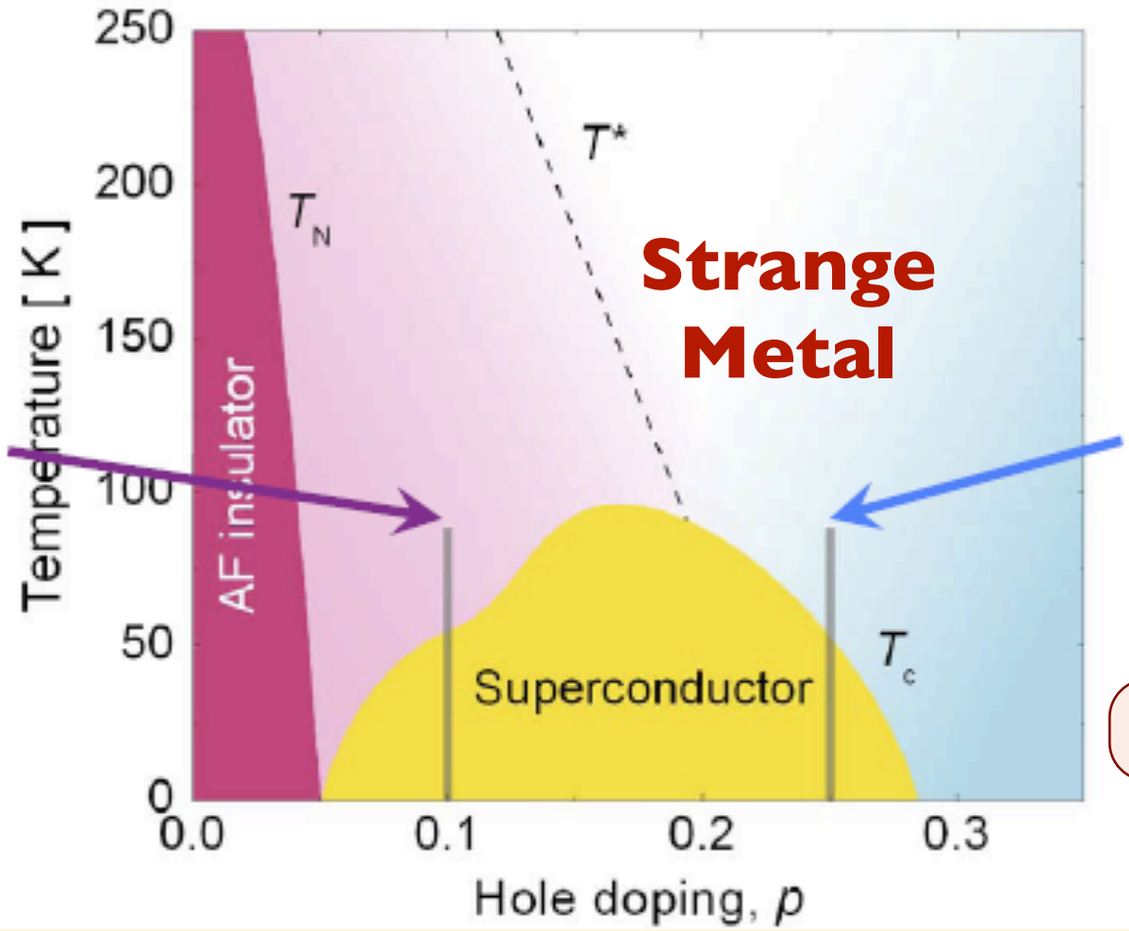

M. Platé et al., PRL 2005

Smaller hole Fermi-pockets

Large hole Fermi surface

Antiferro-
magnetism

d-wave
supercon-
ductivity

Fermi
surface

Antiferro-
magnetism

d-wave
supercon-
ductivity

Fermi
surface

Canonical quantum critical phase diagram of coupled-dimer antiferromagnet

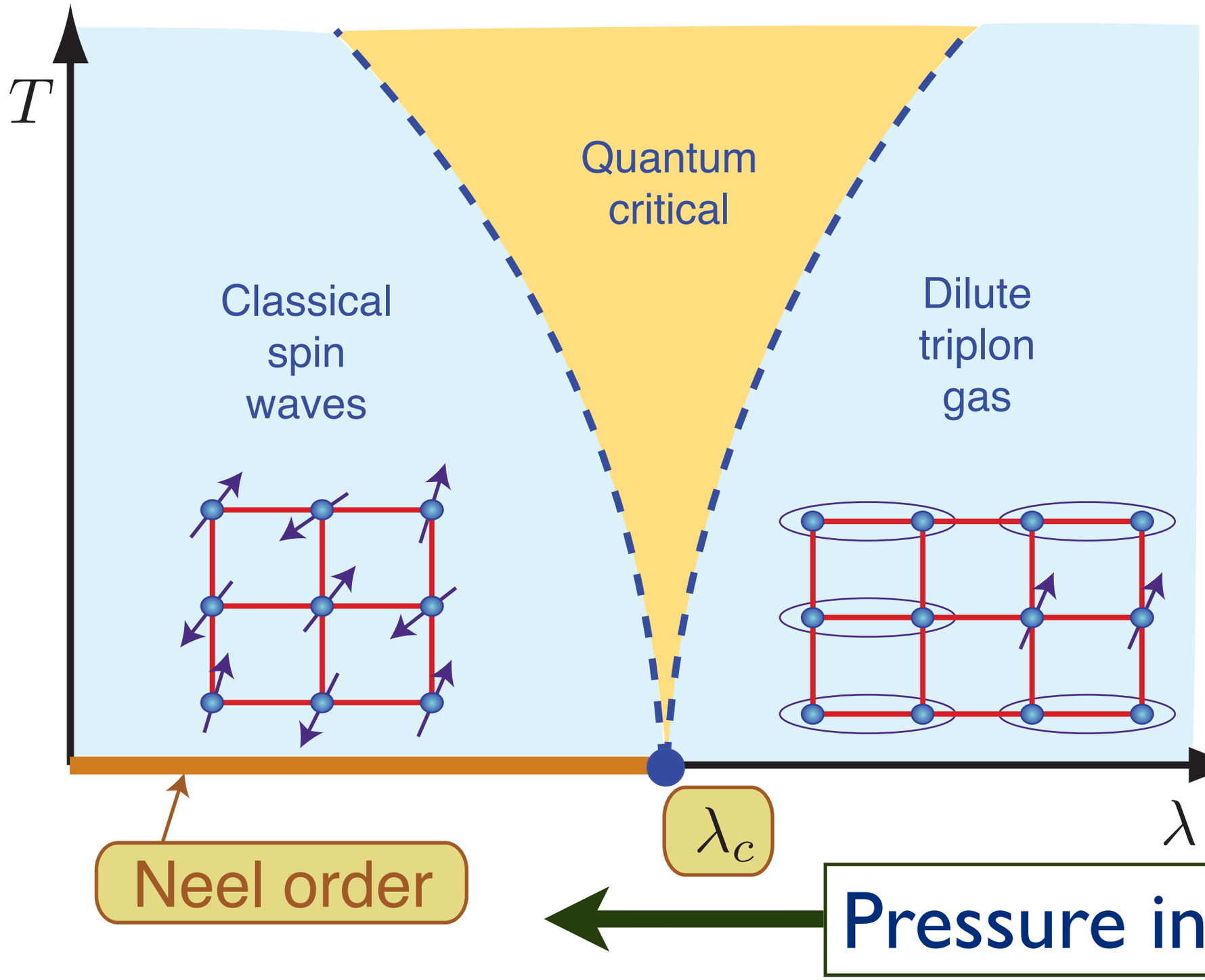

S. Sachdev and J. Ye, *Phys. Rev. Lett.* **69**, 2411 (1992).

Christian Ruegg et al. , *Phys. Rev. Lett.* **100**, 205701 (2008)

Antiferro-
magnetism

d-wave
supercon-
ductivity

Fermi
surface

Antiferro-
magnetism

d-wave
supercon-
ductivity

Fermi
surface

Fermi surface+antiferromagnetism

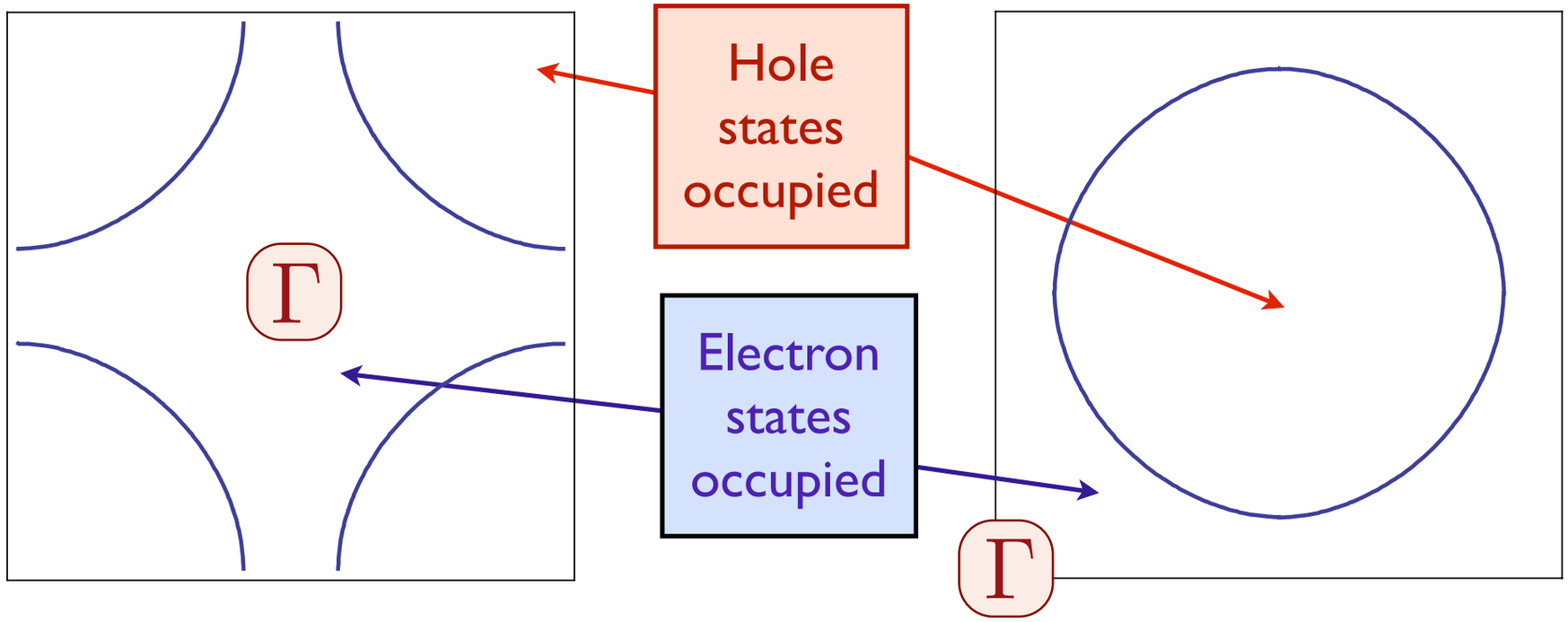

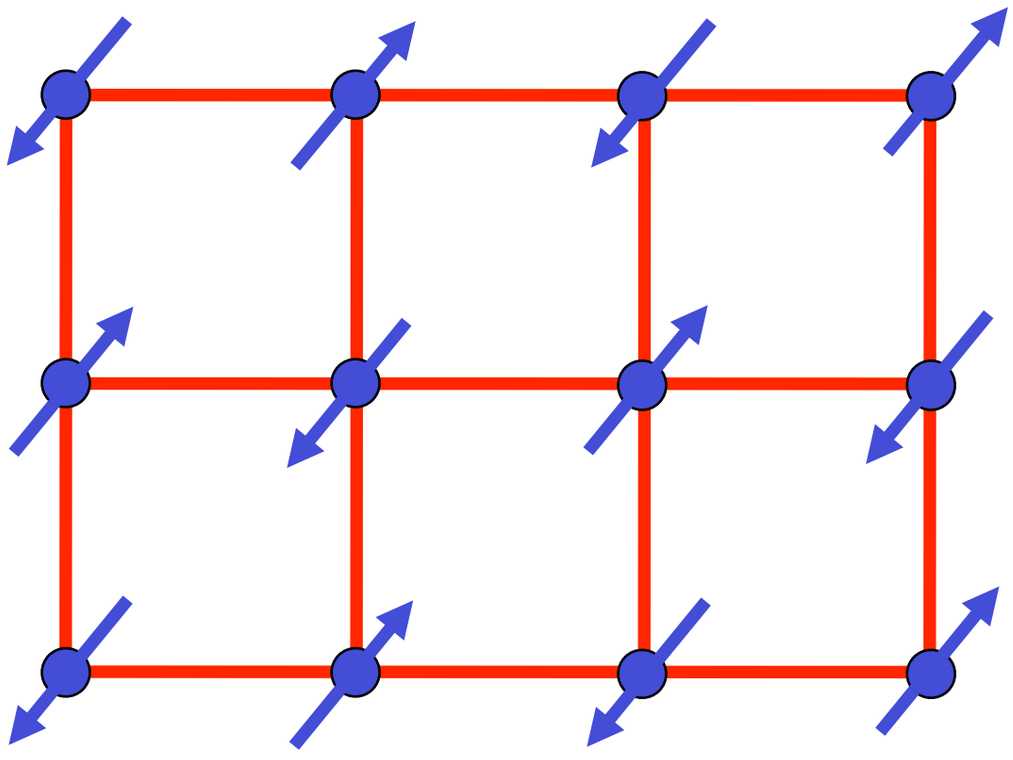

The electron spin polarization obeys

$$\left\langle \vec{S}(\mathbf{r},\tau) \right\rangle = \vec{\varphi}(\mathbf{r},\tau) e^{i\mathbf{K}\cdot\mathbf{r}}$$

where $\mathbf{K}$ is the ordering wavevector.

Hole-doped cuprates

←——Increasing SDW order——

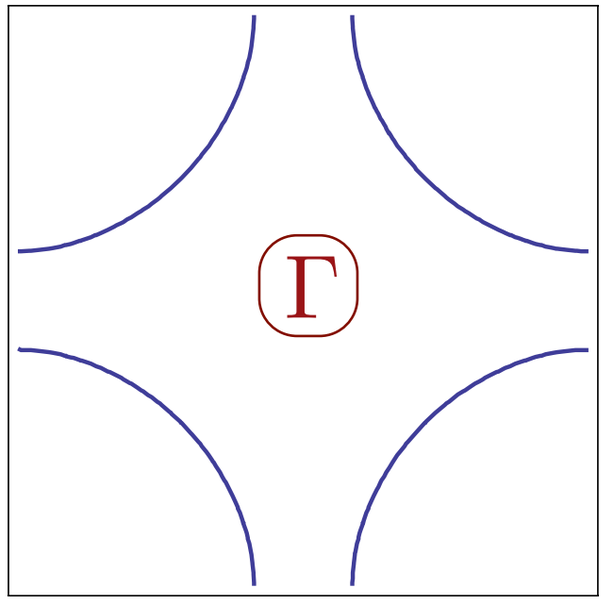

S. Sachdev, A.V. Chubukov, and A. Sokol, *Phys. Rev. B* **51**, 14874 (1995).
A.V. Chubukov and D. K. Morr, *Physics Reports* **288**, 355 (1997).

Hole-doped cuprates

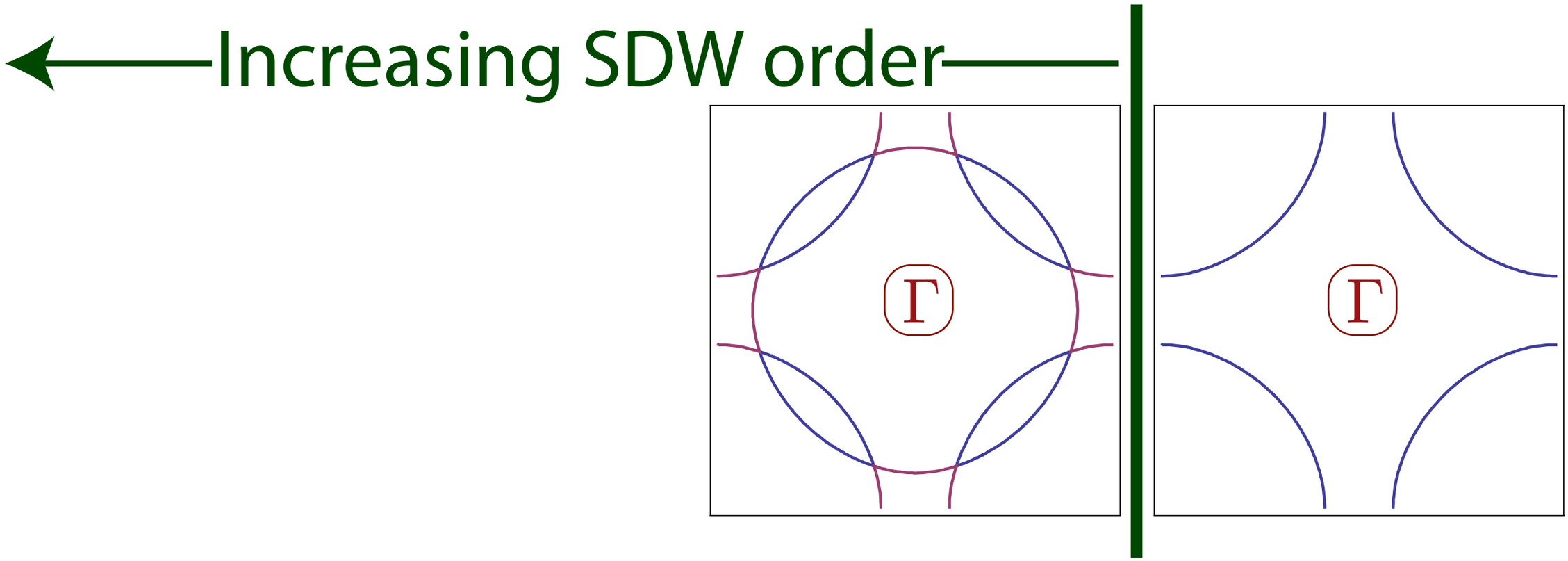

S. Sachdev, A.V. Chubukov, and A. Sokol, *Phys. Rev. B* **51**, 14874 (1995).
A.V. Chubukov and D. K. Morr, *Physics Reports* **288**, 355 (1997).

Hole-doped cuprates

←——Increasing SDW order——

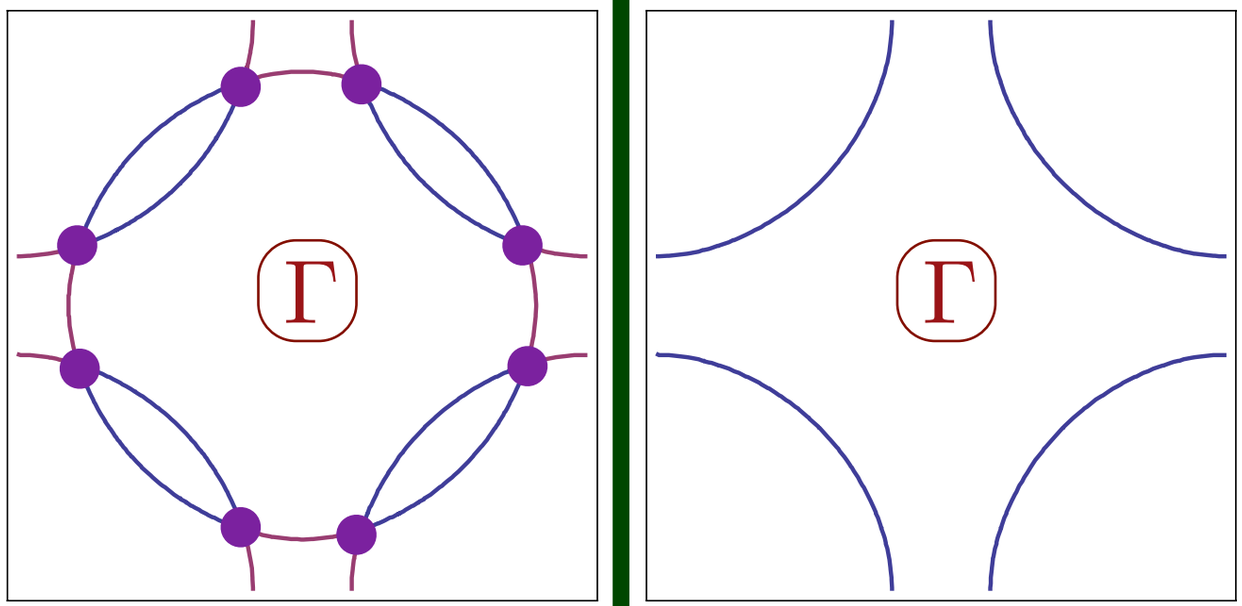

Hot spots

S. Sachdev, A.V. Chubukov, and A. Sokol, *Phys. Rev. B* **51**, 14874 (1995).
A.V. Chubukov and D. K. Morr, *Physics Reports* **288**, 355 (1997).

Hole-doped cuprates

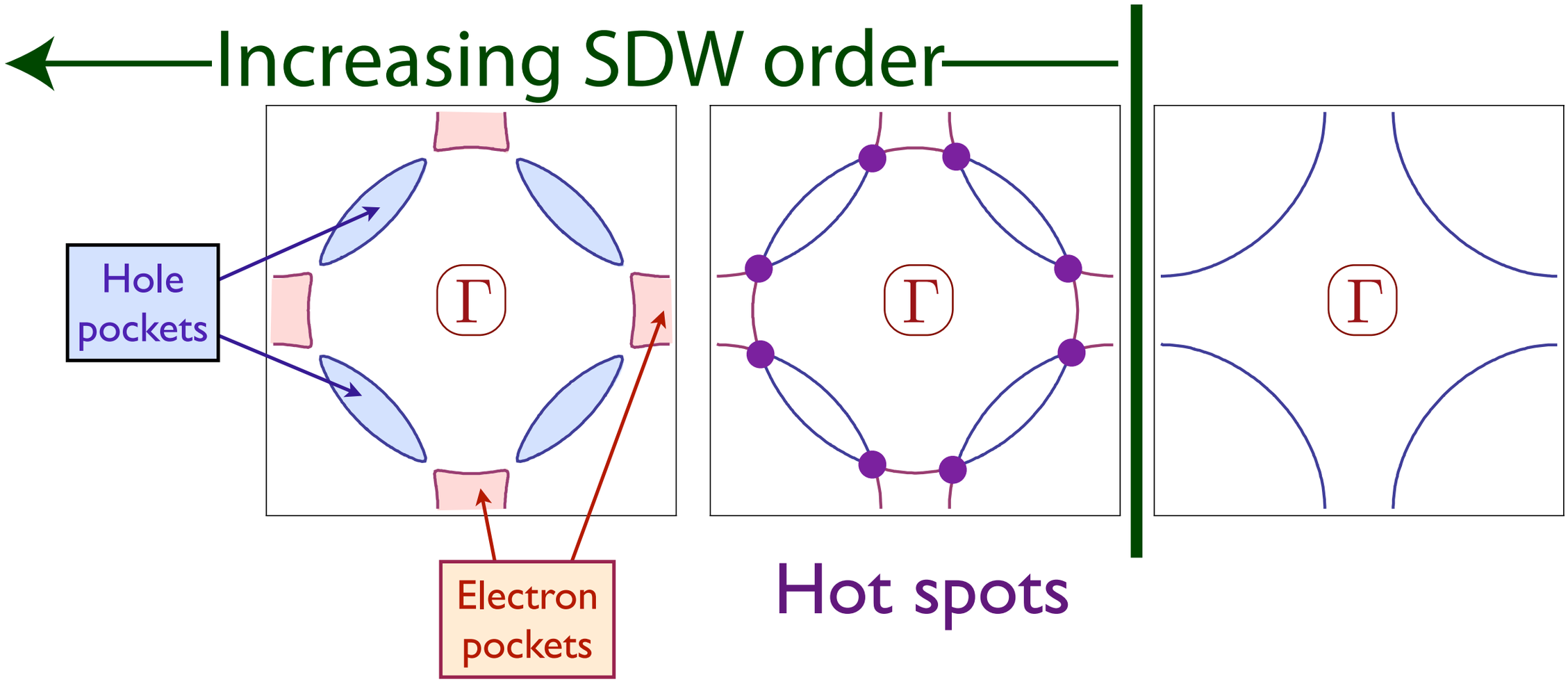

Fermi surface breaks up at hot spots into electron and hole "pockets"

S. Sachdev, A.V. Chubukov, and A. Sokol, *Phys. Rev. B* **51**, 14874 (1995).
A.V. Chubukov and D. K. Morr, *Physics Reports* **288**, 355 (1997).

Hole-doped cuprates

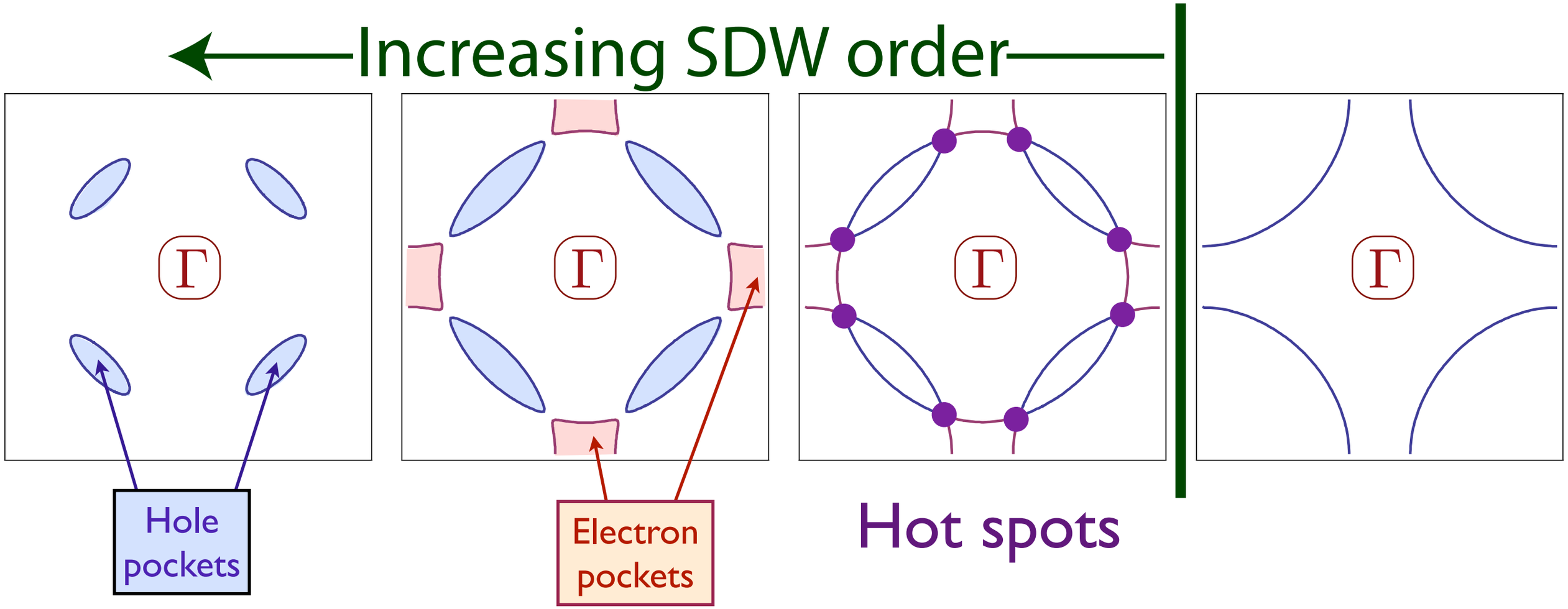

Fermi surface breaks up at hot spots into electron and hole "pockets"

S. Sachdev, A.V. Chubukov, and A. Sokol, *Phys. Rev. B* **51**, 14874 (1995).
A.V. Chubukov and D. K. Morr, *Physics Reports* **288**, 355 (1997).

Theory of quantum criticality in the cuprates

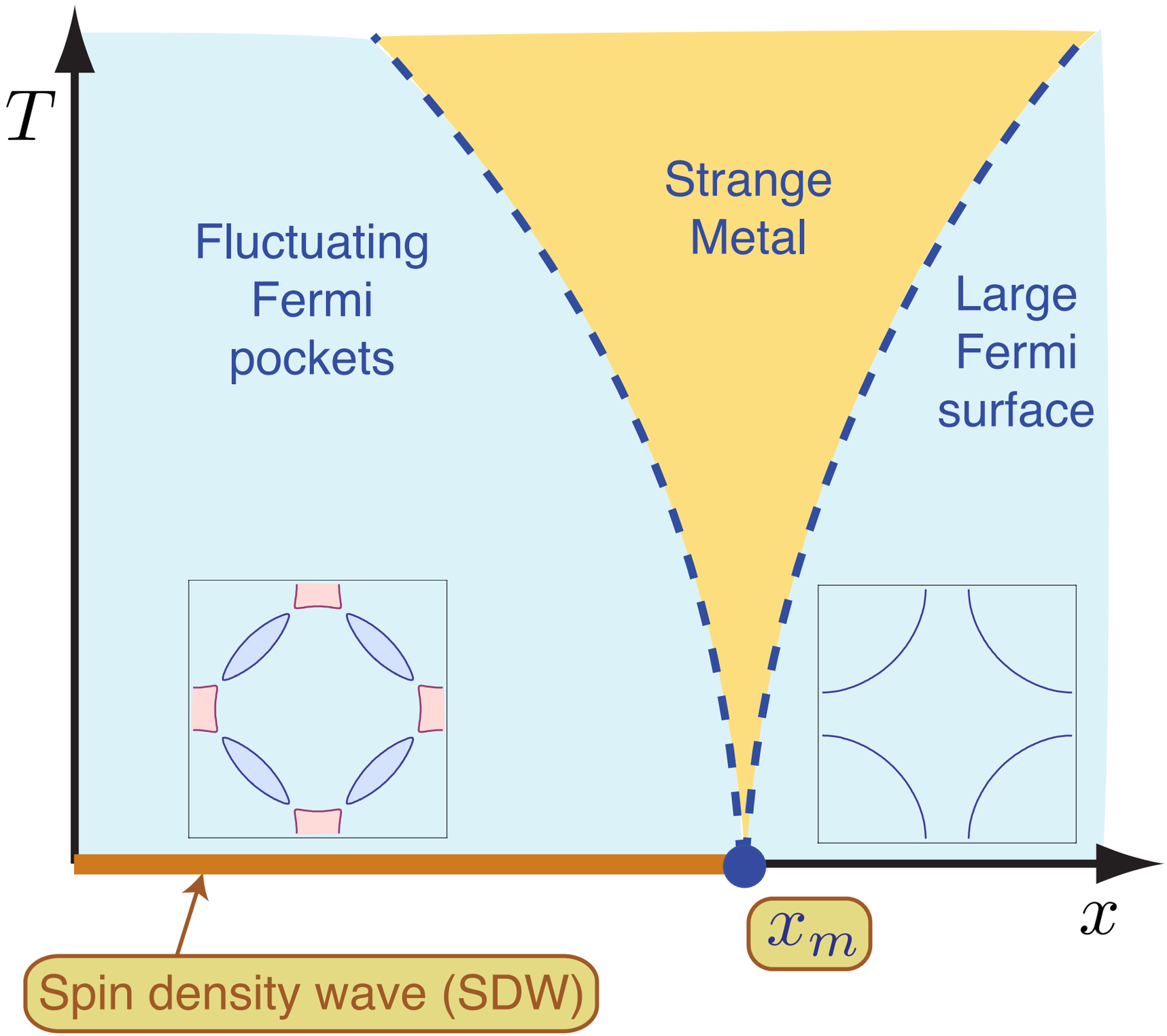

Underlying SDW ordering quantum critical point in **metal** at $x = x_m$

Antiferro-
magnetism

d-wave
supercon-
ductivity

Fermi
surface

Antiferro-
magnetism

d-wave
supercon-
ductivity

Fermi
surface

Theory of quantum criticality in the cuprates

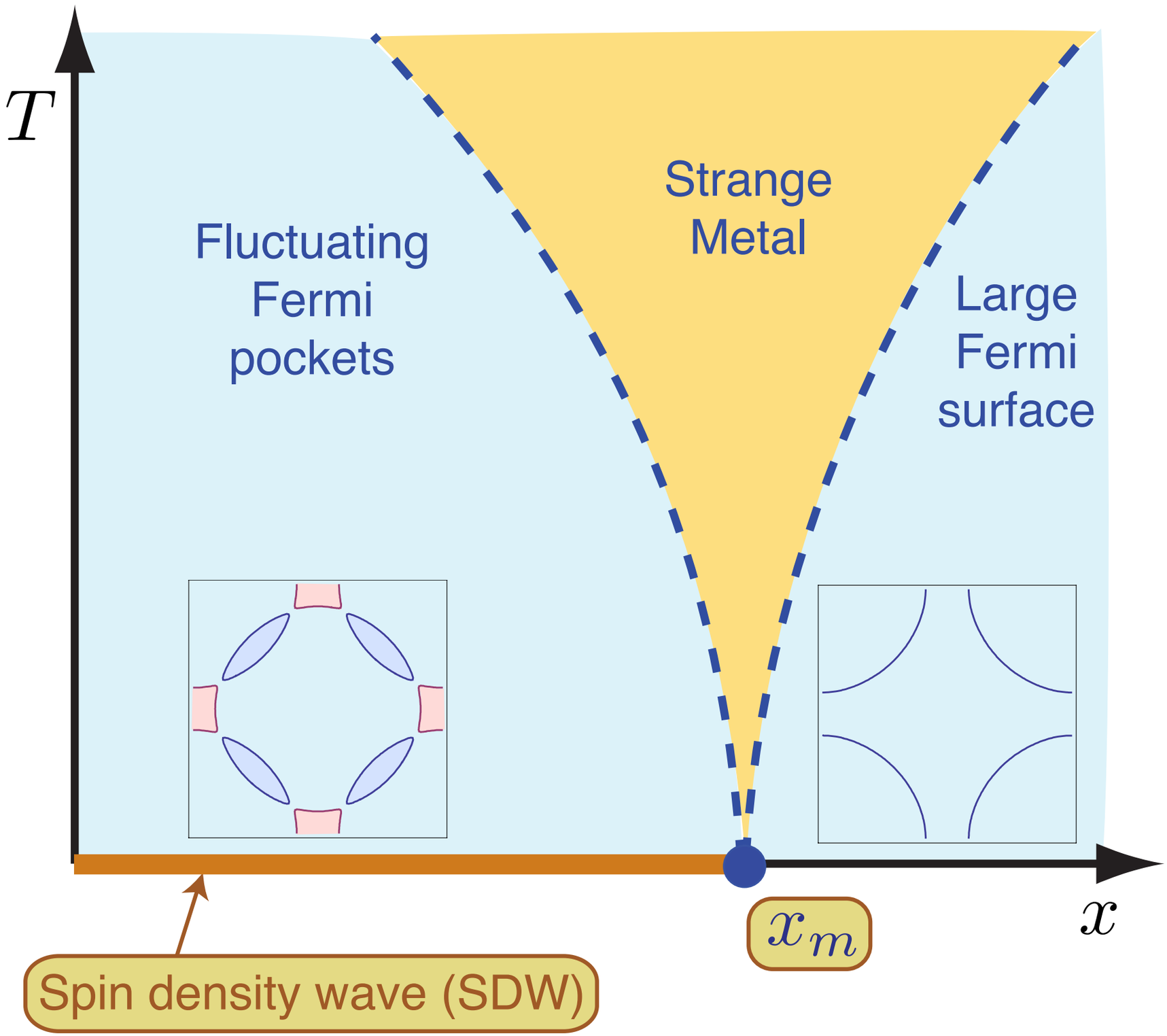

Underlying SDW ordering quantum critical point in **metal** at $x = x_m$

Theory of quantum criticality in the cuprates

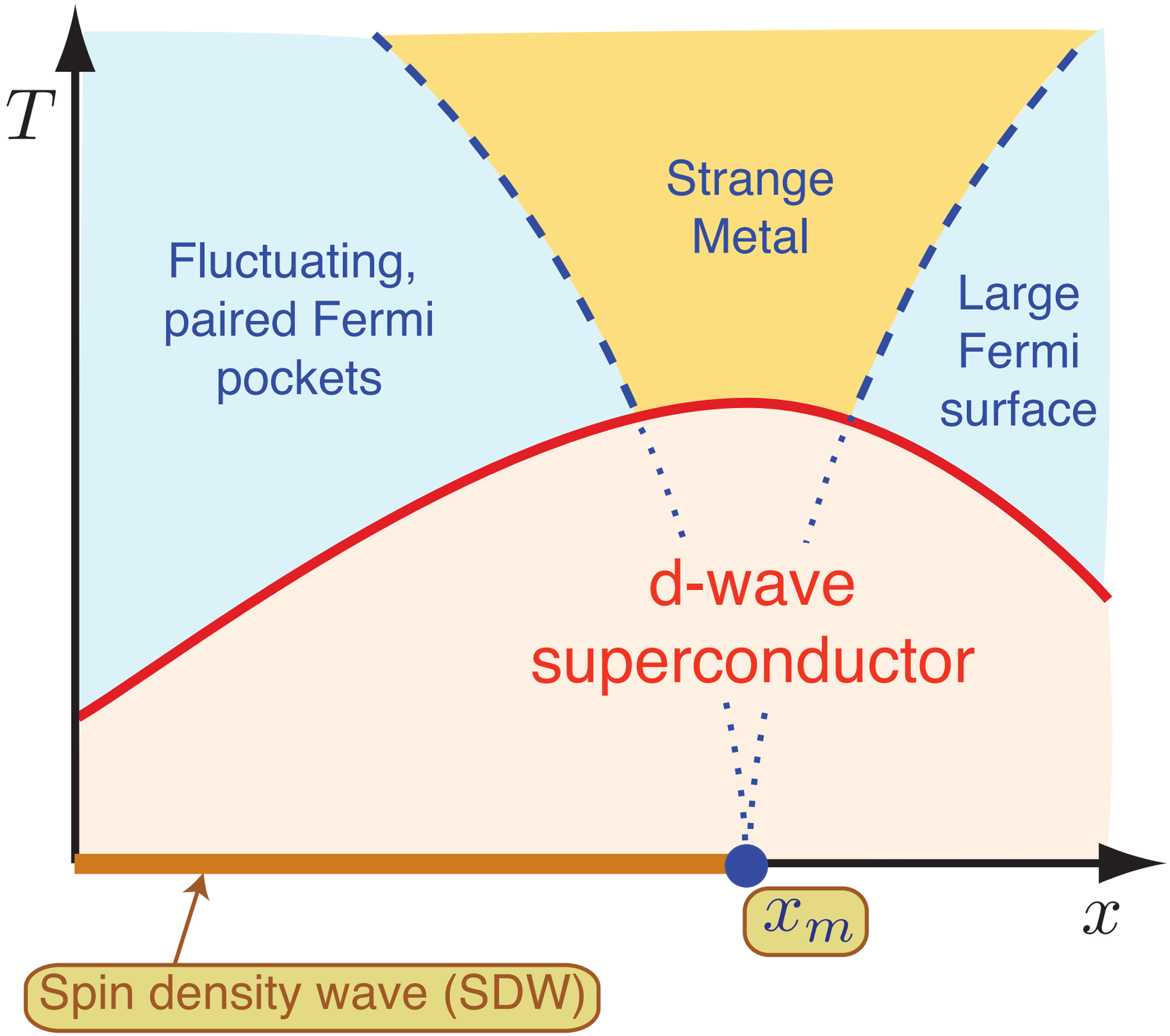

Onset of d-wave superconductivity hides the critical point $x = x_m$

Theory of quantum criticality in the cuprates

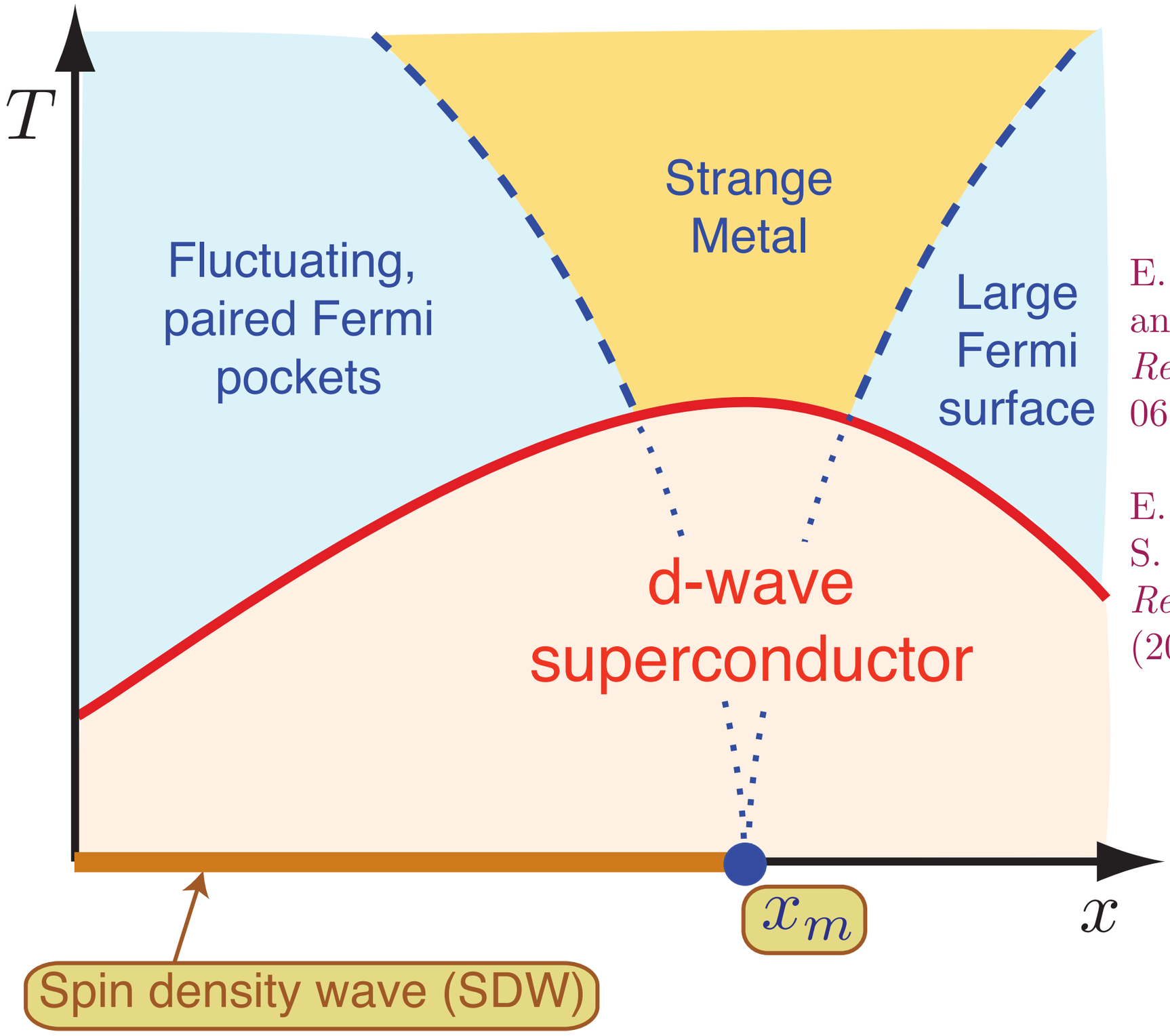

E. Demler, S. Sachdev and Y. Zhang, *Phys. Rev. Lett.* **87**, 067202 (2001).

E. G. Moon and S. Sachdev, *Phy. Rev. B* **80**, 035117 (2009)

Competition between SDW order and superconductivity moves the actual quantum critical point to $x = x_s < x_m$.

Theory of quantum criticality in the cuprates

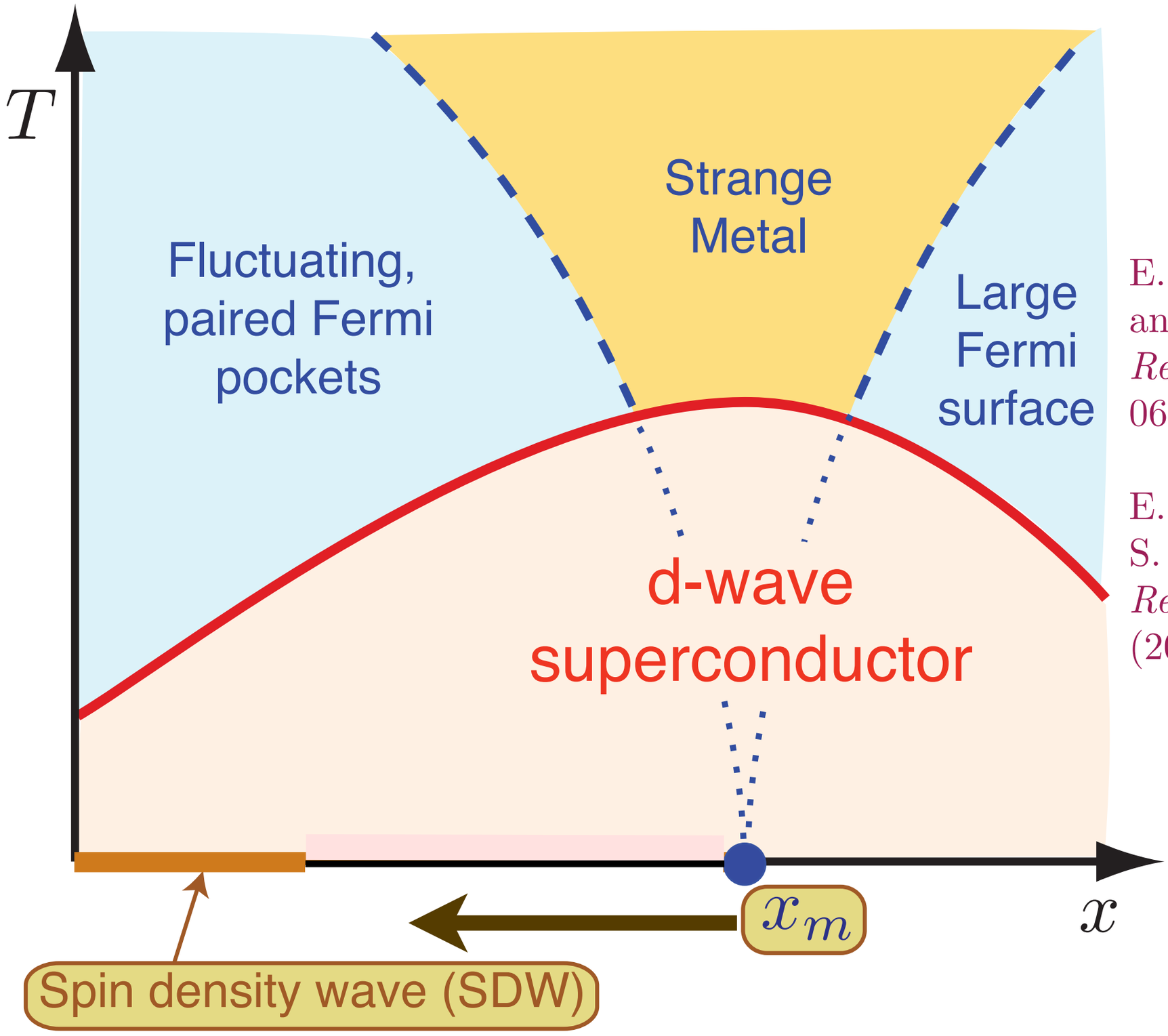

E. Demler, S. Sachdev and Y. Zhang, *Phys. Rev. Lett.* **87**, 067202 (2001).

E. G. Moon and S. Sachdev, *Phy. Rev. B* **80**, 035117 (2009)

Competition between SDW order and superconductivity moves the actual quantum critical point to $x = x_s < x_m$.

Theory of quantum criticality in the cuprates

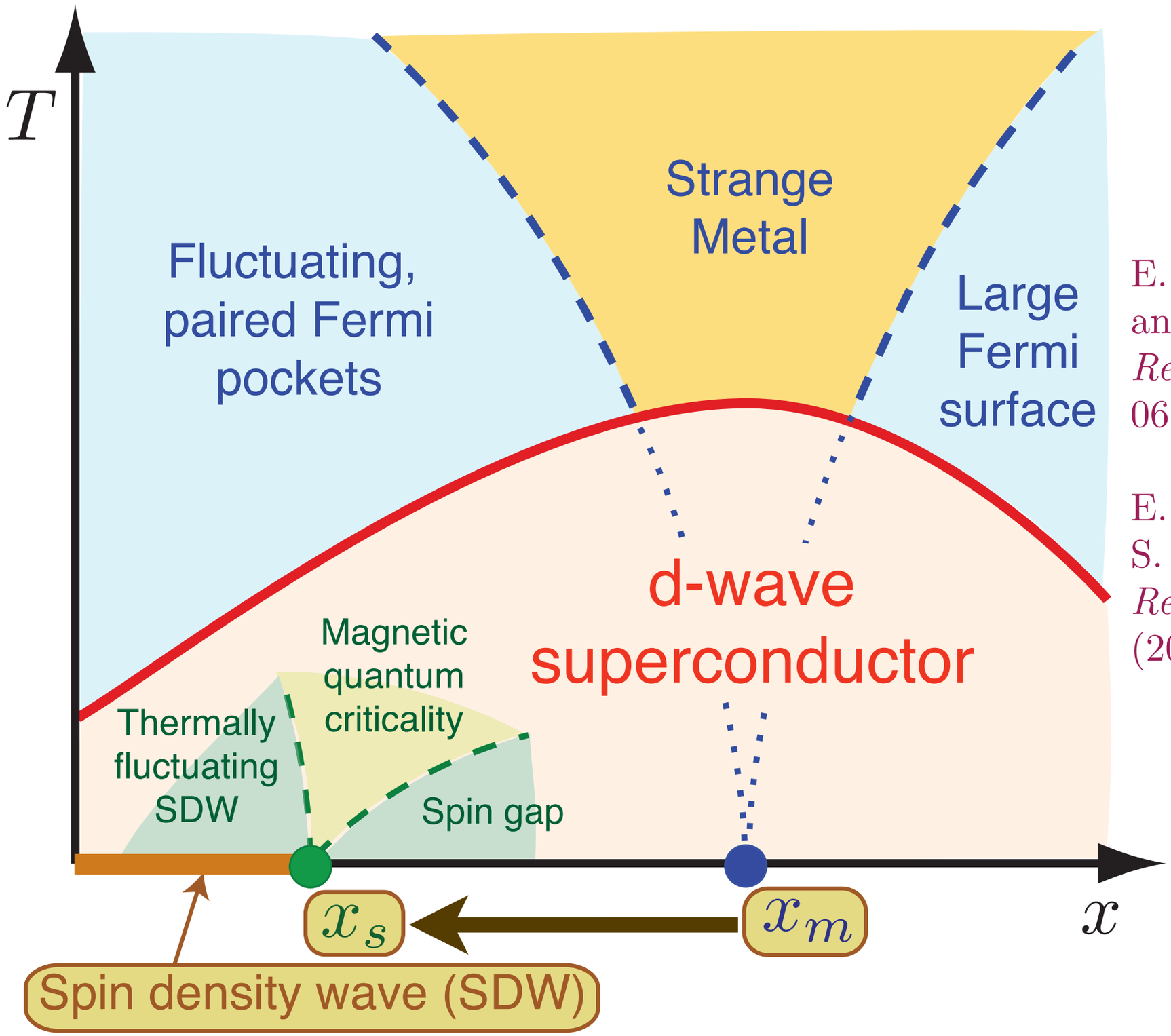

E. Demler, S. Sachdev and Y. Zhang, *Phys. Rev. Lett.* **87**, 067202 (2001).

E. G. Moon and S. Sachdev, *Phy. Rev. B* **80**, 035117 (2009)

Competition between SDW order and superconductivity moves the actual quantum critical point to $x = x_s < x_m$.

Theory of quantum criticality in the cuprates

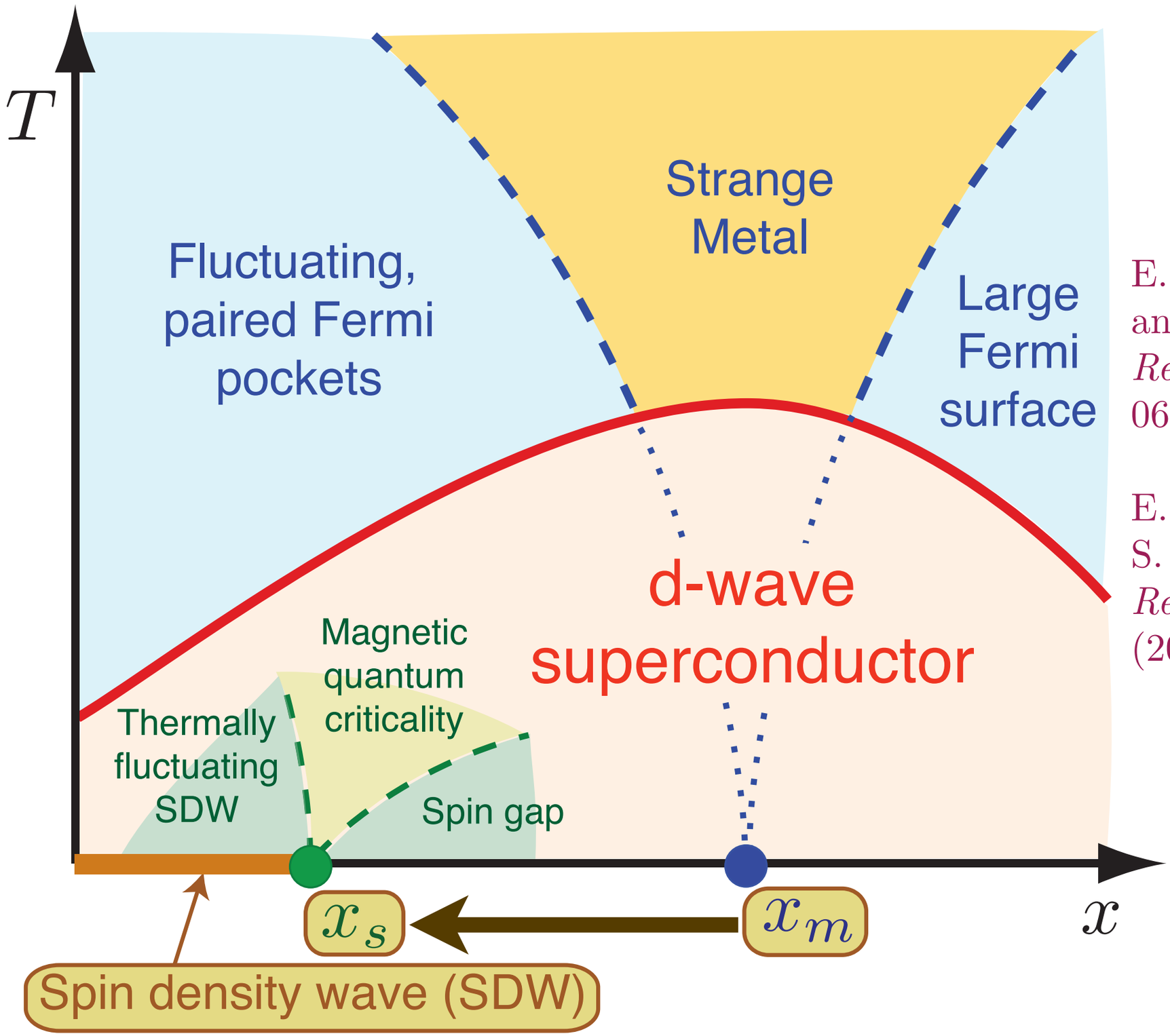

E. Demler, S. Sachdev and Y. Zhang, *Phys. Rev. Lett.* **87**, 067202 (2001).

E. G. Moon and S. Sachdev, *Phy. Rev. B* **80**, 035117 (2009)

Many neutron scattering and quantum oscillation experiments in high magnetic fields are explained by this phase diagram

Theory of quantum criticality in the cuprates

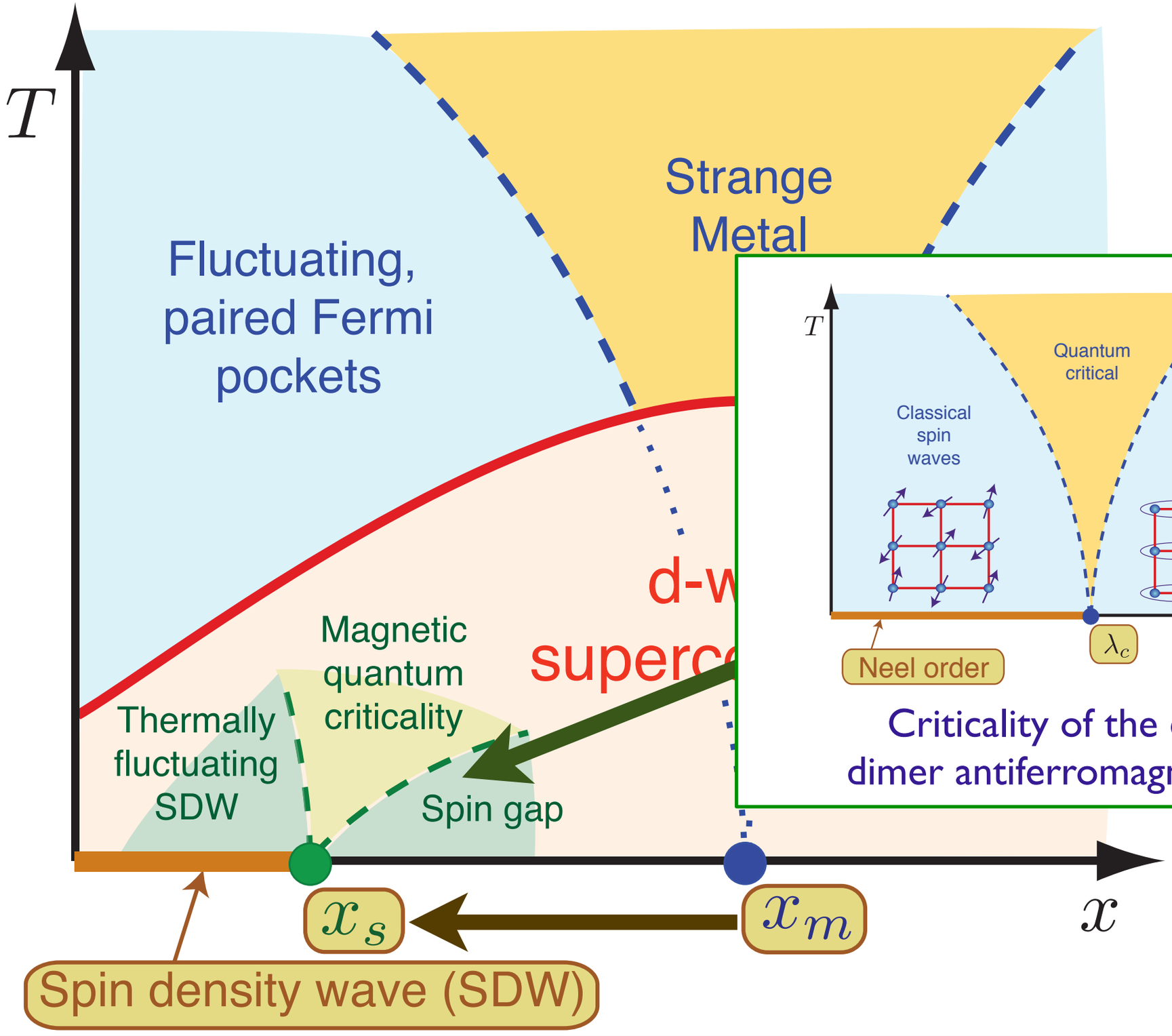

achdev
Phys.
7,
d
y.
117

Many neutron scattering and quantum oscillation experiments in high magnetic fields are explained by this phase diagram

Theory of quantum criticality in the cuprates

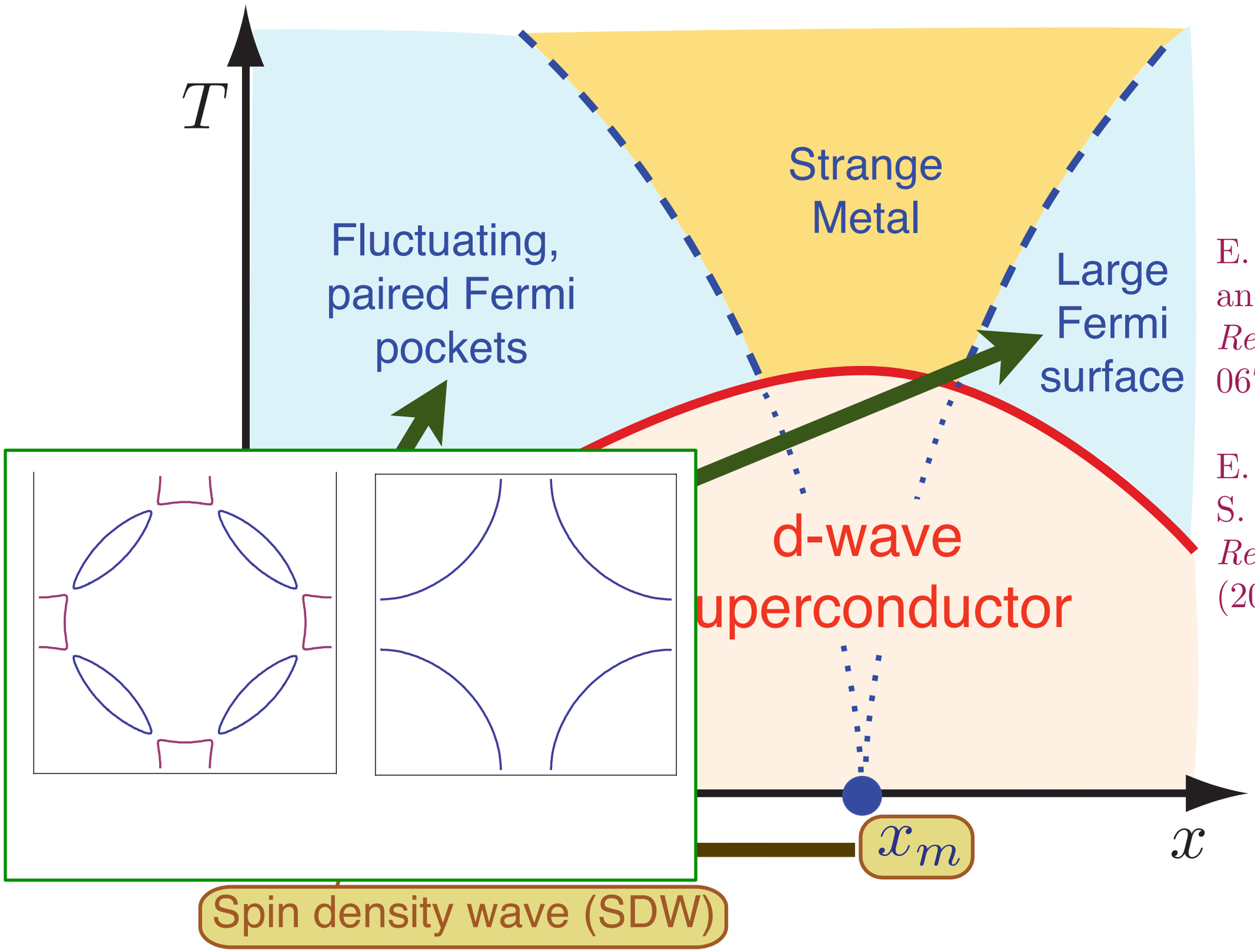

E. Demler, S. Sachdev and Y. Zhang, *Phys. Rev. Lett.* **87**, 067202 (2001).

E. G. Moon and S. Sachdev, *Phy. Rev. B* **80**, 035117 (2009)

Many neutron scattering and quantum oscillation experiments in high magnetic fields are explained by this phase diagram

Theory of quantum criticality in the cuprates

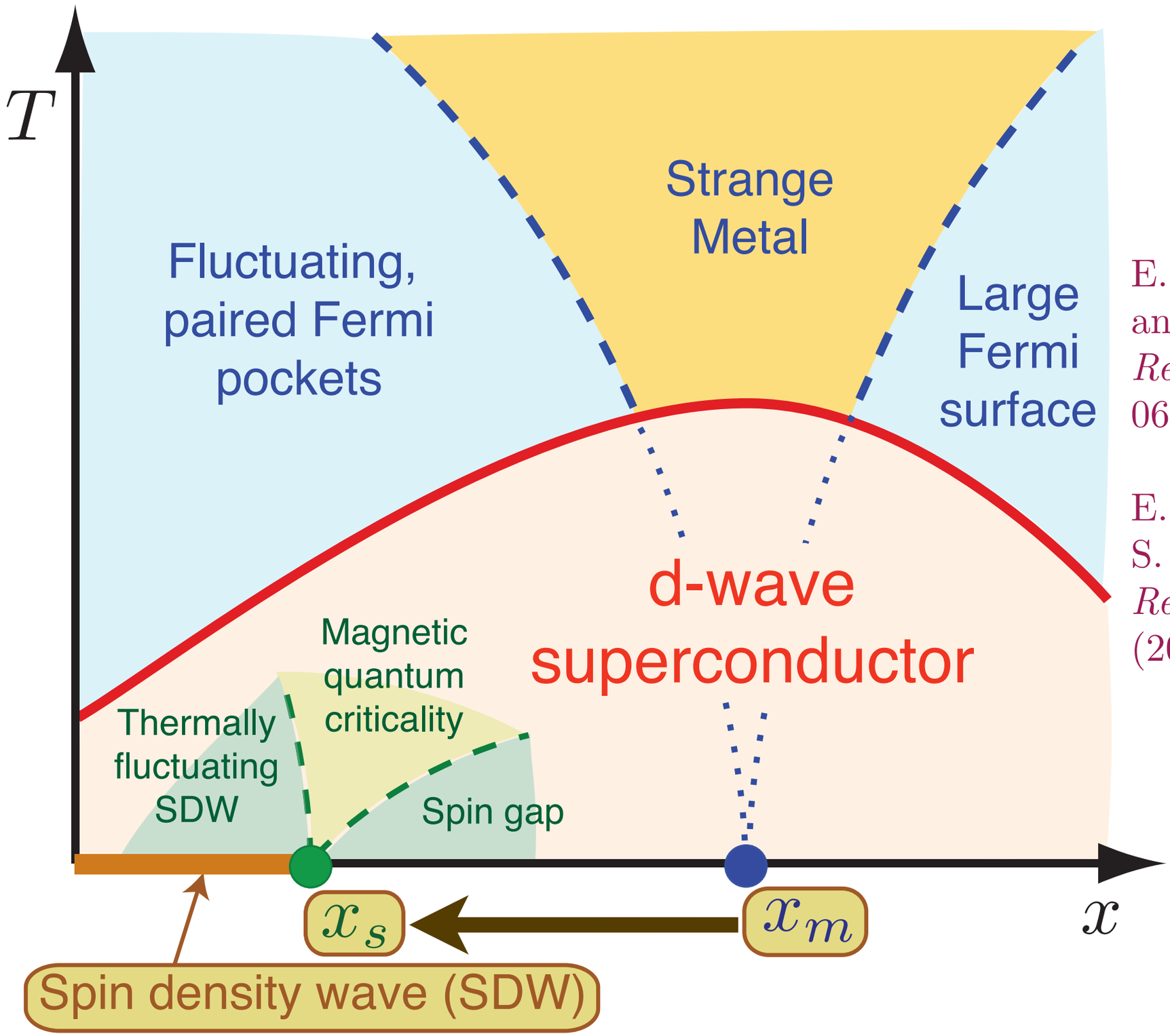

E. Demler, S. Sachdev and Y. Zhang, *Phys. Rev. Lett.* **87**, 067202 (2001).

E. G. Moon and S. Sachdev, *Phy. Rev. B* **80**, 035117 (2009)

Many neutron scattering and quantum oscillation experiments in high magnetic fields are explained by this phase diagram

Theory of quantum criticality in the cuprates

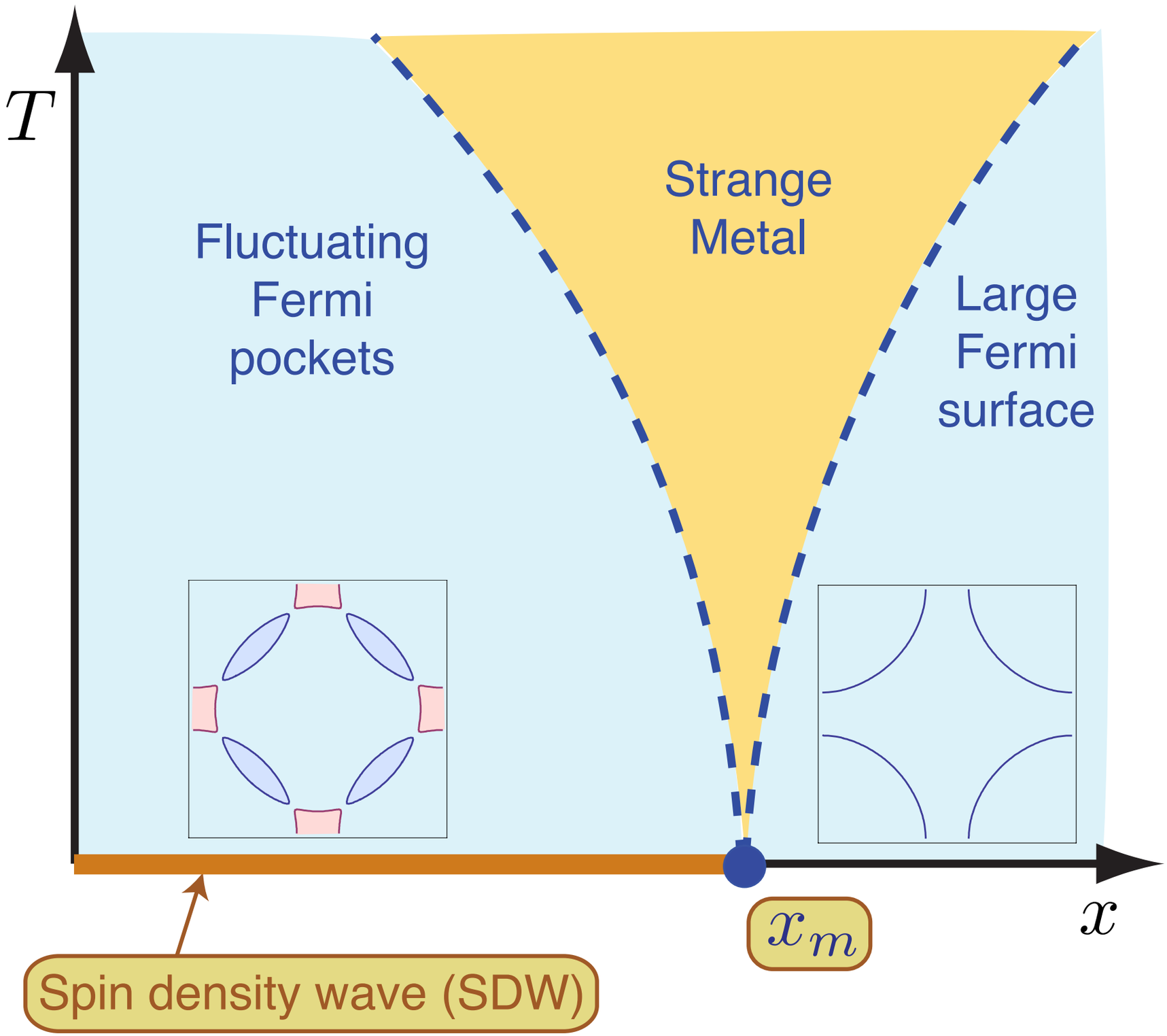

Underlying SDW ordering quantum critical point in **metal** at $x = x_m$

Fluctuations about mean field theory

M. Metlitski

SDW fluctuation $\vec{\varphi}$

Fermions near connected hot spots

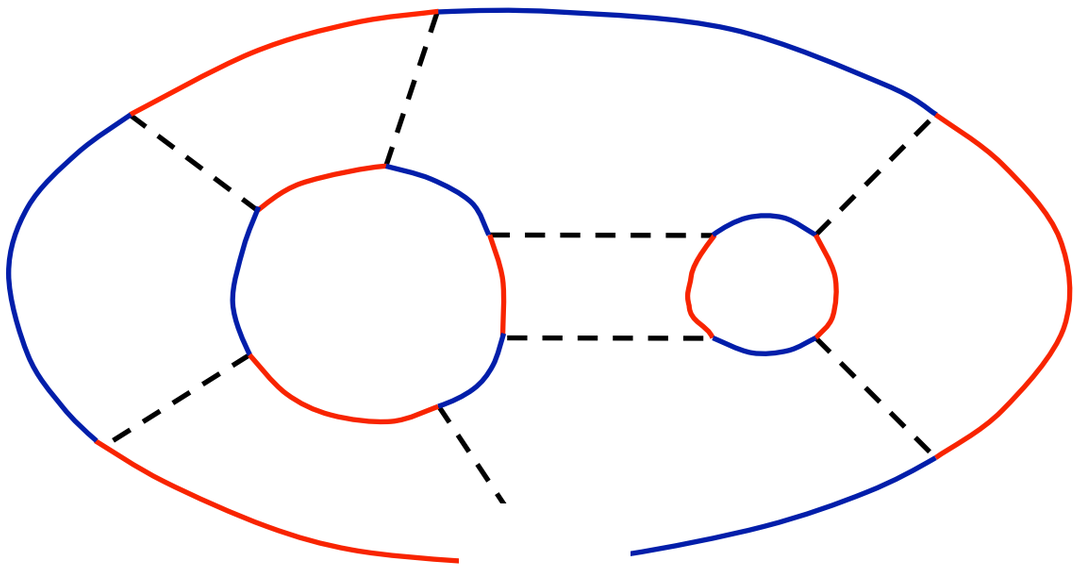

Fluctuations about mean field theory

M. Metlitski

SDW fluctuation $\vec{\varphi}$

Fermions near connected hot spots

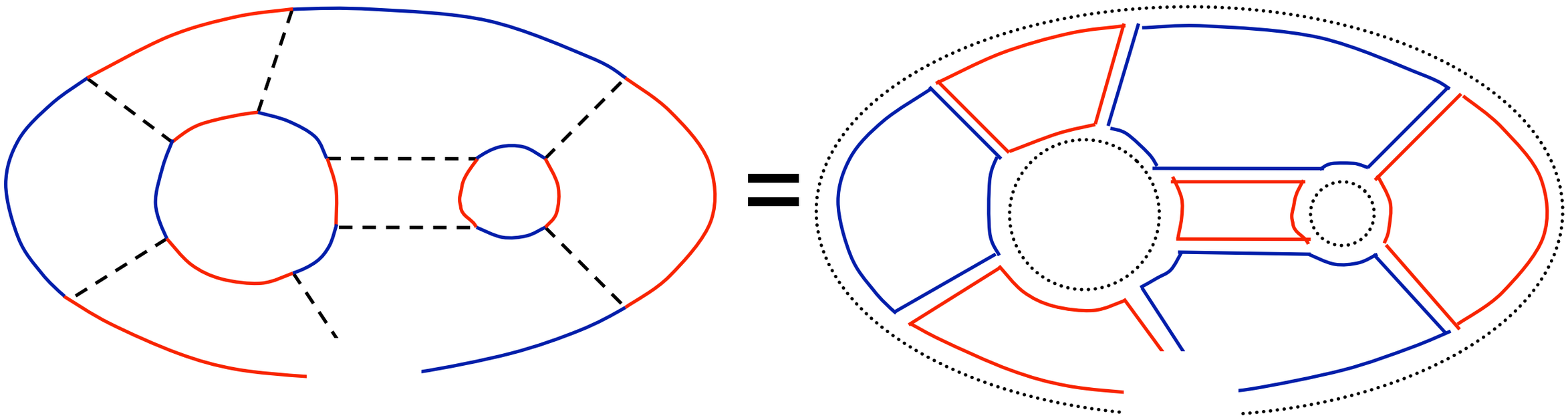

Turn $\vec{\varphi}$ lines into doubled particle-holes lines,
and add dotted lines for fermion loops

Sung-Sik Lee, *Phys. Rev.* B **80**, 165102 (2009); M. Metlitski and S. Sachdev, to appear

Fluctuations about mean field theory

M. Metlitski

SDW fluctuation $\vec{\varphi}$

Fermions near connected hot spots

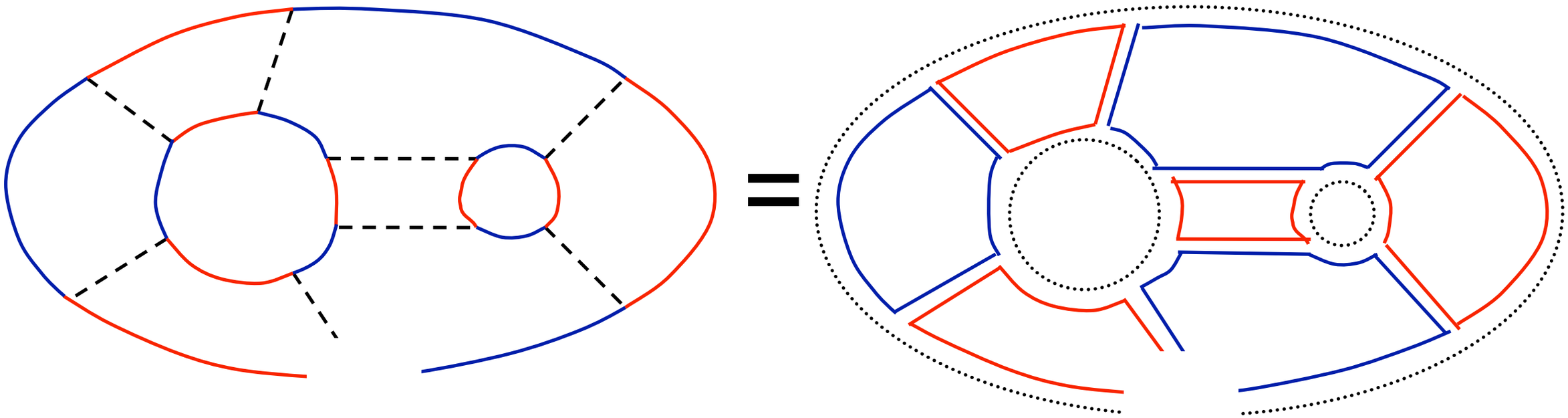

All planar graphs contain the dominant singularity, and have to be resummed for a consistent theory

Sung-Sik Lee, *Phys. Rev.* B **80**, 165102 (2009); M. Metlitski and S. Sachdev, to appear

Fluctuations about mean field theory

M. Metlitski

SDW fluctuation $\vec{\varphi}$

Fermions near connected hot spots

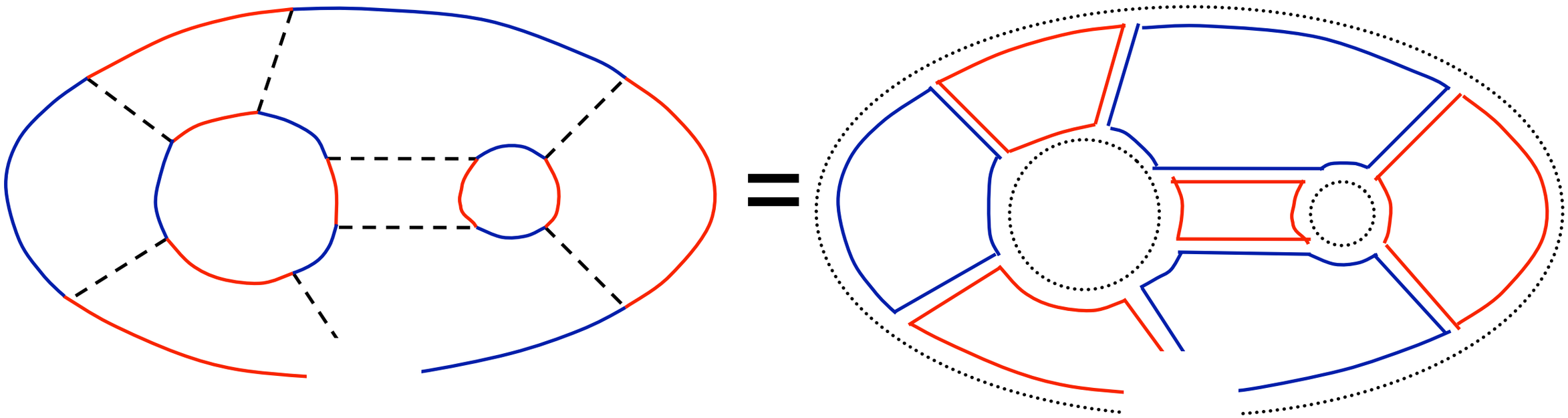

A string theory for the Fermi surface ?

Sung-Sik Lee, *Phys. Rev.* B **80**, 165102 (2009); M. Metlitski and S. Sachdev, to appear

Conclusions

General theory of finite temperature dynamics and transport near quantum critical points, with applications to antiferromagnets, graphene, and superconductors

Conclusions

The AdS/CFT offers promise in providing a new understanding of strongly interacting quantum matter at non-zero density

Conclusions

Identified quantum criticality in cuprate superconductors with a critical point at optimal doping associated with onset of spin density wave order in a metal

Elusive optimal doping quantum critical point has been "hiding in plain sight".

It is shifted to lower doping by the onset of superconductivity